

Head race tunnel evaluation through engineering geological and remote sensing approach - A case of Wabe Hydropower Project, Central Ethiopia

Kibrewossen Jira Dumesso

A Thesis Submitted to

School of Earth Sciences



Presented in Partial Fullfillment of the requirements for the Degree of Masters of Science (Engineering Geology)



ADDIS ABABA UNIVERSITY

Addis Ababa, Ethiopia

August, 2020

Head race tunnel evaluation through engineering geological and remote sensing approach - A case of Wabe Hydropower Project, Central Ethiopia

Kibrewossen Jira Dumesso

A Thesis Submitted to

School of Earth Sciences

Presented in Partial Fullfillment of the requirements for the Degree
of Masters of Science (Engineering Geology)



ADDIS ABABA UNIVERSITY

Addis Ababa, Ethiopia

August, 2020

DECLARATION

I, the undersigned, declare that this thesis is my original work and has not been presented for a degree on any other university and all sources of materials used for the thesis have duly acknowledged.

KIBREWOSSEN JIRA DUMESSO

Signature_____

Place and data of submission: School of Graduate Studies; Addis Ababa University.

August, 2020

SIGNATURE PAGE

**Addis Ababa University
School of Graduate Studies**

This is to certify that the thesis prepared by **Kibrewossen Jira Dumesso**, entitled: **Head race tunnel evaluation through engineering geological and remote sensing approach- A case of Wabe Hydropower Project, Central Ethiopia** and submitted in partial fulfillment of the requirements for the Degree of Master of Science (Engineering Geology) complies with the regulations of the University and meets the accepted standards with respect to originality and quality.

Signed by the Examining Committee:

Examiner _____ **Signature** _____ **Date** _____

Examiner _____ **Signature** _____ **Date** _____

Advisor _____ **Signature** _____ **Date** _____

Chair of School or Graduate Program Coordinator

ABSTRACT

Head race tunnel evaluation through engineering geological and remote sensing approach- A case of Wabe Hydropower Project, Central Ethiopia

Kibrewossen Jira

Addis Ababa University, 2020

The present study was carried out along head race tunnel (HRT) alignment of Wabe hydropower project which is situated in Welkite, Gurage Zone, Southern Nation Nationality and Peoples regional state in Ethiopia. The project is accessible via Addis-Welkite-Jima asphalt road and is about 161 km west of Addis Ababa. The project is proposed to be constructed across Omo River with installed capacity of 450 MW. It envisages a 4m diameter modified-horse shoe shaped, 15821m long horizontal head race tunnel (HRT), a pressurized penstock with 3.2m diameter, and 1394 m long horizontal and 300m vertical shaft tunnel. In order to evaluate the suitability of HRT alignment, tunnel inlet and penstock shaft integrated approach through engineering geological, geophysical and remote sensing methods has been utilized in the present study. The main purpose of this study is to evaluate and characterize the rock mass along the proposed tunnel alignment and to recommend supports for the proposed head race tunnel including slope stability condition at the tunnel inlet portal and, the slope around the surge and penstock shaft. These objectives were met by following systematic approach by utilizing secondary and primary data. The primary data was generated through investigations carried out in the present study area which include, surface mapping, terrain evaluation through remote sensing of satellite images, rock mass classification, in situ testing on rock properties, and laboratory testing on representative samples. Moreover, secondary data from previous investigation was also utilized to analyze and characterize the rock mass along HRT. This includes geotechnical and geophysical investigation reports. Litologically, HRT will be excavated through fresh to moderately weathered aphanitic and porphyritic basalts (BA-3) and moderately weathered to completely weathered aphanitic, porphyritic and vesicular basalt (BA-4). In order to characterize and classify the rock mass along HRT alignment, rock mass classification systems i.e. rock mass rating (RMR), tunnel quality index (Q system) and geological strength index (GSI) were used. The results of rock mass classification through Q system indicates that the rock mass quality in general varies from poor to very good whereas classification through RMR system indicates that the rock mass quality in general varies in the range of Fair to good. The GSI value for rock mass ranges from 67 to 81 which suggests rock mass ranges from good blocky un disturbed to very good massive. Further, 2D resistivity imaging was carried out along the HRT alignment with the objective to characterize geological features and to assess general ground condition prevailing along the headrace tunnel alignment. Based on 2D resistivity imaging analysis and remote sensing interpretations seven normal faults and six fracture zones were identified. Accordingly, these faults were observed to be striking northwest and southwest, dipping from 65 to 80°. These faults were characterized to have vertical displacement (throw) ranging from 10 and 20 m. Furthermore, remote sensing analysis was performed in order to aid the study by providing valuable information for evaluating geological and topographical consideration of the study area. Finally, the study forwards recommendation for tunnel support and Suitability based on the findings.

Key words; Headrace tunnel, Rock mass classification, Rock mass characterization, Tunnel support.

ACKNOWLEDGMENT

First of all, I would like to thank the Almighty God for unspeakable gift and limitless backing of my entire life. It is his help that gives me the patience and strength to accomplish my work.

Next, I would like to offer my sincere gratitude to my esteemed advisor Dr. Tarun Kumar Raghuvanshi, Associate Professor, School of Earth Sciences, College of Natural Science, Addis Ababa University who advised the present research work. His attempt for guidance and constant encouragement strongly supported me to complete the present research work in this manner.

I would also like to express as well my sincere thanks to the Ethiopian Construction Design and Supervision Works Corporation (ECDSWC) which sponsored me during the whole master program and all the staff members for all support and motivation throughout the studies and in the process of writing this thesis.

Finally, I would like to thank my family and for their support and encouragement. Similarly, I am beholden to all my friends and well-wishers for their inspirations and blessings and specifically to those who have directly or indirectly co-operated with me in bringing this thesis at this stage.

TABLE OF CONTENTS

| <u>Contents</u> | <u>Page</u> |
|--|-------------------------------------|
| ABSTRACT | i |
| ACKNOWLEDGMENT | i |
| TABLE OF CONTENTS | iii |
| LIST OF TABLES | viii |
| LIST OF FIGURE | ix |
| LIST OF PLATES | xi |
| LIST OF ACRONYMS | xii |
| CHAPTER – 1 INTRODUCTION | 1 |
| 1.1 General..... | 1 |
| 1.2 Statement of the problem | 2 |
| 1.3 Objectives | Error! Bookmark not defined. |
| 1.3.1 Main Objective..... | 4 |
| 1.3.2 Specific Objectives | 4 |
| 1.4 Methodology..... | 5 |
| 1.5 Significance of the study..... | 6 |
| 1.6 Limitation of the study..... | 6 |
| 1.7 Outline of the study..... | 7 |
| CHAPTER –2 LITERATURE REVIEW | 8 |
| 2.2 Review of previous project study | 8 |
| 2.2.1 Project Layout..... | 8 |
| 2.2.1.1 Intake..... | 9 |
| 2.2.1.2 Head Race Tunnel..... | 9 |
| 2.2.1.3 Power House Area (Surge Shaft, Penstock and Tailrace Tunnel) | 9 |
| 2.2.2 Field Investigations..... | 10 |
| 2.3 Remote sensing Evaluation for Tunnels | 10 |

| | | |
|-------------------------------|--|----|
| 2.3.1 | Selection Criteria for HRT Alignment | 10 |
| 2.3.2 | Topographic Considerations | 11 |
| 2.3.3 | Geologic Considerations | 11 |
| 2.4 | Rock mass Characterization | 12 |
| 2.4.1 | Rock Mass Classification | 12 |
| 2.4.1.1 | Rock Quality Designation (RQD) | 14 |
| 2.4.1.2 | Geomechanics Classification (Rock Mass Rating RMR –System) | 14 |
| 2.4.1.3 | The Q System | 15 |
| 2.4.1.4 | Geological Strength Index (GSI) | 16 |
| 2.4.2 | Hoek-Brown Failure Criterion | 16 |
| 2.5 | Tunnel Support System | 20 |
| 2.5.1 | Tunnel Support Recommendation Based On RMR | 20 |
| 2.5.2 | Tunnel Support Recommendation Based On Q System | 22 |
| 2.6 | Genesis of Methodology for the Present Study | 26 |
| CHAPTER – 3 STUDY AREA | | 26 |
| 3.1 | Location and Accessibility | 26 |
| 3.2 | Climate | 26 |
| 3.3 | Land use Land cover and vegetation | 27 |
| 3.4 | Soil and vegetation | 27 |
| 3.5 | Physiography | 28 |
| 3.6 | Salient features of the project and the project status | 30 |
| 3.7 | Regional Geology and Tectonic Setting | 31 |
| 3.7.1 | Tectonic Setting | 31 |
| 3.7.2 | Regional Geology | 32 |
| 3.7.2.1 | Jima Lower Basalt (E2jl) | 33 |
| 3.7.2.2 | Tarmaber Megezez Formation (E3tm) | 33 |
| 3.7.2.3 | Welded to Partially Welded Pyroclastic Flows (Npp) | 33 |
| 3.7.3 | Regional Geological Structure | 33 |

| | |
|---|-----------|
| 3.8 Geology of the Study Area | 34 |
| 3.8.1 Superficial Deposits (Qal)..... | 34 |
| 3.8.2 Ignimbrite and Tuff (IT) | 35 |
| 3.8.3 Basalt (BA_5) | 35 |
| 3.8.4 Basalt (BA_4) | 36 |
| 3.8.5 Basalt (BA_3) | 36 |
| 3.8.6 Basalt (BA_2) | 37 |
| 3.8.7 Basalt (BA_1) | 37 |
| 3.9 Structure of the study area | 37 |
| 3.10 Groundwater/regional hydrogeology | 37 |
| 3.11 Seismicity..... | 39 |
| CHAPTER – 4 DATA COLLECTION | 42 |
| 4.1 Preamble | 43 |
| 4.2 Secondary Data Collection and Study | 42 |
| 4.2.1 Geophysical Study | 42 |
| 4.2.1.1 2D- Electrical Resistivity Imaging/Electrical Resistivity Data Collection | 43 |
| 4.2.2 Remote Sensing Study | 43 |
| 4.2.3 Permeability Test | 44 |
| 4.2.3.1 Packer Test..... | 44 |
| 4.2.4 Groundwater Condition | 45 |
| 4.3 Primary Data Collection/Engineering Geology | 45 |
| 4.3.1 Geological and Structural Data Collection | 46 |
| 4.3.1.1 Geological Mapping..... | 46 |
| 4.3.1.2 Discontinuities Survey | 46 |
| 4.3.2 Geotechnical Core Drilling | 49 |
| 4.3.3 Laboratory Testing..... | 51 |
| 4.4 Methodology on data collection and analysis | 52 |
| 4.4.1 Preamble | 52 |

| | | |
|--|---|-----------|
| 4.4.2 | Geological and Engineering Geological Investigation | 52 |
| 4.4.3 | Engineering Geological Assessment..... | 53 |
| 4.4.3.1 | Rock Mass Classification..... | 53 |
| 4.4.3.2 | Rock Mass Strength Estimation..... | 54 |
| 4.4.4 | Geophysical Characterization of HRT..... | 54 |
| 4.4.5 | Remote Sensing Study..... | 54 |
| CHAPTER – 5 RESULTS AND DISCUSSION..... | | 55 |
| 5.2 | Engineering Geological Assessment..... | 55 |
| 5.2.1 | Geotechnical Units Intercepted Along the Study Area..... | 55 |
| 5.2.1.1 | Geotechnical Unit One (BA-4)..... | 55 |
| 5.2.1.2 | Geotechnical Unit Two (BA-3)..... | 55 |
| 5.2.2 | Discontinuity Systems | 56 |
| 5.2.3 | Rock Mass Properties | 56 |
| 5.2.4 | Ground Water Condition..... | 59 |
| 5.2.5 | Permeability Test | 60 |
| 5.2.6 | Rock Mass Classification in HRT..... | 60 |
| 5.2.6.1 | Rock Mass Rating (RMR) Classification | 61 |
| 5.2.6.2 | Q - Classification System..... | 63 |
| 5.2.6.3 | Geological Strength Index (GSI) System | 63 |
| 5.3 | Indirect Estimation of Rock Mass Strength..... | 64 |
| 5.4 | Geophysical Results and Discussion | 67 |
| 5.4.1 | 2D- Electrical Resistivity Imaging..... | 68 |
| 5.4.1.1 | Resistivity Imaging Along Section Line-1 | 68 |
| 5.4.1.2 | Resistivity Imaging Along Section Line-2 | 69 |
| 5.4.1.3 | Resistivity Imaging Along Section Line-3 | 69 |
| 5.4.1.4 | Resistivity Imaging Along Section Line-4 | 70 |
| 5.5 | Rock mass study for critical zones..... | 71 |
| 5.5.1 | Weak or Critical Zones | 71 |

| | | |
|--|---|-----|
| 5.6 | Remote sensing study Result | 72 |
| 5.7 | Discussion on results and findings of the study..... | 74 |
| 5.7.1 | Geotechnical Conditions along HRT | 75 |
| 5.7.2 | Discussion on Geophysical Data Results..... | 78 |
| 5.7.3 | Remote Sensing Interpretation..... | 78 |
| 5.7.4 | Overall Assessment of HRT Suitability..... | 79 |
| CHAPTER – 6 HEADRACE TUNNEL SUITABILITY AND SUPPORT | | |
| | ANALYSIS | 83 |
| 6.1 | HRT Topographic Condition | 83 |
| 6.2 | Kinematic Check..... | 84 |
| 6.3 | Engineering Geological Evaluation and HRT Support Analysis..... | 85 |
| 6.3.1 | Recommended HRT Support Based on RMR | 85 |
| 6.3.2 | Recommendation for HRT Support Based on Q System..... | 87 |
| 6.4 | Summery on General Suitability of HRT | 88 |
| CHAPTER – 7 CONCLUSION AND RECOMMENDATIONS | | 90 |
| 7.1 | Conclusion | 90 |
| 7.2 | Recommendations..... | 91 |
| REFERENCE | | 93 |
| APPENDIX | | 100 |

LIST OF TABLES

| | |
|---|----|
| Table 2.1 Major rock mass classification systems (Cosar, 2004)..... | 14 |
| Table 2.2 Summary of RMR rating related to rock mass conditions (Bieniawski, 1989)..... | 15 |
| Table 2.3 Guidelines for excavation and support of 10 m span horseshoe shaped rock tunnels Constructed using drill and blast method at a depth of < 900 m, in accordance with RMR system (after Bieniawski, 1989) | 21 |
| Table 2.4 Values of Excavation Support Ratio, ESR (Barton et al. 1974)..... | 22 |
| Table 2.5 Guidelines for estimating disturbance factor D (After Hoek et al., 2002)..... | 25 |
| Table 3.1 Availability of data in the stations around Wabe River catchment | 27 |
| Table 3.2 Mean monthly Precipitation from Seven stations..... | 27 |
| Table 3.3 LULC coverage area at different period of time in the Wabe River catchment | 28 |
| Table 3.4 Wabe Hydropower Project site Ground motion amplitude determination for rocks and soils (Sources :ECDSWC, 2019) | 40 |
| Table 4.1 coordinates and work volumes of resistivity imaging survey lines | 43 |
| Table 4.2 Pressure magnitudes typically used for each test stage | 45 |
| Table 4.3 Description of degrees of weathering (ISRM, 1981)..... | 47 |
| Table 4.4 Summary of location for Schmidt hammer data collection. | 48 |
| Table 4.5 Details of boreholes along the proposed waterway (Source: ECDSWC, 2019)..... | 49 |
| Table 4.6 Summary of laboratory test..... | 51 |
| Table 5.1 Preferred orientations of Major joint sets in the study area..... | 56 |
| Table 5.2 Summary of Laboratory test results on representative rock samples | 58 |
| Table 5.3 Summary of permeability test result..... | 61 |
| Table 5.4 RMR values for different geomechanical units along the HRT alignment | 62 |
| Table 5.5 Q values for the different geotechnical rock mass units along the HRT alignment | 65 |
| Table 5.6 Classification of rock mass based on RMR and Q-values (Modified after Bieniawski, 1989 and Barton et al 1974) | 76 |
| Table 5.7 Summary of rock mass classification result for each geotechnical rock mass unit | 77 |
| Table 5.8 Summary of Rock mass parameters obtained from analyzing geotechnical rock mass along HRT by using Rock Lab 1 software | 77 |
| Table 6.1 Summary of Rock mass classification results..... | 85 |

| | |
|---|----|
| Table 6.2 Estimated support and excavation based on Guidelines for excavation and support of 10 m span horseshoe shaped rock tunnels constructed using drill and blast method at a depth of < 900 m, in accordance with the RMR system (after Bieniawski, 1989)..... | 86 |
| Table 6.3 Maximum unsupported span and reinforcement categories for geotechnical rock mass unit (according to Q system) | 88 |

LIST OF FIGURE

| | |
|--|----|
| Fig.2.1 Modified table for estimating the Geological Strength Index (Hoek et al., 1998).... | 20 |
| Fig.2.2 Relationship between the stand-up time and roof span for various rock masses (after Bieniawski, 1989) | 22 |
| Fig.2.3 Different Support Categories (type of support) for different rock mass classes defined by the Q or Qc relationships and the support width or height (Grimstad and Barton, 1993)..... | 23 |
| Fig.3.1 Location map of the study area..... | 26 |
| Fig.3.2 Soil types in the Wabe River catchment..... | 28 |
| Fig.3.3 Physiographical map of the study area produced by using DEM at 20m resolution. | 29 |
| Fig.3.4 Regional Geologic Map of the study area (simplified after Efrem Beshawered, 2012 , Ethiopian Institute of Geological survey)..... | 34 |
| Fig.3.5 Structural sketch map of the Ethiopian and Somali plateaus, Afar depression, and Main Ethiopian Rift (Northern, Central, and Southern MER) with the main transversal tectonic line and major volcanic edifices (modified from Abbate E. and Sagri M., 1980)..... | 35 |
| Fig.3.6 Geological map (above) at offset of 500 m from headrace tunnel alignment (HRT) and Cross section (below) along HRT alignment..... | 36 |
| Fig.3.7 Geological map of the area (simplified after Efrem Beshawered, 2012) | 39 |
| Fig.3.8 (a) Earthquakes recorded in the Horn of Africa region from 1900 to 2010. (b) Seismicity data for the Addis Ababa region and the Wabe project site; red circles represent earthquakes that occurred for the last 110 years in the region and size of the circles is proportional with magnitude. The green rectangle shows the locations of the planned Wabe Hydroelectric power project site. | 41 |
| Fig.3.9 Seismicity Map of Ethiopian Rifts (Including Red Sea and Gulf of Aden rifts) from the new catalog. The legend color bar on the right bottom of the map indicates the Hypocentral depths variations of Earthquake. The rectangular legend on the top right of the map indicates the size of the of the Earthquakes magnitude's ranges in Moment magnitude scale in the regions (After Geremew Lemessa et al., 2019)..... | 41 |
| Fig.4.1 Procedures used for Data collection and interpretation..... | 42 |

| | | |
|----------|--|----|
| Fig.4.2 | BN- Hammer Conversation curve for N type Silver Schmidt hammer (from silver Schmidt operating instructions) (Source: http://www.proceq.comproceq_silverschmidt_user_manual_en) | 48 |
| Fig.5.1 | Rosette diagram for joints in the study area. | 57 |
| Fig.5.2 | Fisher concentrations of joint sets in the study area. | 57 |
| Fig.5.3 | GSI for BA-4 geotechnical unit. The drilled Core box shown on left is from BH-9 borehole and GSI value ..is shown on the right marked over standard chart proposed by Rock Lab Guide by Hoek and Brown, 2002 | 66 |
| Fig.5.5 | Analysis of rock strength using Rock lab for BA-4geotechnical rock unit along HRT alignment | 67 |
| Fig.5.6 | Analysis of rock strength using Rock lab for BA-3geotechnical rock unit along HRT alignment | 67 |
| Fig.5.7 | (a) Topographic contour map showing morphology of study area and(b)Terrain condition of the study area, as seen through Google Earth image | 74 |
| Fig.5.8 | Terrain View of the study area (above) with section along the tunnel alignment (bottom) | 75 |
| Fig.5.9 | Geological structures extracted from DEM (resolution 20m) along HRT tunnel | 79 |
| Fig.5.10 | Cross section along HRT alignment showing geotechnical rock units and various structures..... | 80 |
| Fig.5.11 | (a) drainage patterns map showing drainage systems that cross HRT and (b) ridges along HRT route that indicate geological structures | 81 |
| Fig.6.1 | Effect of valley side on stress condition in tunnel..... | 83 |
| Fig.6.2 | Topographic analysis results A) section of near Tunnel entrance. B) HRT entrance profile and C)Tunnel profile near to penstock. | 84 |
| Fig.6.3 | Kinematics cheek for potential mode of failure (a) for tunnel entrance slope. (b) for slope near to penstock | 84 |
| Fig.6.4 | Estimated support categories on the bases of the tunneling quality index Q (After Grimstad and Barton, 1993 , reproduced from Palmstrom and Broch, 2006)..... | 87 |
| Fig.6.5 | Stereographic plot of major joint set and tunnel axis orientation..... | 89 |

LIST OF PLATES

| | | |
|-----------|--|----|
| Plate 3.1 | (a) Photographic view near to the tunnel portal (b) Surge shaft slope..... | 30 |
| Plate 3.2 | Rock units exposed in the study area. (A) Fresh columnar basalt mapped as BA_3 rock unit (Fig. 3.5) (B) Closely jointed fresh basalt mapped as rock unit BA_3 (Fig. 3.5) and (C) Fresh basalt exposure mapped in BA_5 rock unit (Fig. 3.5) | 38 |
| Plate 4.1 | (a) Bore hole logging during field work and (b) Field compressive strength estimation using Schmidt hammer | 50 |
| Plate 5.1 | Surface exposures of weak zones or fractured rock along the fault zone in BA_3 rock unit gully exposure | 72 |

LIST OF ACRONYMS

| | |
|-----------------|---|
| ASTM | American Society for Testing and Materials |
| BH | Borehole |
| BS | British standard |
| C | Cohesion (KPa) |
| D | Disturbance factor |
| ECDSWC | Ethiopian construction Design and Supervision Works Corporation |
| Ed | Deformation Modulus(GPa) |
| EMA | Ethiopian Map Agency |
| ENEL ELC | Eneland Electro Consult |
| ESR | Excavation Support Ratio |
| FAO | Food and Agriculture Organization |
| GSI | Geological Strength Index |
| ha | Hectare |
| HRT | Head race tunnel |
| ISRM | International Society for Rock Mechanics |
| m.a.s.l | meter above sea level |
| mb | Material Constant |
| MER | Main Ethiopian Rift |
| MW | Mega Watt |
| MPa | Mega Pascal |
| MoWIE | Ministry of Water, Irrigation and Energy |
| mm | Millimeter |
| Mm ³ | Million cubic meter |
| RMR | Rock Mass Rate |
| RQD | Rock Quality Designation |
| UCS | Unconfined Compressive Strength |
| USACE | United States Arms Corps Engineers |
| UTM | Universal Traverse Mercator |
| Φ | Internal Friction Angle (°) |
| g | Density of the rock (N/m ³) |
| σ_1 | Major principal stress |

| | |
|---------------|--|
| σ_3 | Minor principal stress |
| σ_c | Uniaxial compressive strength (Mpa) |
| σ_v | Vertical stress (Mpa) |
| σ_{cm} | Unconfined Compressive Strength of Rock Mass |
| σ_{ci} | Unconfined Compressive Strength of Intact Rock |

CHAPTER – 1

INTRODUCTION

1.1 General

Energy production directly governs the development of a country. This energy may develop with the mechanism of Hydropower generation project. Ethiopia is one of the countries in Africa having ample water resources distributed across 12 major basins with an exploitable hydropower potential of 45,000 MW. Wabe hydropower development project is one of such projects that has good potential, selected by the government, to be studied in Omo-Gibe river basin (ECDSWC, 2019).

Wabe hydropower project is proposed to construct across Omo River for the intended use of hydropower production. The project envisages a 4m diameter modified-horse shoe shaped, 15,821m long horizontal head race tunnel (HRT), a pressurized penstock with 3.2m diameter, and 1,394 m long horizontal and 300m vertical shaft tunnel. At downstream end of the pressurized penstock it trifurcates into three 1.8m diameter steel pipes through a manifold to join the turbine. Each turbine will have an installed capacity of 150 MW (ECDSWC, 2019).

A HRT is a typical component of hydropower plant that conveys water from reservoir to the penstock and powerhouse. It is a pressurized tunnel in which the inner applied hydraulic pressure may exceed the overburden/ground load (Strauss et al., 2020). Stability evaluation of HRT is one of the most important concerns in the design of Underground projects. According to Rahimi et al. (2014) stability of an underground opening depends on the behavior of the ground surrounding it. Therefore, it is necessary to understand the actual type of behavior, as a prerequisite for rock support and other evaluation. In this regard, evaluation by determining the rock mass properties along the HRT, tunnel entrance and penstock slope is very crucial to have long term life span of the hydro power project (Mohammad et al., 2017 and Marie, 1998). The evaluation has been carried out by engineers and scientists on the basis of rock mass classification (Gupta et al., 2011) and application of remote sensing (Gupta, 2018).

The rock mass classification systems are used to classify the rock masses into different categories having more or less similar geological and geotechnical properties on the basis of results obtained from the rock mass characterization (Bieniawski, 1989; Sopac, 2008). Knowledge and understanding of the complexity of the ground are essential for a good

geotechnical design of a tunnel excavation. Therefore, guideline for selection of suitable design methods of tunnel is based on ground behavior (Rahimi et al.,2014).

Most of the rock mass classification systems provide the empirical value to different rock mass parameters according to their conditions and the overall rating value of the rock mass is determined by combining these parameters such as; (i) the strength of the intact rock material (compressive strength, modulus of elasticity), (ii) the rock quality designation (RQD) which is a measure of drill core quality or intensity of fracturing, (iii) parameters of rock joints such as; orientation, spacing, and condition (aperture, surface roughness, infilling and weathering), (iv) groundwater pressure and flow, (v) in situ stress and (vi) major geological structures (Bieniawski, 1989; Rahimi et al.,2014).

For the present study, Remote sensing application was applied to cover a wider area to minimize the effort of ground survey and cost by providing early prediction of potential problematic areas. This approach can effectively recognize terrain conditions, geologic formations, escarpments and surface reflection of faults, buried stream beds, site access conditions and general soil and rock formations (Soldo et al., 2019).Therefore, remote sensing helps not only in evaluating ground conditions but it also helps in assessing general suitability of HRT alignment.

Further, for the present study HRT alignment, inlet portal, surge and penstock shaft were selected for the evaluation and characterization of the rock mass.As such, detailed site geological investigations, geotechnical evaluations and design aspects related tasks were carried out by using three rock mass classification systems i.e., Rock mass rating (RMR) by Bieniawski (1989), Tunneling quality index (Q -system) by Barton et al. (1974), and Geological strength index (GSI) by Hoek et al. (1997-1998). Further, based on the rock mass characterization the support systems and blasting method were proposed for each geotechnical unit within the HRT, surge and the shaft.

1.2 Statement of the problem

Ethiopia is characterized by diverse geographical land forms, which varies from top mountainous area to deep lowlands and because of its diverse topographical formations the country is endowed with long rivers, lakes and streams. Therefore, hydropower is favorable option in Ethiopia in order to satisfy demand of power. Nowadays in Ethiopia, large hydropower projects have been developed, which involves long tunnels. These tunnels are

constructed to convey water to the power house. Six such hydropower projects which involve tunnels are; Fincha hydropower project, Beles hydropower project, Tekeze hydropower project, and Gilgel Gibe – III hydropower projects (Abichu Lule, 2016).

Ethiopia has faced tunnel collapses in different time in hydropower development projects of Gilgel Gibe (I, II and III). These problems had been resulted due to the unforeseen geological conditions encountered during the construction works, which has significantly affected the project's progress for a year and increased the construction cost unexpectedly (ENEL and ELC, 2004; Samuel Kidane and Samison Engida, 2010).

Engineering design associated with rock mechanics problems is a challenging issue due to the variation of rock strength properties. This is due to the presence of fractures (which govern the stability of surface structures) and in situ stress conditions (which govern the stability of deep structures) in rock masses (Marie, 1998; Jones, 1989). Furthermore, groundwater conditions, squeezing and swelling or stability conditions of rock masses and filling materials in joints will scale their effects (Hudson and Harris, 1997; Panthee et al., 2016). In this regard, proper engineering design is one of the major concerns to avoid failure of engineering structures (Akin, 2013).

Tunneling possesses various kinds of challenges or problems that influences the stability such as rock burst, swelling, squeezing and spalling. Generally, these challenges are associated with frequently changing of geological setup and ground water along tunnel route (Shrestha, 2006). Also, factors influencing the stability of underground excavations in rock are stratigraphy, geological structures, ground water conditions, strength of the rock masses, geometry, excavation methods, and type of support systems and method of support installations (EM1110-2-2901, 1997).

Geology is the most important factor that determines the nature, form and the cost of a tunnel. According to Edlebro (2004), knowledge of the rock mass behavior, the failure processes and the strength are important for the design of drifts, ore passes, Panel entries, tunnels, and rock caverns. Reliable estimates of the strength and deformation characteristics of rock masses are required for almost any form of analysis used for the design of slopes, foundations and underground excavations. Further, many tunneling problems are caused by the unexpected changes in the strength or deformability of the rock mass where it is being excavated. When such a mass is disturbed, it undergoes a re-distribution of stresses, accompanied by a

deformation of rock mass is very often. These changes can be either inconsequential or catastrophic, depending on the distribution of stresses in the rock, its strength, deformability etc. Early assessment of such changes in tunneling projects can be of great importance in identifying potential unstable zones, and also in devising appropriate remedial measures (Kolymbas, 2005). Moreover, slope instability remains a major concern for tunnel entrance and slope near to penstock located in hilly terrain. Many factors such as topography, gradient of the slope, overburden depth, geological and rock mechanics properties of the rock mass constituting the hill slope, amount of precipitation and surface run off, design and support of the cut slope, influences the stability of the slope (https://www.academia.edu/6546821/managing_power_house-back-slope-Acase-study&sa=u&ved.pdf).

1.3 Objectives

1.3.1 Main Objective

The main objective of this study is to evaluate and characterize the rock mass along the proposed tunnel alignment and to recommend supports for the proposed head race tunnel. Also, it is intended to study the Slope stability conditions at the tunnel inlet portal and the slope around the surge and penstock shaft.

1.3.2 Specific Objectives

In order to meet out the aforementioned main objective, the following specific objectives were formulated;

- ❖ To evaluate the suitability of tunnel alignment based on general topography and geological conditions by using remote sensing and other secondary data.
- ❖ To evaluate and characterize rock mass likely to be encountered along the head race tunnel (HRT), inlet portal, surge and penstock shaft with the help of surface geological mapping, rock mass classification, borehole logging and geophysical data.
- ❖ To classify the zones in HRT with potential difficulties on account of geological, hydrogeological and construction difficulties.
- ❖ To workout possible support measures in HRT based on rock mass characterization.
- ❖ To carry out slope stability studies at HRT inlet portal, slope at surge and Penstock shaft for existing and anticipated adverse conditions.

1.4 Methodology

The present study consist step wise procedures of desk study, field investigations, in situ tests, laboratory tests, data processing, interpretation of the result and report writing. Generally, it consists of following five stages;

❖ **Desk study:** In the initial stage, desk study work like relevant literature review of available sources was undertaken. Literature review has helped to recognize geological features and geotechnical conditions that may have impact on design and construction (database on the classification systems, tunnel support applications and slope stability) of tunneling projects, and gives clue/frame work on acquiring and understanding engineering geological and geotechnical information from similar projects or sites.

Also, emphasis was paid to review previously conducted geotechnical and geological investigation for head race tunnel construction for hydropower and irrigation projects. Relevant back ground material for review was obtained from geological maps, aerial photos, reports, investigation reports for Wabe hydropower project (geophysical data and other related secondary data which was valuable for the specific research topic), journals, books and online materials.

❖ **Detailed field studies:** Detailed geological, structural and geomorphological mapping with the scale of 1 to 5000 at offset of 500 m from the center of proposed tunnel alignment was prepared including hydrogeological conditions of the study area with aid of remote sensing and field mapping. Discontinuities description and characterization was performed on surface and through core drilling. Core drilling is crucial for estimating RQD value, provides samples from underground for laboratory test and analysis. Besides, information from bore holes was used as a supplement material to support information from surface geological mapping. Core drilling along the tunnel route has been in progress by ECDSWC. For this study, core log data and packer tests were conducted. In order to obtain specimens for laboratory test analysis, core samples were also taken.

❖ **Laboratory tests:** from samples taken from the field, laboratory tests were carried out in order to assess quantitative properties of the rock mass. The analysis consists of intact rock properties such as; uniaxial compressive strength (UCS), unit weight, and point load, modulus of elasticity and also water absorption tests were determined in the laboratory.

- ❖ **Engineering geological characterization:** Rock mass classification was performed along the tunnel alignment in order to quantify various engineering properties of the rock mass. On the basis of field work and laboratory test results, rock mass within the tunnel alignment was evaluated using rock mass classification systems. The classification systems for estimating quality of the rock mass that were used for the present study are Rock mass rating system (RMR; Bieniawski, 1989), Geologic strength index (GSI; Hoek, 2002) and Q-system (Barton et al., 1974).
- ❖ **Slope stability assessment:** slope stability assessment of entrance of the tunnel and near to surge shaft, and penstock was executed by stereographic kinematical analysis method.
- ❖ **Data analysis and interpretation:** lastly after completion of the field engineering geological studies and laboratory rock property tests, geotechnical data analysis and interpretation in terms of engineering geological aspect was carried out.

Software such as; AutoCAD, ArcGIS, Global Mapper, Surfer, RockLab and Microsoft offices (word and excel) was used as an assisting tool in this research.

1.5 Significance of the study

The present study provides information about the site investigation and rock mass evaluation, and characterization of tunnel of Wabe hydropower development project along the proposed alignment. The main significance of this study is to obtain/predict reliable estimates of tunnel constraints as early as possible to carry out construction without/minimum difficulties.

Further, the major output of the study has significance for determination of tunnel support design and devises possible remedial measures for adverse ground tunneling conditions as per conditions in the field. Besides, it may also improve the knowledge of site investigation and geological aspects of rock tunneling projects in Ethiopia.

1.6 Limitation of the study

The present research was mainly focused on HRT alignment and on the slope near to tunnel entrance, and surge shaft. The design presented in this study was limited to availability of sufficient and appropriate literature on the specific thesis title and for geotechnical investigation there were limited number of joint exposures. Thus, the quality of the results

and the findings of the present study may be affected to certain degree of inaccuracy. However, all attempts are being made to carry out the present research work in a very systematic and organized manner, well supported by the actual field data laboratory tests and the secondary data gathered from various sources.

1.7 Outline of the study

The present research presents systematic detailed geotechnical site investigation, engineering geological evaluation and design consideration for proposed HRT alignment of Wabe hydropower project. The present study consists following seven chapters;

Chapter I covers introduction of the study, justifies the relevance of the study, describes the study objective, methodologies, defines the scope and limitations of the research and finally outline of the study.

Chapter II presents literature review in detail which includes remote sensing study, rock mass characterization using rock mass classification and tunnel support, and genesis of methodology for the present study.

Chapter III briefly presents the study area which includes location and accessibility, climate, physiography, salient features and project status, regional geology, tectonic setup, local geology, geological structures, ground water condition and seismicity of the study area.

Chapter IV describes the applied methodology and data collection for the present study.

Chapter V presents results and discussion of the study in detail. Evaluation of the study area from the results of engineering geological assessment of the study area which includes geotechnical rock mass condition, deformability and strength estimation, permeability, study of geophysical data and remote sensing study.

Chapter VI Discusses Head race tunnel support analysis which includes Head race tunnel topographic condition and recommendation on tunnel support.

Chapter VII Briefly summarizes and gives conclusion and recommendations that includes the researchers' scientific and logical recommendations for further necessary works on unattended problems and matters in this thesis.

CHAPTER – 2

LITERATURE REVIEW

2.1 Preamble

Prior to detailed geotechnical site investigations, review on previous works was undertaken in order to understand the geological features and geotechnical conditions associated with such tunneling project. Emphasis has been given to review pertinent previous works on rock mass characterization and support analysis of tunneling mainly on hydropower tunnel evaluation with engineering geological and remote sensing methods. For the present study different literature sources were utilized which include topographic data, boreholes drilling logs, geophysical investigations, geological maps and design geotechnical reports of Wabe hydropower project, books, journals and on-line materials available on internet.

2.2 Review of previous project study

The Ministry of Water, Irrigation and Electricity (MoWIE) gave a mandate with contractual agreement for Ethiopian Construction Design and Supervision Works Corporation (ECDSWC) in order to conduct the pre-feasibility/ feasibility study and design of Wabe hydropower project. Under this mandate geological and geotechnical investigation tasks of the project were included. Geological study and mapping, geophysical survey (using 2D-Electrical Resistivity Imaging and Seismic Refraction Methods), seismic hazard study, geotechnical investigation and corresponding reports are covered under geological and geotechnical investigation tasks.

2.2.1 Project Layout

Wabe hydropower project is proposed to be constructed across Omo River for the intended use of hydropower production. The project consists of dam, HRT, intake structure, surge shaft and underground power house. The runoff river hydropower scheme result shows there are two scenarios. The first scenario shows the reservoir area at full supply level (FSL) and reservoir volume at FSL is considered 1504.5ha and 528.96 Mm³, respectively. Based on the second scenario the dam crest elevation will be at 1803m, the reservoir capacity at FSL will become 784.71Mm³ and reservoir area at FSL for this scenario will be 1914.31ha (ECDSWC 2019).

The elevation difference (river drop) between intake invert level and tail water level is 661m. Along the water way Wabe River flow is led in to HRT through the main dam, shaft, tailrace

tunnel and power house. The flow through HRT is controlled from a vertical gate shaft located at 657.50m from the intake structure (ECDSWC, 2019).

2.2.1.1 Intake

According to ECDSWC (2019) a rounded bell mouth intake structure with flat bottom is provided at 350m upstream of the dam axis on the left abutment. Typical power water way ranging intake to tail race is designed on the left side. A 7x6m trash rack inclined at 75° from the horizontal is provided at the upstream of the intake structure to screen debris and trashed from entering the power water way and power house. A mesh size that allows a permissible velocity of 0.7m/s through the racks, when 50% of the gross area is clogged, is designed.

2.2.1.2 Head Race Tunnel

For annual mean discharge of 30m³/s, a 4m diameter modified-horse shoe shaped tunnel is provided to convey the water to power house. The headrace tunnel has 15,821m long horizontal tunnel with bed slope of 0.1% and 342.2m high vertical shaft. The flow through the tunnel is controlled from a vertical gate shaft located at 657.50m from the intake structure (ECDSWC, 2019).

2.2.1.3 Power House Area (Surge Shaft, Penstock and Tailrace Tunnel)

Since the mean discharge from the reservoir is small, 30m³/s, and this discharge is conveyed through a minimum workable area of 4m diameter, the velocity of flow is 2.4m/s which give a velocity coefficient of 14.58. The computation in general indicates a 1 to 1.3m diameter surge tank which is impractical to construct. Hence a 5m diameter surge tank is adopted. The propagated wave in the penstock during sudden closure creates a maximum upsurge of 4.8m in the surge tank. Adding 2m free board in the surge tank the top tank level becomes 1800 m. a. s. l. (ECDSWC, 2019).

The pressurized penstock is with 3.2m diameter and 1394m long horizontal and 300m vertical shaft tunnel. At its downstream end it trifurcates into three 1.8m diameter steel pipes through a manifold to join the turbine. Each turbine will have an installed capacity of 150MW. The water, after generating electricity, will be collected from the three turbines and conveyed to the Wabe River through a tail race tunnel. The flow through the tail race tunnel is made to be an open channel flow with 75% full flow. This required a gross area of 7m diameter. The tail race has a total of 3177m length (ECDSWC, 2019).

2.2.2 Field Investigations

During the present study, the feasibility investigation work by the project authorities was under progress. The resulting feasibility investigation report from this study was used as a basis for the present research work. With the background information obtained from the feasibility study, there were some other sources from the field investigation carried out after the end of the feasibility report that were utilized for the present study. Further, before the primary data collection for the present study, the Wabe hydropower project investigation has been under preliminary investigation stage. For this 2D seismic imaging for 17,269m was accomplished along the tunnel alignment. Also, along the tunnel alignment six bore holes have been proposed and all bore holes are located along the HRT alignment except BH-16. Out of bore holes along HRT alignment, BH-9 and BH-13 were completed and the remaining was under progress (BH-12 and BH-13) and was not completed during the present study.

2.3 Remote sensing Evaluation for Tunnels

In tunnel design, prediction of ground response to tunneling work is the most essential task. Assessment of ground behavior is inevitably associated with ground characterization, which is the process of quantified description of the ground conditions anticipated along a proposed tunnel alignment for engineering design purposes (Alexandris et al., 2016). Remote sensing observation of earth delivers large amount of data on the earth surface (Rengers et al., 2002) and the application of remote sensing technology cover many fields of studies, such as; structural geology, and mineral exploration, it is also useful for fault structure features extractions (Abdullah et al., 2013) such structures have negative impact on tunneling or fault zones in general is associated with frequently changing ground and ground water conditions together with large and occasionally long lasting displacements (Goricki et al. 2006).

2.3.1 Selection Criteria for HRT Alignment

Collecting data for remote sensing is possible to recognize effectively for large-scale regional interpretation of geologic structure, analyses of regional lineaments, drainage patterns, rock types, soil characteristics, erosion features, and availability of construction materials (Rasher and Weaver, 1990; Gupta, 1991 and soldo et al., 2019). Thus, characterization of the above mentioned geological features are the most influential aspect for the tunnel design (soldo et al., 2019). Accordingly, remotely acquired data are required to be utilized in the construction of both surface and subsurface geologic maps which could be used to predict subsurface conditions in possible tunneling sites (WRLIST, 1972).

2.3.2 Topographic Considerations

Topographic or morphology of tunnel alignment is evaluated using the application of remote sensing. According to [Martínek \(2018\)](#) morphology could be easily visualized using DEMs in the form of colored elevation maps combined with shaded relief. Digital elevation models (DEMs) data were used to trace tectonic features and mapping geologically and, topographically defined structures in many areas ([Sarapirome et al., 2002](#)). Extraction of topographic feature information using DEMs has become increasingly popular in structural analysis ([Gans et al., 2005](#)) and DEMs are used for mapping and, characterization of tunnel alignment in hilly region ([Jeganathan et al., 2017](#)).

2.3.3 Geologic Considerations

The geological characteristics of potential Hydropower electric power sites and their surroundings have high importance in suitability analysis. These characteristics may be studied using multispectral data and field evidences to ensure that geologically, the sites fall in stable zone ([Jeganathan, et al., 2017](#)). According to [Abdullah et al. \(2013\)](#) geological features are any alignment of features on satellite images such as the various types recognized including topographic, drainage, vegetative, and color alignments. For the classification of landforms to many purposes such as recognition of drainage patterns DEMs are very useful tools.

Structural characteristics of an area can be accessed on remotely sensed images by interpretations of linear features. Satellite images allows for recognition of features that would be difficult to follow and interpret during field campaigns because of their large synoptic view of study area ([Martínek, 2018](#)). The application of remote sensing techniques to the identification of faults is important ([WRLIST, 1972](#)), since tunneling in fault zones in general is associated with frequently changing ground (weathered and brecciated fault zones)and water-saturated conditions together are one of the most difficult and expensive problems ([Goricki et al.,2006](#)).

Further, it is necessary that the geotechnical features or conditions of the rock mass (shear zones, faults, joints, bedding, rock types, groundwater conditions etc.) as observed in the field, interpreted from satellite images and or deduced from drilling, are integrated and projected to tunnel axis for their proper appraisal ([Gupta, 2018](#)). Lineation may be detected in air photographs that are essentially invisible in ground surface field examinations. The lineation maybe a guide to the identification of formation boundaries, wide shear or fault

zones, and different joint systems that will have a marked influence on evaluation of geologic conditions at the tunnel grade (Irwin et al., 2000).

2.4 Rock mass Characterization

Rock mass characteristics are not measured, but estimated from observations, descriptions and indirect tests, supported by laboratory test on small specimens, from which characterizations of relevant parameters in the rock mass are made (Sharma and Saxena, 2001). According to Ocepec (2006) rock mass characterization is the process of collecting and analyzing qualitative and quantitative data that provide indices and descriptive terms of the geometrical and mechanical properties of a rock mass. Rock mass characterization is required for many applications in rock engineering practice including excavation and tunnel design. For these purposes, it is necessary to obtain the geological characteristics of the rock material, together with the visual assessment of the rock mass as input parameters such as; strength parameters for further analysis.

Rock mass characterization forms the bases for design and estimation of the required amount and type of rock support and groundwater control measures. The rock mass classification systems were designed to act as an engineering design aid and were not intended to substitute field observations, analytical considerations, measurements, and engineering judgment (Bieniawski, 1993; Bieniawski, 1989 and Hoek, 2007). Ideally rock mass classification should provide a quick means to estimate the support requirement and to estimate the strength and deformation properties of the rock mass (Ocepec, 2006).

2.4.1 Rock Mass Classification

Rock Mass Classification is the process of placing a rock mass into groups or classes on defined relationships (Bieniawski, 1989; Syed, 2015) and assigning a unique description (or number) to it on the basis of similar properties/characteristics such that the behavior of the rock mass can be predicted. Most classification systems were developed from case histories of civil engineering (Wickham et al., 1972, Bieniawski (1973, 1989) and Barton et al., 1974). According to Bieniawski (1989) the classification systems are not suitable for use in the elaborated and final design, particularly for complex underground openings. Such use of classification needs further development of these systems. These systems form an essential part of foremost design approaches (the empirical and the numerical design methods) and are increasingly used in both design approaches as computing power improves. It should be used

in conjunction with other design schemes to devise an overall rationale compatible with the design objectives and site geology.

The objectives of rock mass characterization and classification are: (i) to identify the most significant parameters influencing the behavior of a rock mass, (ii) to divide a particular rock mass formation into a number of rock mass classes of varying quality, (iii) to provide a basis for understanding the characteristics of each rock mass class, (iv) to derive quantitative data for engineering design, (v) to recommend support guidelines for tunnels and mines, (vi) to provide a common basis for communication between engineers and geologists and (vii) to relate the experience on rock conditions at one site to the conditions encountered and experience gained at other (Bieniawski, 1989).

In practice, rock mass classification systems have provided a valuable systematic design aid on many engineering projects especially on underground constructions, tunneling and mining projects (Hoek, 2007). At the preliminary design stage, comprehensive information related to the rock mass parameters, its stress, and hydrologic characteristics is mostly unavailable, so to apply a rock mass classification system it is useful to characterize the rock mass and estimate the rock mass properties (Syed, 2015).

Different classification systems place different emphases on the various parameters, and it is recommended that at least two methods be used at any site during the early stages of a project (Palmstrom, 2003). The rock mass classification schemes that are often used in rock engineering for assisting in designing underground structures are RMR, Q and GSI systems (Palmstrom, 2003). Some well-known systems are listed in Table 2.1.

Based on Bieniawski (1993) different important parameters used in order to describe and classify rock mass. Those are; (i) the strength of the intact rock material (compressive strength, modulus of elasticity), (ii) the rock quality designation (RQD) which is a measure of drill core quality or intensity of fracturing, (iii) parameters of rock joints such as; orientation, spacing, and condition (aperture, surface roughness, infilling and weathering), (iv) groundwater pressure and flow, (v) in situ stress and (vi) major geological structures (folds and faults).

Table 2.1 Major rock mass classification systems (Cosar, 2004)

| Rock Mass Classification System | Originator | Country of Origin | Application Areas |
|---|--|------------------------|--|
| Rock Load | Terzaghi, 1946 | USA | Tunnels with steel Support |
| Stand-up time | Lauffer, 1958 | Australia | Tunneling |
| New Austrian Tunneling Method (NATM) | Pacher et al., 1964 | Austria | Tunneling |
| Rock Quality Designation (RQD) | Deere et al., 1967 | USA | Core logging, tunneling |
| Rock Structure Rating(RSR) | Wickham et al., 1972 | USA | Tunneling |
| Rock Mass Rating (RMR) Modified Rock Mass Rating (M-RMR) | Bieniawski, 1973 (last modification 1989-USA) Ünal and Özkan, 1990 | South Africa Turkey | Tunnels, mines, (slopes, foundations) Mining |
| Rock Mass Quality (Q) | Barton et al., 1974 (last modification 2002) | Norway | Tunnels, mines, foundations |
| Strength-Block size | Franklin, 1975 | Canada | Tunneling |
| Basic Geotechnical Classification | ISRM, 1981 | International | General |
| Rock Mass Strength (RMS) | Stille et al., 1982 | Sweden | Metal mining |
| Unified Rock Mass Classification System (URCS) | Williamson, 1984 | USA | General |
| Communication Weakening Coefficient System (WCS) | Singh, 1986 | India | Coal mining |
| Rock Mass Index (RMi) | Palmstrom, 1996 | Sweden | Tunneling |
| Geological Strength Index (GSI) | Hoek and Brown, 1997 | Canada | All underground excavation- |

2.4.1.1 Rock Quality Designation (RQD)

The Rock Quality Designation index (*RQD*) was developed by Deere (Deere et al., 1967) to provide a quantitative estimate of rock mass quality from drill core logs. *RQD* is defined as the percentage of intact core pieces longer than 100 mm (4 inches) in the total length of core. *RQD* only represents the degree of fracturing of the rock mass and does not account for the strength of the rock or mechanical and other geometrical properties of the joints. This parameter has been used in the rock mass classification systems, including the RMR and the Q systems (Syed, 2015).

2.4.1.2 Geomechanics Classification (Rock Mass Rating RMR –System)

Geo mechanics Classification or the Rock Mass Rating (RMR) system was developed by Bieniawski (1973; 1974; 1989) for detailed rock mass classification. Significant changes have been made over the years with revisions in 1974, 1975, 1976, and 1989. The following six parameters are used to classify a rock mass using the RMR (Bieniawski, 1989) system:

$$RMR = A1 + A2 + A3 + A4 + A5 + B \quad \dots\dots\dots \text{eq. 2.1}$$

Where; A1 is the rating for Uniaxial compressive strength of rock material, A2 is the rating for Rock Quality Designation (RQD), A3 is the rating for spacing of discontinuities, A4 is the rating for condition of discontinuities, A5 is the rating for groundwater conditions and B is the rating for orientation of discontinuities.

In accordance to [Bieniawski \(1989\)](#) work, these classification parameters are evaluated by field measurements using the table A-1 (see in Appendix TableA-1) that gives numerical rating value to each parameter to give a value of RMR. This value can be used to define rock mass quality and its class as shown on Table 2.2.

Table 2.2 Summary of RMR rating related to rock mass conditions ([Bieniawski, 1989](#))

| S.N | Sum of RMR rating | 81 - 100 | 61 - 80 | 41-60 | 21 - 40 | <20 |
|-----|---|-------------------|-----------------|--------------------|-------------------|-----------------------|
| 1 | Class number | I | II | III | IV | V |
| 2 | Description | Very good rock | Good rock | Fair | Poor rock | Very poor rock |
| 3 | Average Stand up time | 20yr for 15m span | 1yr for 10m spa | 1 week for 5m span | 10hrfor 2.5m span | 30 minute for 1m span |
| 4 | Cohesion of the rock mass(kPa) | > 400 | 300 - 400 | 200 - 300 | 100 - 200 | < 100 |
| 5 | Friction Angle of the rock mass(degree) | > 45 | 35 - 45 | 25 - 35 | 15 - 25 | < 15 |

2.4.1.3 The Q System

The Q-system was developed at NGI between 1971 and 1974 for estimating rock support in tunnels on the bases of various numbers of case histories on tunnel projects ([Barton et al. 1974](#)).

The Q-system is a classification system developed as an empirical design method for rock masses with respect to stability of underground openings. The numerical value of the index Q ranges from 0.001 to a maximum of 1,000 on a logarithmic scale ([Bieniawski, 1989](#)). The value of Q is calculated by six rock mass parameters combined in the following equation no 2.2:

$$Q = \left[\frac{RQD}{J_n} \right] * \left[\frac{J_r}{J_a} \right] * \left[\frac{J_w}{SRF} \right] \quad \dots\dots\dots \text{eq. 2.2}$$

where; RQD is the Rock Quality Designation (≥ 10 measuring the degree of fracturing), J_n is the rating for the number of joint sets (number of discontinuity sets), J_r is the rating for the joint roughness (for critically oriented joint set roughness of discontinuity surfaces), J_a is the

rating for the joint alteration (degree of alteration or weathering and filling of discontinuity surfaces), J_w is the joint water reduction factor (pressure and inflow rates of water within discontinuities) and SRF is the stress reduction factor (presence of shear zones, stress concentrations, squeezing or swelling rocks).

The numerical estimation of these six input parameters are presented on a series tables of Barton (2002) as shown in Appendix, Table A-2. It gives the classification of individual parameters used to obtain the Tunnelling Quality Index Q for a rock mass (Barton et al., 1974).

2.4.1.4 Geological Strength Index (GSI)

The Geological Strength Index (GSI) was introduced by Hoek (1994). It was aimed to estimate the reduction in rock mass strength for different geological conditions. GSI is qualitative or descriptive system that is used for estimating the engineering design and the only rock mass classification system that is directly linked to engineering parameters such as, GSI value is related to Hoek–Brown strength parameters (Hoek, 1994; Hoek and Brown, 1997; Hoek et al., 2002) or rock mass modulus (Hoek et al., 2002 and Hoek and Diederichs, 2006). The most well developed criterion is the Hoek–Brown Failure Criteria used to estimate the strength and deformation modulus of jointed rock mass using the GSI as an input (Hoek and Brown, 1997; Lu, 2015).

The GSI characterization scheme was devised for engineering geologists and geologists who can utilize all the information contained in the chart presented as Fig. 2.1, to arrive at a range of probable GSI numbers for each rock unit (Hoek et al., 1998). This simple, fast and reliable system represents nonlinear relationship for weak rock mass, can be tuned to computer simulation of rock structures (Singh and Geol, 1999) and can provide means to quantify both the strength and deformation properties of a rock mass (Hoek et al., 2002 and Syed, 2017). Average GSI value is estimated based on the relationship between rock mass conditions and rock discontinuity surface conditions and provides a set of mechanical properties such as Hoek–Brown strength parameters (m_b , a and s) or the equivalent Mohr–Coulomb strength parameters (C and ϕ) and Young's modulus for design purposes (Hoek and Brown, 1997).

2.4.2 Hoek-Brown Failure Criterion

Knowledge of the rock mass strength or reliable estimation of the strength and deformation characteristics of rock mass is required for the design of underground excavation. Hoek and

Brown (1980a;1980b), proposed a method for obtaining estimates of the strength of jointed rock mass, based upon an assessment of the interlocking of rock blocks and the conditions of the surfaces between these blocks. This method was modified over the years in order to meet the needs of users who were applying it to the problems that were not considered when the original criterion was developed (Hoek 1983; Hoek and Brown 1988). The application of the method to very poor quality rock mass required further changes (Hoek et al., 1992) and eventually the development of a new classification called the Geological Strength Index (Hoek et al., 1995; Hoek, 1995; Hoek and Brown, 1997). There were still some uncertainties and inaccuracies which made the criterion inconvenient to apply in numerical models and limit equilibrium programs particularly the difficulty of finding an acceptable friction angle and cohesive strength for a given rock mass which were later solved in “Hoek and Brown Failure Criterion-2002 Edition” (Hoek et al.,2002). Hoek and Brown (2002) proposed application of the Generalized Hoek Brown criterion to jointed rock mass which is expressed as eq. 2.3,

$$\sigma_1 = \sigma_3 + \sigma_{ci} [m_b \sigma_3 / \sigma_{ci} + s]^a \quad \dots\dots\dots \text{eq. 2.3}$$

Where; ‘m_b’ is a reduced value of the material constant m_i and is given by eq.2.4;

$$m_b = m_i \exp[(GSI - 100) / (28 - 14D)] \quad \dots\dots\dots \text{eq. 2.4}$$

‘s’ and ‘a’ are constants for the rock mass given by the following relationships eq. 2.5 and 2.6;

$$s = \exp\left(\frac{GSI - 100}{9 - 3D}\right) \dots\dots\dots \text{eq.2.5}$$

$$a = \frac{1}{2} + \frac{1}{6} (e^{-GSI/15} - e^{-20/3}) \quad \dots\dots\dots \text{eq.2.6}$$

D is the factor which depends on the degree of disturbance to which the rock mass has been subjected by blast damage and stress relaxation and estimated from for estimating guidelines disturbance factor (Table 2.5). It varies from 0 for undisturbed in situ rock masses to 1 for very disturbed rock masses.

The uniaxial compressive strength for rock mass is obtained by following equation;

$$\sigma_c = \sigma_{ci} \cdot s^a \quad \dots\dots\dots \text{eq. 2.7}$$

The tensile strength is determined as;

$$\sigma_t = \frac{s \cdot \sigma_{ci}}{m_b} \quad \dots\dots\dots \text{eq. 2.8}$$

Further, normal and shear stresses are related to principal stresses by the equations proposed by [Balmer \(1952\)](#);

$$\sigma'_n = \frac{\sigma'_1 + \sigma'_3}{2} - \frac{\sigma'_1 - \sigma'_3}{2} \cdot \frac{d\sigma'_1/\sigma'_3 - 1}{d\sigma'_1/\sigma'_3 + 1} \dots\dots\dots \text{eq. 2.9}$$

$$\tau = (\sigma'_1 - \sigma'_3) \frac{\sqrt{d\sigma'_1/\sigma'_3}}{d\sigma'_1/\sigma'_3 + 1} \dots\dots\dots \text{eq. 2.10}$$

Where; $\frac{d\sigma'_1}{\sigma'_3} = 1 + am_b(m_b \rho'_3 / \sigma_{ci} + s)^{a-1} \dots\dots\dots \text{eq. 2.11}$

The rock mass modulus of deformation is given by;

$$E_m(GPa) = \left(1 - \frac{D}{2}\right) \sqrt{\frac{\sigma_{ci}}{100}} \cdot 10^{((GSI/10)/40)} \quad \dots\dots\dots \text{eq. 2.12}$$

Eq. 4.35 applies when $\sigma_{ci} \leq 100 \text{ MPa}$

For $\sigma_{ci} > 100 \text{ MPa}$

$$E_m(GPa) = \left(1 - \frac{D}{2}\right) \cdot 10^{((GSI/10)/40)} \quad \dots\dots\dots \text{eq.2.13}$$

The relation for Mohr – Coulomb in terms of c and ϕ can be related by following equations;

Angle of friction for rock mass;

$$\phi' = \sin^{-1} \left[\frac{6am_b(s+m_b\sigma'_{3n})^{a-1}}{2(1+a)(2+a)+6am_b(s+m_b\sigma'_{3n})^{a-1}} \right] \quad \dots\dots\dots \text{eq. 2.14}$$

Cohesive strength for rock mass;

$$c' = \frac{\sigma_{ci}[(1+2a)s+(1-a)m_b\sigma'_{3n}](s+m_b\sigma'_{3n})^{a-1}}{(1+a)(2+a)\sqrt{1+(6am_b(s+m_b\sigma'_{3n})^{a-1})/((1+a)(2+a))}} \dots\dots\dots \text{eq. 2.15}$$

Where; $\sigma_{3n} = \sigma'_{3max} / \sigma_{ci} \quad \dots\dots\dots \text{eq. 2.16}$

For tunnels;

$$\frac{\sigma'_{3max}}{\sigma_{ci}} = 0.47 \left(\frac{\sigma'_{cm}}{\gamma \cdot H} \right)^{-0.94} \quad \dots\dots\dots \text{eq. 2.17}$$

σ_{cm} is the rock mass strength and Υ is the unit weight of rock mass above tunnel and H is depth of tunnel from surface.

From Mohr Coulomb criteria;

$$\sigma'_{cm} = \frac{2c' \cos \phi}{1 - \sin \phi} \quad \dots\dots\dots \text{eq. 2.18}$$

$$\sigma'_{cm} = \sigma_{ci} \cdot \frac{m_b + 4s - a(m_b - 8s)(m_b/4 + s)^{a-1}}{2(1+a)(2+a)} \quad \dots\dots\dots \text{eq. 2.19}$$

For Slopes;

$$\frac{\sigma'_{3max}}{\sigma_{ci}} = 0.72 \left(\frac{\sigma'_{cm}}{\gamma \cdot H} \right)^{-0.91} \quad \dots\dots\dots \text{eq. 2.20}$$

σ_{cm} is the rock mass strength and γ is the unit weight of rock mass on slope and H is height of slope.

An associated windows program called RocLab has been developed to provide a rigorous and unambiguous method for calculating or estimating the input parameters required for the analysis (Hoek- Brown,2002).This program includes tables and charts for estimating the uniaxial compressive strength of the intact rock elements (σ_{ci}), the material constant m_i and the Geological Strength Index (GSI). This program can be downloaded (free) from www.roscience.com.







| GEOLOGICAL STRENGTH INDEX FOR JOINTED ROCKS (Hoek and Marinos, 2000) | | SURFACE CONDITIONS | | | | |
|--|------------------------------|---|--|---|--|--|
| <p>From the lithology, structure and surface conditions of the discontinuities, estimate the average value of GSI. Do not try to be too precise. Quoting a range from 33 to 37 is more realistic than stating that GSI = 35. Note that the table does not apply to structurally controlled failures. Where weak planar structural planes are present in an unfavourable orientation with respect to the excavation face, these will dominate the rock mass behaviour. The shear strength of surfaces in rocks that are prone to deterioration as a result of changes in moisture content will be reduced if water is present. When working with rocks in the fair to very poor categories, a shift to the right may be made for wet conditions. Water pressure is dealt with by effective stress analysis.</p> | | SURFACE CONDITIONS | | | | |
| | | VERY GOOD Very rough, fresh unweathered surfaces | GOOD Rough, slightly weathered, iron stained surfaces | FAIR Smooth, moderately weathered and altered surfaces | POOR Slackensided, highly weathered surfaces with compact coatings or fillings or angular fragments | VERY POOR Slackensided, highly weathered surfaces with soft clay coatings or fillings |
| STRUCTURE | DECREASING SURFACE QUALITY → | | | | | |
|  INTACT OR MASSIVE - intact rock specimens or massive in situ rock with few widely spaced discontinuities | 90 | | | N/A | N/A | |
|  BLOCKY - well interlocked undisturbed rock mass consisting of cubical blocks formed by three intersecting discontinuity sets | 80 | 70 | | | | |
|  VERY BLOCKY- interlocked, partially disturbed mass with multi-faceted angular blocks formed by 4 or more joint sets | | 60 | | | | |
|  BLOCKY/DISTURBED/SEAMY - folded with angular blocks formed by many intersecting discontinuity sets. Persistence of bedding planes or schistosity | | | 50 | | | |
|  DISINTEGRATED - poorly interlocked, heavily broken rock mass with mixture of angular and rounded rock pieces | | | 40 | 30 | | |
|  LAMINATED/SHEARED - Lack of blockiness due to close spacing of weak schistosity or shear planes | | | | 20 | | |
| | | | | | 10 | |
| | N/A | N/A | | | | |

Fig.2.1 Modified table for estimating the Geological Strength Index (Hoek et al., 1998)

2.5 Tunnel Support System

2.5.1 Tunnel Support Recommendation Based On RMR

Bieniawski (1989) published a set of guidelines for the selection of support in tunnels in rock for which the value of *RMR* has been determined. These guidelines depend on factors such as; depth below the surface (in-situ stress), tunnel size and shape, and method of excavation. It is recommended in many mining and civil engineering applications to consider steel fibre reinforced shotcrete instead of wire mesh and shotcrete (Hoek, 2007). These guidelines are

reproduced in Table 2.3. Note that these guidelines have been published for a 10m span horseshoe shaped tunnel, constructed using drill and blast methods, in a rock mass subjected to a vertical stress < 25 MPa (equivalent to a depth below surface of <900 m).Further, the RMR is also related to stand-up time and the value gives a set of guidelines for estimating the standup time for selecting rock support in tunnels as shown in Fig. 2.2.

Table 2.3 Guidelines for excavation and support of 10 m span horseshoe shaped rock tunnels Constructed using drill and blast method at a depth of < 900 m, in accordance with RMR system (after Bieniawski, 1989) *

| Rock mass class | Excavation | Rock bolts (20 mm diameter, fully grouted) | Shotcrete | Steel sets |
|----------------------------------|--|---|--|---|
| I- Very good rock RMR: 81–100 | Full face, 3 m advance | Generally, no support required except spot bolting | | |
| II- Good rock RMR: 61–80 | Full face, 1–1.5 m advance complete support 20 m from the face. | Locally, bolts in crown 3m long, spaced 2.5 m with occasional wire mesh | 50 mm in crown where required | None |
| III- fair rock RMR: 41–60 | Top heading and bench 1.5–3 m advance in top heading. Commence support after each blast. Complete support 10m from the face. | Systematic bolts 4 m long, spaced 1.52 - 2m in crown and walls with wire mesh in the crown. | 50–100 mm in crown and 30 mm insides | None |
| IV- Poor rock RMR: 21–40 | Top heading and bench 1.0–1.5 m advance in top heading Install support currently with excavation, 10 m from the face. | Systematic bolts 4–5 m long, spaced 1–1.5 m in crown and wall with wire mesh | 100–150 mm in crown and 100 mm insides | Light to medium ribs spaced 1.5m where required |
| V- Very poor rock RMR: <20 | Multiple drifts 0.5–1.5 m advance in top heading. Install support currently with excavation. Shotcrete as soon as possible after blasting. | Systematic bolts 5–6 m long, spaced 1–1.5 m in crown and walls with wire mesh, Bolt invert | 150–200 m in the crown, 150 mm in sides, and 50 mm on the face | Medium to heavy ribs spaced 0.75 m with steel lagging and forepoling if required. Close invert. |

* Shape: horseshoe. Width: 10 m. Vertical stress: 25 MPa. Construction method: drilling and blasting.

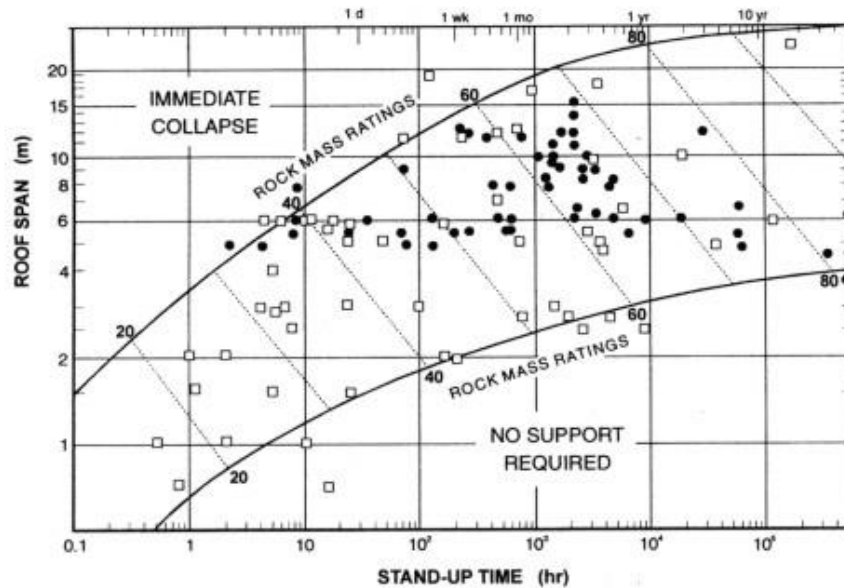


Fig. 2.2 Relationship between the stand-up time and roof span for various rock masses (after Bieniawski, 1989).

2.5.2 Tunnel Support Recommendation Based On Q System

Q value is applied to estimate the support measure for a tunnel of a given dimension, and the usage of excavation by defining the Equivalent Dimension (D_e) of the excavation (Barton et al., 1974) and this is defined as given by the equation 2.21;

$$D_e = \frac{\text{Excavation span (s), diameter (d)}}{\text{Excavation Support ratio (ESR)}} \quad \dots\dots\dots \text{eq. 2.21}$$

Span/diameter is used for analyzing the roof support, and height of the wall is used in case of wall support. The value of *ESR* is related to the intended use of the excavation and to the degree of security which is demanded of the support system installed to maintain the stability of the excavation. Barton et al (1974) suggest the values of *ESR* as presented in Table 2.4.

Table 2.4 Values of Excavation Support Ratio, *ESR* (Barton et al. 1974)

| | Excavation category | ESR |
|---|---|-----|
| A | Temporary mine openings | 3-5 |
| B | Permanent mine openings, water tunnels for hydro power (excluding high-pressure penstocks), pilot tunnels, drifts and headings for large excavation | 1.6 |
| C | Storage rooms, water treatment plants, minor road and railway tunnels, surge chambers, access tunnels | 1.3 |
| D | Power stations, major road, and railway tunnels, civil defense chambers, portal intersections. | 1.0 |
| E | Underground nuclear power stations, railway stations, sports and public facilities, factories | 0.8 |

Based on the relationship between the index Q and the equivalent dimension of the excavation, 38 different support categories have been suggested and permanent support has

been recommended for each category (Barton et al., 1974). The support recommendations made by Barton et al. (1974) has been updated by Grimstad and Barton (1993) to reflect the increasing use of steel fibre reinforced shotcrete in underground excavation support (Fig.2.3).

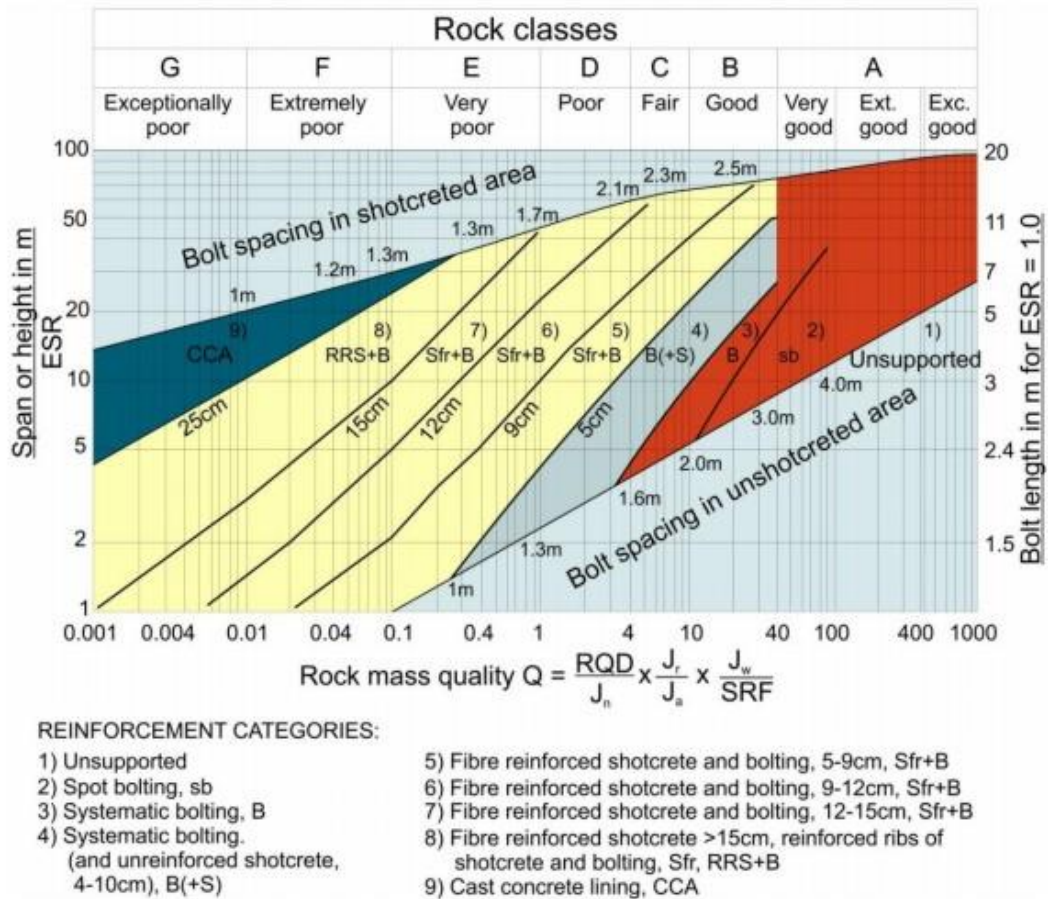


Fig.2.3 Different Support Categories (type of support) for different rock mass classes defined by the Q or Qc relationships and the support width or height (Grimstad and Barton, 1993).

Barton et al (1980) also proposed empirical relationships to determine rock bolt length (L), maximum unsupported spans (Smax) to supplement the support recommendations.






$$L = 2 + (0.15 * B / ESR) \quad \dots\dots\dots \text{eq. 2.22}$$

Where, B is the excavation width.

The maximum unsupported span can be estimated,

$$S_{\max} = 2 ESR Q^{0.4} \quad \dots\dots\dots \text{eq. 2.23}$$

Table 2.5 Guidelines for estimating disturbance factor D (After Hoek et al., 2002)

| Appearance of rock mass | Description of rock mass | Suggested value of <i>D</i> |
|---|---|--|
|  | Excellent quality controlled blasting or excavation by Tunnel Boring Machine results in minimal disturbance to the confined rock mass surrounding a tunnel. | $D = 0$ |
|  | Mechanical or hand excavation in poor quality rock masses (no blasting) results in minimal disturbance to the surrounding rock mass. Where squeezing problems result in significant floor heave, disturbance can be severe unless a temporary invert, as shown in the photograph, is placed. | $D = 0$ $D = 0.5$ No invert |
|  | Very poor quality blasting in a hard rock tunnel results in severe local damage, extending 2 or 3 m, in the surrounding rock mass. | $D = 0.8$ |
|  | Small scale blasting in civil engineering slopes results in modest rock mass damage, particularly if controlled blasting is used as shown on the left hand side of the photograph. However, stress relief results in some disturbance. | $D = 0.7$ Good blasting $D = 1.0$ Poor blasting |
|  | Very large open pit mine slopes suffer significant disturbance due to heavy production blasting and also due to stress relief from overburden removal. In some softer rocks excavation can be carried out by ripping and dozing and the degree of damage to the slopes is less. | $D = 1.0$ Production blasting $D = 0.7$ Mechanical excavation |

2.6 Genesis of Methodology for the Present Study

For the present study various literatures were studied in detail to have basic background and frame work on acquiring and understanding engineering geological and geotechnical information from similar projects or sites. Materials for reviewing included under both published and unpublished geological maps, aerial photos, reports, investigation reports of hydropower project (geophysical data and other related secondary data which was valuable for the specific research topic), journals, books and online materials. Literature review work has helped to recognize geological features and geotechnical conditions that may have impact on design and construction of tunneling projects, and it has been the basis for evaluation of the engineering geological conditions along the headrace tunnel. Hence, Wabe hydropower project HRT alignment require surface and subsurface suitability evaluation for planning, design and implementation of engineering structures such as dams, spillways, powerhouses, tunnel alignments, etc. detailed investigation is essential. Because of the aforementioned justifications, a theoretical and/or empirical methodology for evaluation of head race tunnel was initiated. This evaluation was undertaken by using an integrated approach mainly the rock mass classification and remote sensing as a tool.

CHAPTER – 3

STUDY AREA

3.1 Location and Accessibility

The Wabe Hydropower project is found in Welkite, Gurage Zone which is part of Southern Nation Nationality and Peoples regional state (SNNPRS). Geographically the dam site is located approximately at 37°48' longitude and 8° 14' latitude. The project site is accessible via Addis-Welkite-Jima asphalt road and is about 158 km west of Addis Ababa and 3 km south of Welkite Town, on the highway road from Welkite to Indibir (Fig. 3.1). The tunnel alignment lies between 33 ° 48' longitude and 8° 14' latitude at the intake structure and the power house is located at 37° 39' longitude and 8° 13'latitude.

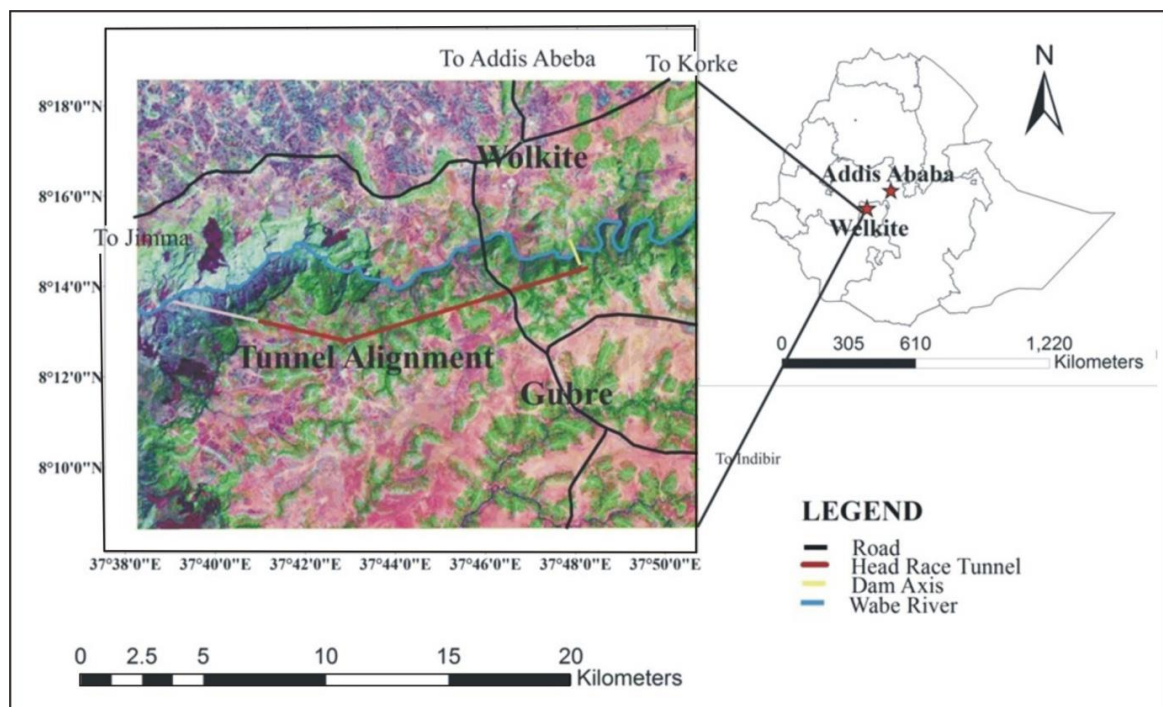


Fig.3.1 Location map of the study area

3.2 Climate

According to Ethiopian Meteorological Agency (EMA, 1981) climate of Ethiopia has been classified based on distribution of land above sea level and the vegetation coverage. The average annual temperature of the study area is 18.6 °C. Long daily precipitation data records are available from seven meteorological stations located in the vicinity of Wabe River catchment. The precipitation data from these stations has many gaps and are not of the same length (Table 3.1). Moreover, some stations are not spatially consistent with the surrounding

Pellic vertisols is the dominant soil type and covers 54% of the catchment followed calcic and eutric fluvisols which covers an area of 13% and 9%, respectively. Eutric nitisols covers the smallest area (0.2%).

Table 3.3 LULC coverage area at different period of time in the Wabe River catchment

| Land use land cover | 1986 | | 2000 | | 2017 | |
|--------------------------|----------|------|----------|------|----------|------|
| | Area(ha) | % | Area(ha) | % | Area(ha) | % |
| Bare land | 9246 | 5 | 12,701 | 6.8 | 6905 | 3.7 |
| Afro-alpine vegetation | 8856 | 4.8 | 5079 | 2.7 | 4700 | 2.5 |
| Built up | 45 | 0.03 | 230 | 0.1 | 801 | 0.4 |
| Cereal crop | 50,431 | 27.1 | 57,407 | 30.8 | 60425 | 32.5 |
| Enset-based agroforestry | 31,431 | 16.9 | 32,405 | 17.4 | 32,684 | 17.6 |
| Forest | 21,072 | 11.3 | 17,425 | 9.4 | 17,259 | 9.3 |
| Grazing land | 46,635 | 25.1 | 34,906 | 18.8 | 36,069 | 19.4 |
| Shrub land | 14,059 | 7.6 | 21,661 | 11.6 | 23,023 | 12.4 |
| Wet land | 305 | 0.23 | 280 | 0.2 | 266 | 0.1 |
| Wood land | 4035 | 2.2 | 4021 | 2.2 | 3983 | 2.1 |

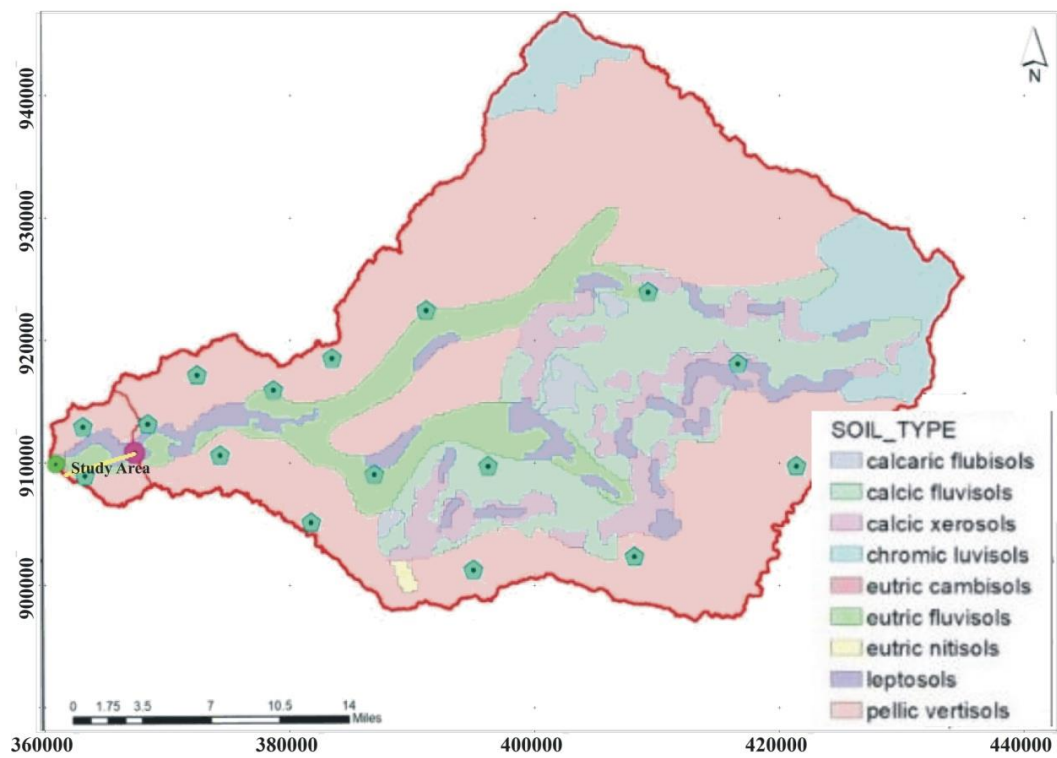


Fig.3.2 Soil types in the Wabe River catchment

3.5 Physiography

Ethiopia is characterized by a wide variety of landscapes and landforms thus; Geomorphology is largely controlled by its geological structure, weathering, erosion, and

deposition processes. The Ethiopian region is formed by three main physiographic provinces: the highlands, represented by the northern and southern Ethiopian plateaus and Somali plateau, the Afar depression, and the MER (Abbate et al., 2015).

The present study area lies in the southwestern highlands which assumes landscape more or less typical mountainous configuration consisting of deep valleys and mountain groups. The north and southeastern sides coincide with the margins of the main and the southern Ethiopian Rift Valley, respectively. The highest mountain peaks are; Mt Gurage (3,721 m.a.s.l.) in the northernmost part, Mt. Guge (4,200 m.a.s.l.) west of Arba Minch and Mt. Malgudo (3,390 m.a.s.l.) southeast of Jimma (Paolo Billi, 2015).

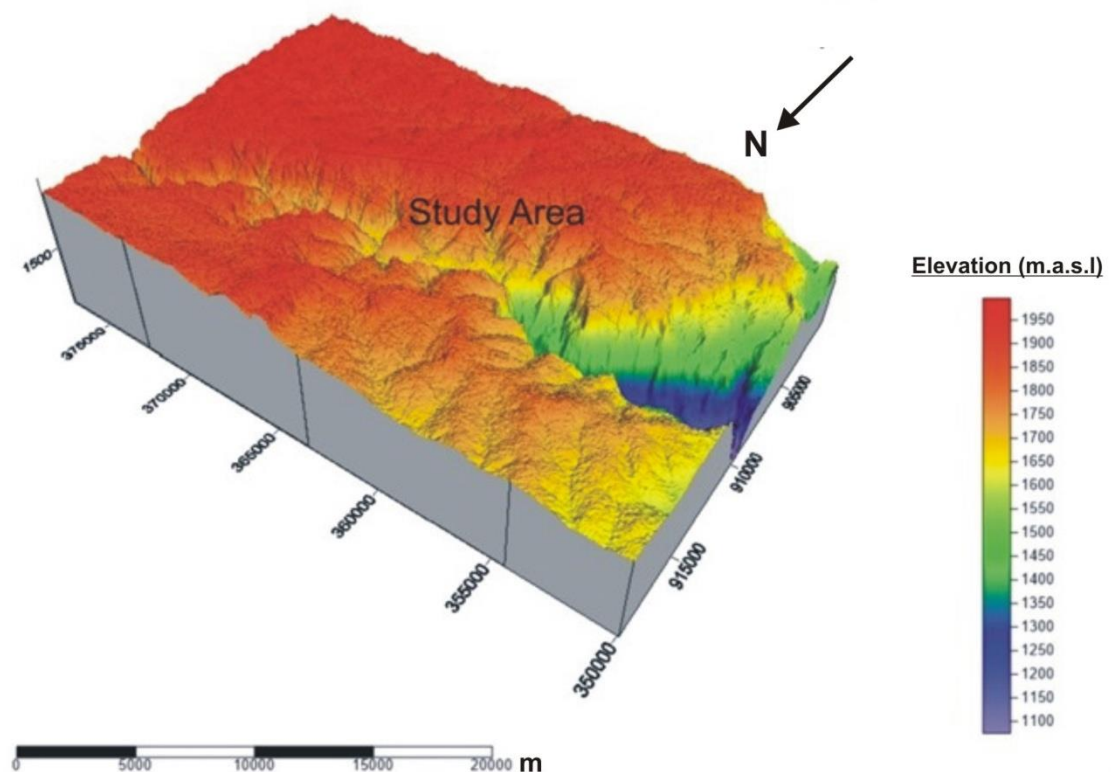


Fig.3.3 Physiographical map of the study area produced by using DEM at 20m resolution

The Wabe Hydropower Project area is located in the upper reaches of Omo-Gibe River basin which is characterized by flat-topped plateau, narrow to wide elevated ridges, low-lying plains and wide to narrow deep valley formed due to dissections of Gibe and Wabe Rivers (Fig.3.3).



Plate 3.1 (a) Photographic view near to the tunnel portal (b) Surge shaft slope

3.6 Salient features of the project and the project status

The Wabe hydropower Dam project is under investigation work and based on information obtained from prefeasibility and feasibility study, the main dam is designed with two dam material zoning alternative design options i.e. Rock Fill with central clay core and Rock and Shell fill with central clay core, with following design features (ECDSWC,2019);

- ✚ Spillway with width; 50m at 1775 m.a.s.l
- ✚ Dead storage level; 1741, 100-year sediment level
- ✚ Normal water level; 1775masl
- ✚ Reservoir Volume at FSL; 528.96 Mm³
- ✚ Reservoir Volume at MWL; 667.03 Mm³
- ✚ Reservoir Area at FSL; 1504.5ha
- ✚ Dam Crest Elevation; 1788 m.a.s.l

This study also has additional simulation that included increasing the spillway crest level to 1790m.a.s.l i.e. 115m above the riverbed. On this the dam crest elevation will be at 1803m.a.s.l. thus, the reservoir capacity at FSL will become 784.71 Mm³ and reservoir area at FSL for this scenario will be 1914.31ha.

Regarding Water way and Power house

For annual mean discharge of 30m³/s the following components are proposed (ECDSWC, 2019).

- ✚ 4m diameter modified-horse shoe shaped tunnel is provided to convey the water to power house. The elevation difference between intake invert level (1741 m.a.s.l) and tail water level (1080 m.a.s.l) is 661m.
- ✚ 17215 m long horizontal tunnel in order to connect power house and intake with vertical shafts of 300 m and 342.20 m.
- ✚ 15821m horizontal HRT with bed slope of 0.1% and 342.2m high vertical shaft.
- ✚ The pressurized penstock is with 3.2m diameter and 1394m long horizontal and 300m vertical shaft tunnel.
- ✚ Total of 3177m length tail race tunnel.
- ✚ Three 1.8m diameter steel pipes through a manifold to join the turbine and each turbine will have an installed capacity of 150 MW.

The present research is conducted when Wabe hydro power project investigation work was under progress. During the present research the project investigation work has been under preliminary feasibility study. Further, before the primary data collection for the present study, the Wabe hydropower project investigation has been under preliminary investigation stage. For this 2D seismic imaging for 17,269m was accomplished along the tunnel alignment. Also, along the tunnel alignment six bore holes have been proposed and all bore holes are located along the HRT alignment except BH-16. Out of bore holes along HRT alignment, BH-9 and BH-13 were completed and the remaining were under progress (BH-12 and BH-13) and were not completed during the present study. For this study, information from boreholes as a primary and seismic imaging and, preliminary investigation reports made by ECDSWC in 2019 (as secondary data) were utilized as mentioned in section 2.4.

3.7 Regional Geology and Tectonic Setting

3.7.1 Tectonic Setting

According to [Abbate et al. \(2015\)](#) geodynamic and geomorphic processes result have shaped the birth, evolution and present day morphology/spectacular land scape of Ethiopia since the Oligocene. These processes, which came relatively late in the one-billion-year geological history of East Africa, were triggered by the impingement of a mantle plume or plumes under the Afro Arabian continental crust. The plume action gave rise to extrusion of huge amounts of magma, uplift, and fragmentation of the continental crust and contributed to the birth of the Red Sea, Gulf of Aden, East Africa Rift valley, and the adjoining Afar depression. Further, according to [Abbate and Sagri \(1980\)](#) the volcanic rocks that cover most of Ethiopia

have been subdivided into five major provinces on the basis of their lithological development, type of activity, frequency of volcanic centers, and age of effusion (1) the northern plateau volcanites; (2) the southern plateau volcanites; (3) the Somali plateau volcanites; (4) Afar volcanites; and (5) Main Ethiopian Rift (MER) volcanites (Merla et al., 1979).

3.7.2 Regional Geology

The Study area is formed on the transition of north western plateau to the south western plateau volcanites which is marked by a 700 km long and 80 km wide east–west trending volcano-tectonic alignment (Addis Ababa-Nekempt line in Abbate and Sagri, 1980; Yerer-Tullu Wellel alignment, (Abbate et al., 1998) consisting of a line of Late Miocene to recent volcanic centers gradually shifting in age from Late Miocene in the west to Quaternary in the east (Abbate et al., 1998). Northern Ethiopian plateau has peculiar feature of the frequent occurrence of shield volcanoes, about 30 major centers according to Mohr and Wood (1976), some of which reach as much as 100 km in diameter and 1,000–2,000m in elevation above the plateau (e.g., Semien, Guna, Choke, and Gugufu). Based on Blanford's (1870) the northern plateau volcanites were subdivide into a lower Ashangi Group unconformably overlain by a Magdala Group. Moreover, Zanettin and Justin Visentin (1973), Gregnanin and Piccirillo (1974) have proposed detailed litho stratigraphic approach with the distinction of the Ashangi and Aiba basalts, Alaji Rhyolites, and Tarmaber Basalts. Near to volcanic centers thickness of Tarmaber basalts reaches 1,000 m. They are made of lenticular, often zeolitized, alkali basalts with a large amount of tuffs, scoriaceous lava flows, peralkaline rhyolites, and typical red paleosoils.

The Southern Ethiopia Plateau traps are less thick than those of the northern plateau and are characterized by much thicker and more widespread siliceous rocks. They are resting directly on the crystalline basement or, more rarely, on the Eocene basalts and Mesozoic sandstones. Merla et al. (1979) subdivides the southwestern Ethiopia flood basalts into three stages: - (1) the Omo Basalts (40 to 25 Ma), (2) the Jimma Volcanics (30 to 21 Ma) and (3) the Wollega Basalts (15 to 7 Ma). Davidson and Rex (1980) also recognized three units of these flood basalts: - (1) the Main Volcanic Sequence (49.4 to 30.5 Ma), (2) the Makonen Basalts (32.8 to 21.2 Ma), and (3) a Post-rift sequence (13.0 Ma to present day).

The succession begins with a hundred meters of mildly alkaline basalts (Omo Basalts), capped by a thick unit, up to 1,000 m, of rhyolites, acidic tuffs, and subordinate basalts (Jima Volcanites). The Omo Basalts are commonly fine grained with columnar flows up to 10 m

thick alternating with minor tuffs and red paleosols. There are some sparse dates ranging around 30 Ma (Merla et al., 1979; Davidson and Rex, 1980). Further, the Jima Volcanites, reaching one thousand meters of thickness in the Omo valley, represent most of the effusive in southwestern Ethiopia with a wide fringe in the southern portion of the Somali plateau northwest of the Amaro Mountain and south of the E–W Bonga–Goba lineament (Abbate and Sagri, 1980).

Efrem Beshawered (2010) presented the regional geology of the study area in 1:250,000 scale geological mapping of Akaki map sheet (Fig. 3.4). Accordingly, the Cenozoic Volcanic is classified in to 1) Jimma volcanics, 2) Makonen basalts, 3) Tarmaber Megezez Formation, and 4) Nazret pyroclastic. The study area is formed on Jimma lower basalt (E2jl), Tarmaber Megezez Formation (E3tm) and Welded to Partially Welded Pyroclastic Flows (Npp).

3.7.2.1 Jima Lower Basalt (E2jl)

This unit is mapped by Efrem Beshawered (2012) as the oldest unit and covers the flat lying plateau, often tilted (Fig.3.4). It also developed a horizontal stratification with intense hexagonal columnar jointing. The rock is characterized by dark-grey medium to coarse grained and partly weathered.

3.7.2.2 Tarmaber Megezez Formation (E3tm)

This unit is dark grey in fresh samples, but reddish brown in weathered specimens. It is fine-grained volcanic rock composed of plagioclase, pyroxene, and opaque minerals (Efrem Beshawered, 2012).

3.7.2.3 Welded to Partially Welded Pyroclastic Flows (Npp)

It is light to dark-grey in fresh samples and reddish to yellow to pink in weathered ones. It is fine grained; densely welded rock containing vitro phytic fiamme and lithic fragments with associated rhyolitic lava flows interleaved with ash and un-welded tuffs (Efrem Beshawered, 2012).

3.7.3 Regional Geological Structure

The study area is situated in the vicinity of the active tectonic zone of the East African Rift System (Giday Woldegebriel and Aronson, 1990). The E-W rift transversal structure called Addis Ababa-Nekemte tectonic line (Abbate and Sagri, 1980). Or Yerer-Tulu Wollel Volcano Tectonic Lineament (YTVL); Abebe Tesegaye et al., 1998) separates the

Southwestern Ethiopia plateau volcanics in the north from the Northwestern Ethiopia Plateau volcanics. Structural sketch map of the Ethiopian and Somali plateaus, Afar depression, and Main Ethiopian Rift is presented in Fig. 3.5 (Abbate et al., 2015).

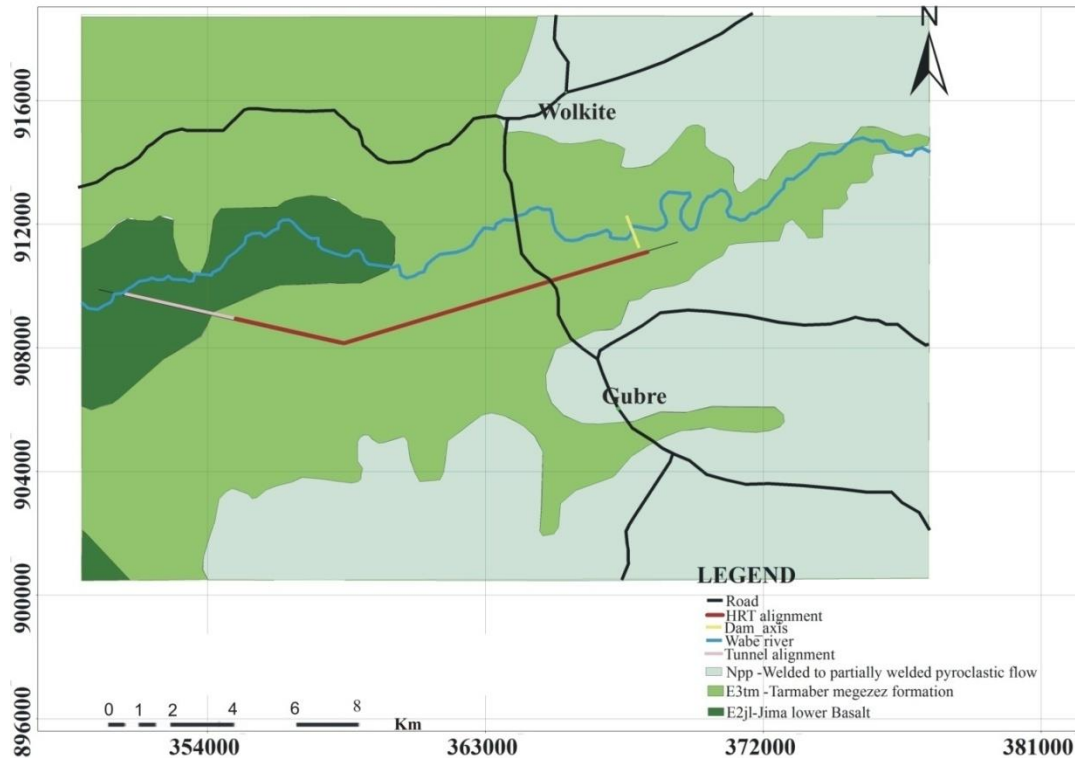


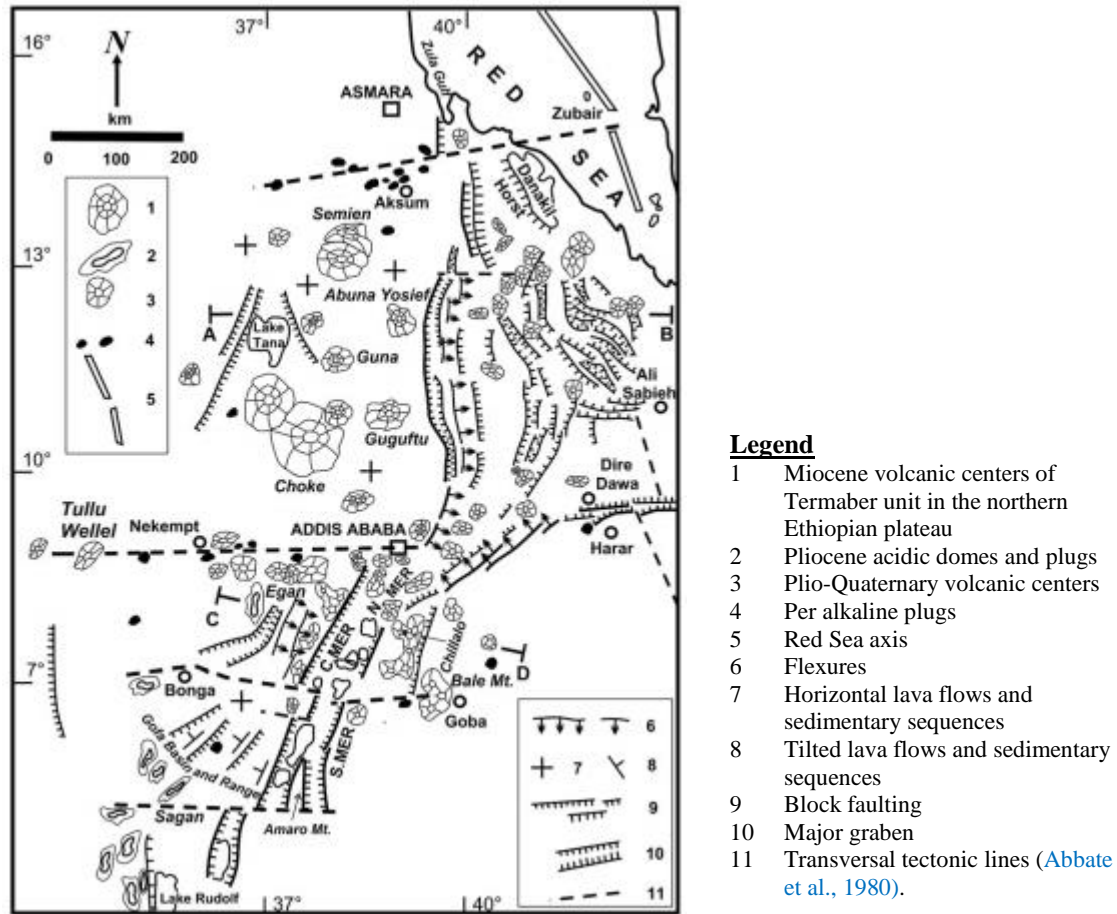
Fig.3.4 Regional Geologic Map of the study area (simplified after Ephrem Beshawered, 2012, Ethiopian Institute of Geological survey)

3.8 Geology of the Study Area

Geological mapping of the study area was undertaken by reviewing and modifying previously available geological maps i.e. Akaki Beseka sheet that was mapped by Ephrem Beshawered (2012) and geological map of Wabe hydropower project site that was prepared by ECDSWC (2019). Based on information gathered from previous works and from the field visit, Geological mapping of the study area was carried out at offset of 500 m from headrace tunnel alignment. Accordingly, different mappable rock unit was identified (Fig. 3.6).The local geology of study area is mainly covered by the following mappable rock units;

3.8.1 Superficial Deposits (Qal)

These units are silty clay quaternary alluvial deposits and encountered mostly on the root of gentle sloped hills and flat portions of the study area. They are dark brown in color and black cotton soil with light density or less compacted property.



(Source: Abbate et al., 2015)

Fig.3.5 Structural sketch map of the Ethiopian and Somali plateaus, Afar depression, and Main Ethiopian Rift (Northern, Central, and Southern MER) with the main transversal tectonic line and major volcanic edifices (modified from Abbate, E. and Sagri, M., 1980)

3.8.2 Ignimbrite and Tuff (IT)

This unit encompasses ignimbrite and tuff. The tuff is grayish white massive to rarely bedded and exposed as grey to light grey, and massively bedded with agglomerate that consists of angular to sub angular fragments of mainly basalt. Ignimbrite represent the dominant part of the unit of brownish and grayish green, crystal rich commonly contains crystals of quartz, and trace mafic minerals. The ignimbrite unit is exposed as extensive exposure in the inlet area of the tunnel and few exposures along the headrace of the tunnel.

3.8.3 Basalt (BA_5)

It is mainly comprised of fresh to slightly weathered porphyritic (plagioclase) basalts with subordinate aphanitic basalt and minor layers of amygdaloidal basalts. This rock is exposed on the upper portion of the study area by forming plateau and the average thickness reaches 65 m. This unit is also encountered as columnar basalt in some locality.

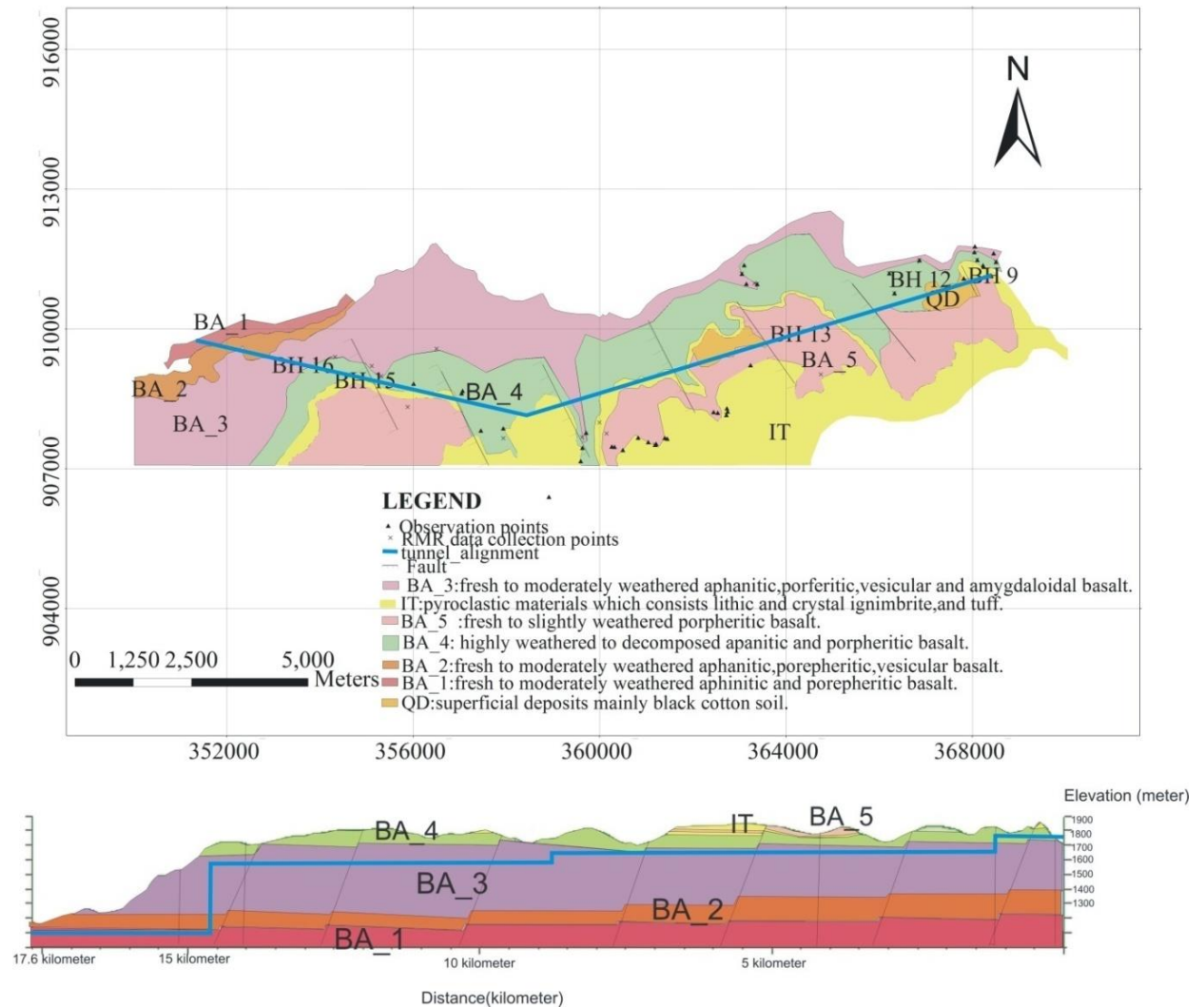


Fig.3.6 Geological map (above) at offset of 500 m from headrace tunnel alignment (HRT) and Cross section (below) along HRT alignment

3.8.4 Basalt (BA_4)

This rock unit is moderately weathered to completely weathered aphanitic, porphyritic and vesicular basalt that is exposed in flat topped plateau covering extensive area of the Head race tunnel (HRT) alignment. It is unconformably overlies unit BA_3 and underlies unit BA_5. A laterite horizon separating the flow from the underlying basalt flow of unit BA_3, and a pyroclastic deposit (IT) is separating this flow from the overlying basalt flow of unit BA_5.

3.8.5 Basalt (BA_3)

This rock unit consists of fresh to moderately weathered aphanitic and porphyritic (plagioclase) basalts, which attains a maximum thickness of 250m. Almost all portions of

HRT length will be drives through this rock unit. The aphanitic basalt, which represents the largest part of the succession, is dark grey and grayish black, fresh to slightly weathered massive to weakly jointed. Porphyritic (plagioclase) basalts observed towards the top part of the succession as inter layers measured in thickness up to 10m; generally weakly to moderately jointed.

3.8.6 Basalt (BA_2)

This map unit is comprised of fresh to slightly and moderately weathered inter-layered phyric (plagioclase) basalt and aphanitic basalt with subordinate vesicular basalt, which attains a thickness of 70-100m. The phyric (plagioclase) basalt is slightly weathered to fresh and frequently observed a sinter-layered with the aphanitic basalt, which attains a thickness of 5-10m (ECDSWC, 2019).

3.8.7 Basalt (BA_1)

Based on ECDSWC (2019) this map unit is exposed in the river bed of Wabe River, which is composed of aphanitic and phyric (plagioclase) basalts which attains an exposed thickness of 10 to 30m. Aphanitic basalt is the dominant rock type and is fresh, grayish black, and commonly massive, however at places, it is jointed with joints striking west-northwest and east-northeast.

3.9 Structure of the study area

The structures in the Wabe hydropower project area are characterized by brittle deformation, which has resulted in the development of fractures, faults and joints. The normal faults are striking northwest and southwest-dipping (65-80°), characterized by vertical displacement (throw) measured between 10 and 20m. They are commonly filled with iron oxides and clays, however at places they are also filled by silica veins.

3.10 Groundwater/regional hydrogeology

The most important work in understanding the regional hydrogeology of the area is the review of the 1:250,000 scale hydrogeological mapping made on the Akaki map sheet by Ephrem Beshawered (2012). This map has characterized the Wabe Hydropower Project area as area of shallow groundwater of fractured aquifers (ECDSWC, 2019). Interception of ground water is one of the major challenges faced during the excavation of the tunnel. Ingress of ground water during tunneling may result in face and roof collapse hampering the progress

(Sharma and Tiwari, 2015). High pore pressure behind the tunnel periphery may also adversely affect the support system and cause its failure (Maurya et al., 2010).

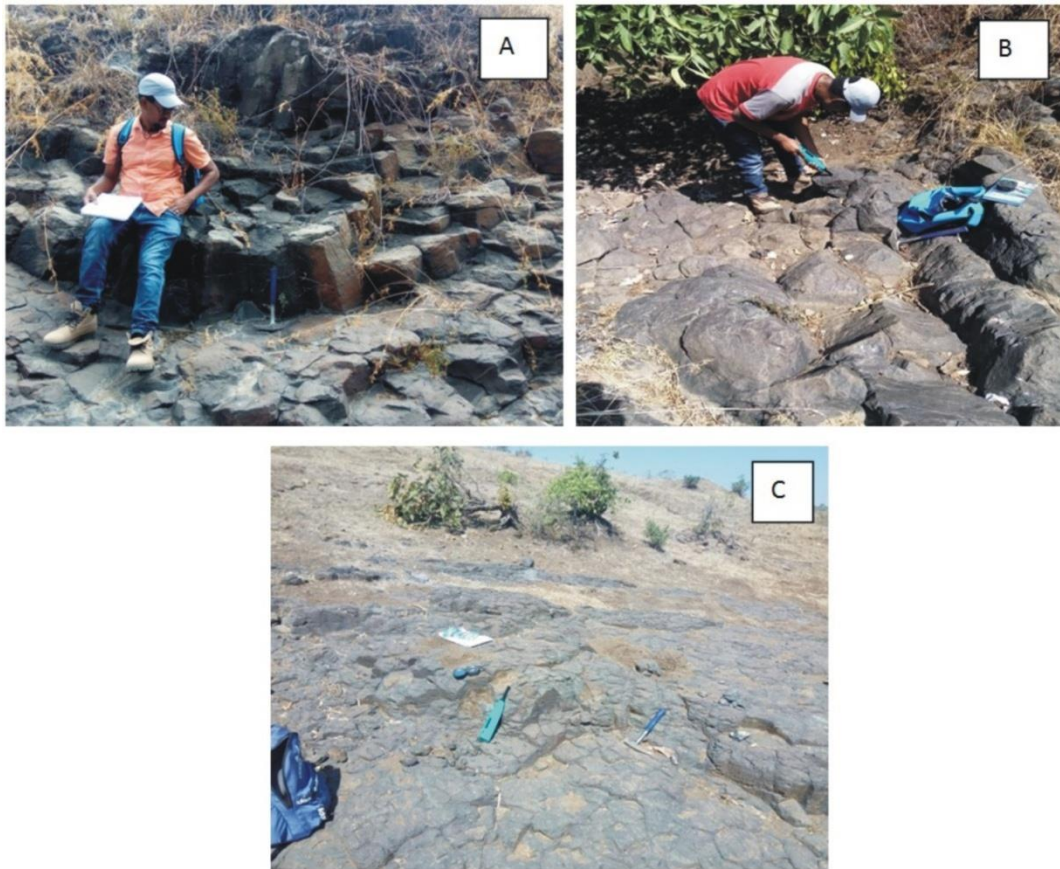


Plate 3.2 Rock units exposed in the study area. (A) Fresh columnar basalt mapped as BA_3 rock unit (Fig. 3.5) (B) Closely jointed fresh basalt mapped as rock unit BA_3 (Fig. 3.5) and (C) Fresh basalt exposure mapped in BA_5 rock unit (Fig. 3.5).

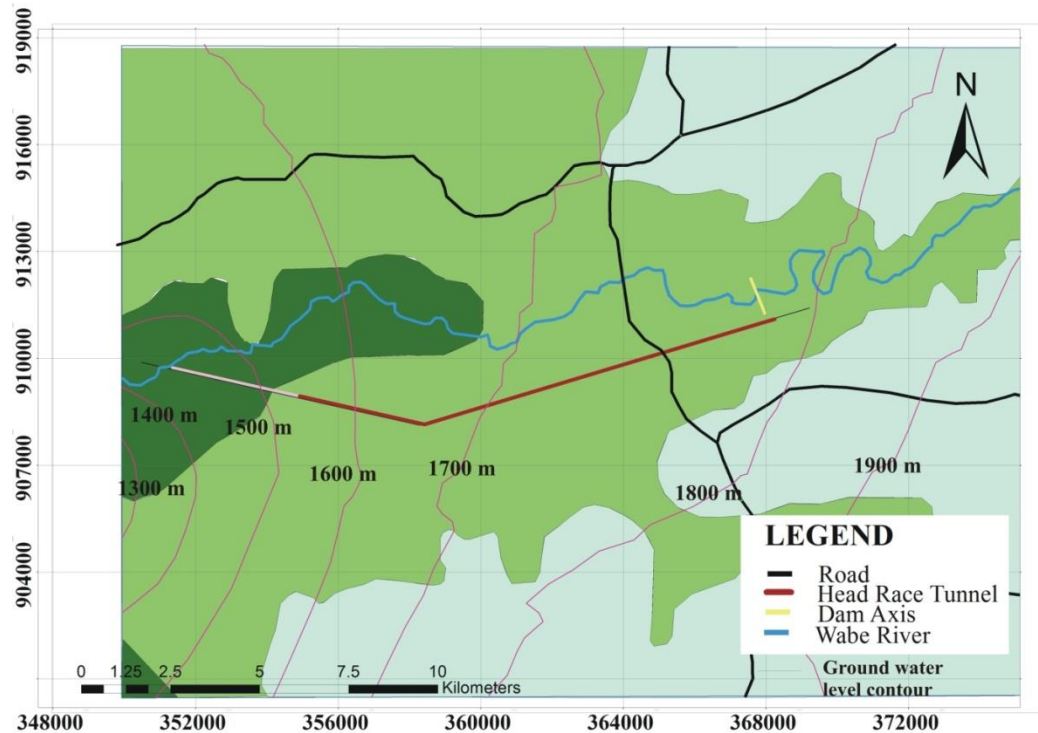


Fig.3.7 Geological map of the area (simplified after [Efrem Beshawered, 2012](#))

3.11 Seismicity

The seismic hazard can be defined as the probability that a ground motion at a specific site will be exceeded during a time period, i.e. return period, T (years). Alternatively, it is the probability that a ground motion will be exceeded with an annual frequency of $1/T$. Seismic hazard due to natural earthquakes is, rather haphazardly, presented as the probability that a Peak ground acceleration (PGA) will be exceeded in T years ([Bommer and Pinho, 2006](#); [GSHAP, 1999](#)). Earthquakes occur along the Ethiopian rift system. Fig. 3.8 (a) depicts the seismicity of the Horn of Africa region by mapping the earthquakes that have occurred in the region from 1900 to 2010 ([IGSSA, 2018](#)). In Fig.3.8 (a), the sizes of the red dots represent the magnitude of earthquakes ranging from 3.5 to 7.2. The yellow stars are the major towns in Ethiopia, revealing that the seismic areas are often inhabited areas. The study area lies on Central Main Ethiopian Rift (CMER) which west of the seismically active Gurage Border Fault or Gurage Mountain. It is close to the active rift margin where destructive earthquakes are common and in 2015 there was a swarm of earthquake close to the dam site with maximum magnitude 4.0 ([IGSSA, 2018](#)).

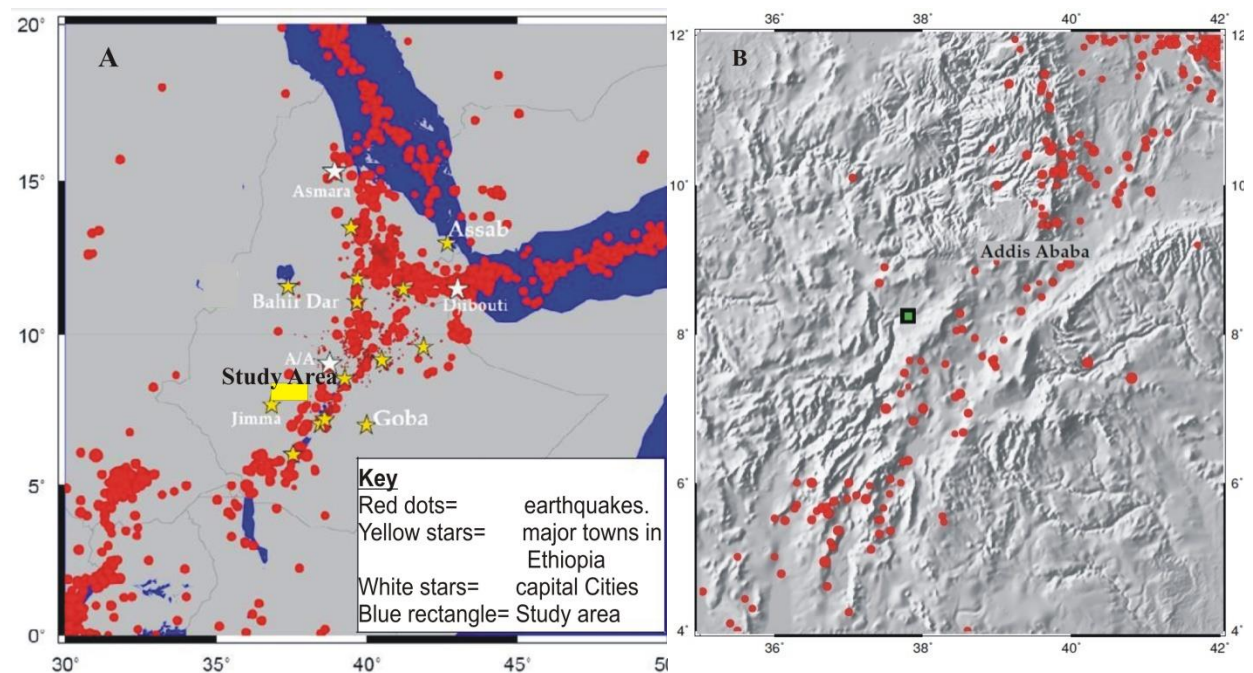
According to [Geremew Lemessa et al., \(2019\)](#) CMER has a-value = 4.33 and b-value = 0.826, magnitude of Completeness (M_c) = 3.1 and, period of completeness from 2001 to

2003 are determined. These authors also concluded low b value anomalies indicate low activity (high stress region). According to IGSSA (2018), the Wabe Hydropower dam site is a point of concern as it is located in the western margin of the Gurage border fault which is close to the active rift margin. As shown in Table 3.4, for 0.2 second period and for both rock and soil sites and by considering all return periods, Wabe dam site has relatively higher hazard values.

The value of b becomes less from 7 km depth beneath the Gurage Border Fault (see Fig. 3.9) which means that the Gurage Border Fault exists only up to a depth of 7 km (Geremew Lemessa et al., 2019).

Table 3.4 Wabe Hydropower Project site Ground motion amplitude determination for rocks and soils (Sources :ECDSWC, 2019)

| Return Period Years | in | Ground Motion Amplitude in % of g for Boore-Joyner-Fumal (1993, 1997) | | | | | |
|---------------------|----|---|-------|-------------------|-------|------------------|------|
| | | Period = 0.2 sec | | Period = 1.0 sec. | | Period = 2.0 sec | |
| | | Rock | Soil | Rock | Soil | Rock | Soil |
| 100 | | 9.39 | 9.91 | 4.32 | 4.81 | 2.96 | 3.26 |
| 500 | | 16.29 | 17.41 | 6.44 | 7.27 | 4.28 | 4.78 |
| 1,000 | | 20.55 | 21.82 | 7.65 | 8.68 | 5.03 | 5.65 |
| 2,500.0 | | 26.68 | 28.54 | 9.60 | 10.97 | 6.20 | 7.03 |



Source; (a) Atalay Ayele (Addis Ababa University), via private correspondence on 15 January 2014, based on data from: Institute of Geophysics Space Science and Astronomy of Addis Ababa University; United States Geological Survey; and International Center of Seismology in UK. (b) Atalay Ayele (Addis Ababa University), via private correspondence on 15 December 2018, based on data from: ECDSWC (2019).

Fig.3.8 (a) Earthquakes recorded in the Horn of Africa region from 1900 to 2010. (b) Seismicity data for the Addis Ababa region and the Wabe project site; red circles represent earthquakes that occurred for the last 110 years in the region and size of the circles is proportional with magnitude. The green rectangle shows the locations of the planned Wabe Hydroelectric power project site.

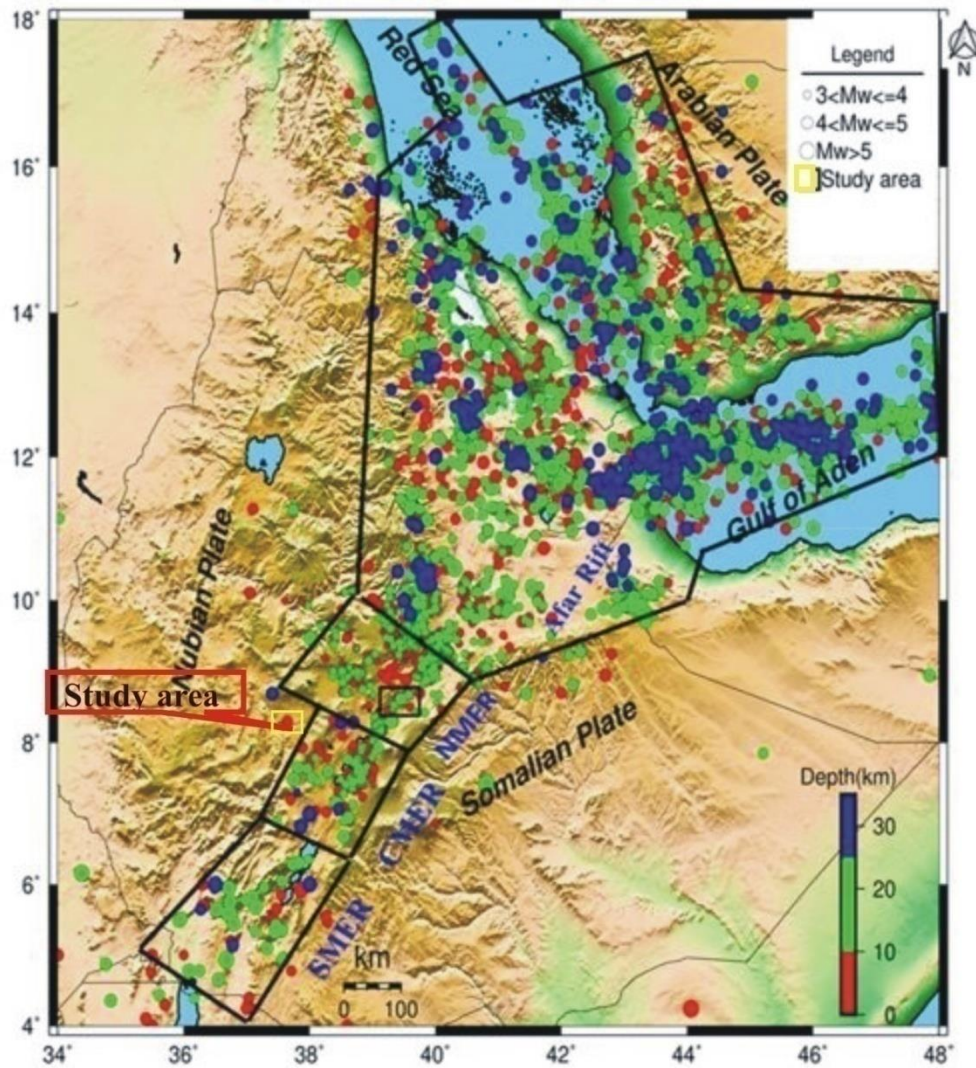


Fig.3.9 Seismicity Map of Ethiopian Rifts (Including Red Sea and Gulf of Aden rifts) from the new catalog. The legend color bar on the right bottom of the map indicates the Hypocentral depths variations of Earthquake. The rectangular legend on the top right of the map indicates the size of the Earthquakes magnitude's ranges in Moment magnitude scale in the regions (After Geremew Lemessa et al., 2019)

CHAPTER – 4

DATA COLLECTION

4.1 Preamble

For the present study, data was collected from field as well laboratory testing and analysis was conducted. Data used in this study can be considered as primary and secondary data. Primary data includes data obtained from core logging, surface mapping as well as data generated through laboratory tastings on representative samples. Secondary data sources include databases such as; geophysical data obtained from [ECDSWC \(2019\)](#) aerial photos, technical journal articles, geological map, reports and DEMs (Fig.4.1).

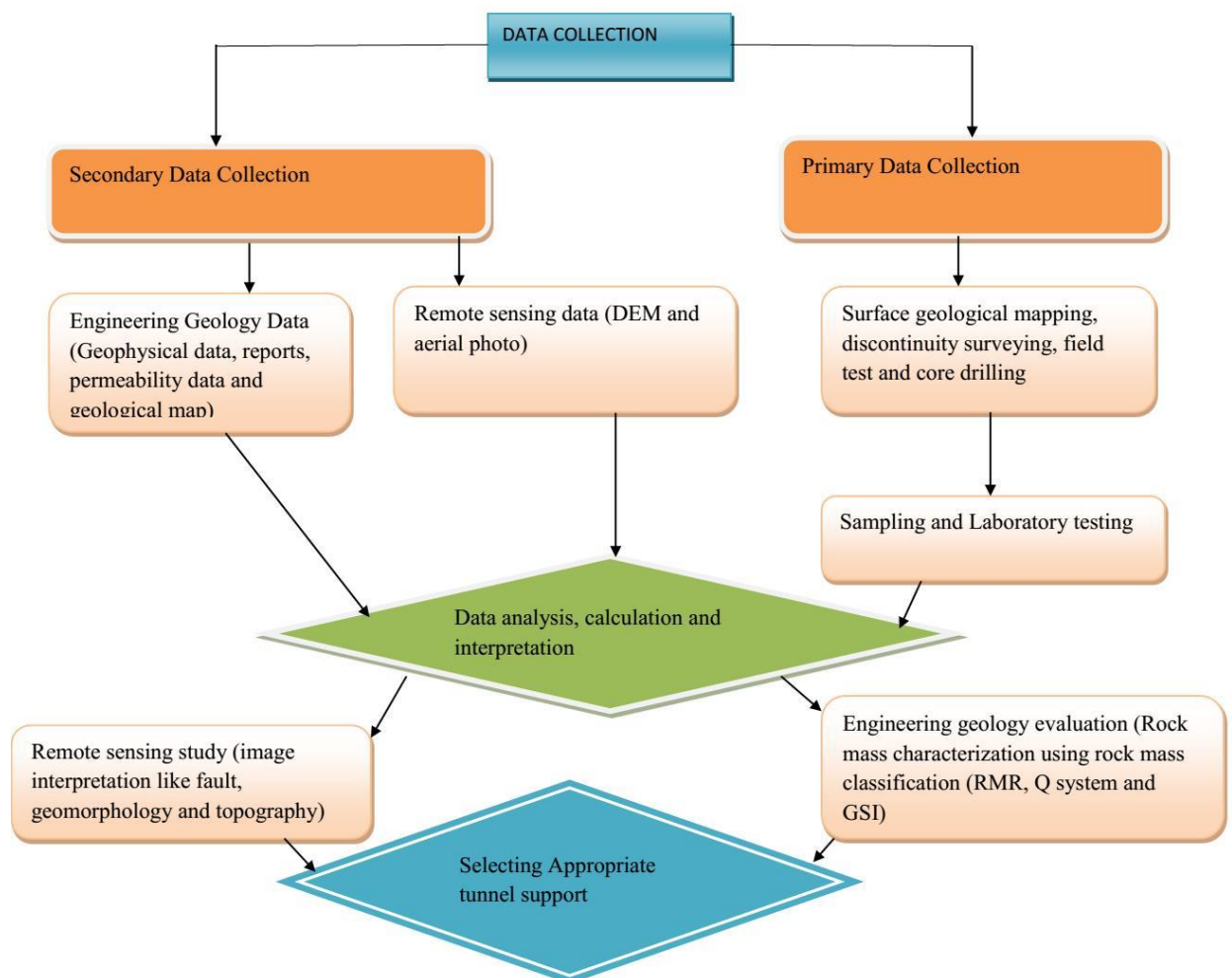


Fig.4.1 Procedures used for Data collection and interpretation

4.2 Secondary Data Collection and Study

4.2.1 Geophysical Study

For the present study geophysical data was procured from ECDSWC. 2D Electrical resistivity imaging was used for preliminary investigation at Wabe Hydropower site ([ECDSWC, 2019](#)).

The geophysical survey works at the project site was carried out with objectives to know: (i) the thickness of overburden/depth of bed rock, (ii) Lateral and vertical variation of subsurface stratification, (iii) the Ground water condition, (iv) the presence and extent of seams (shear zones, fault zones, etc.) and (v) the information for borehole locations and adjustment of boreholes based on information.

4.2.1.1 2D- Electrical Resistivity Imaging/Electrical Resistivity Data Collection

On the basis of proposed survey line a total length of 18500m with 190m depth of investigation the resistivity imaging was conducted to characterize the geological features of foundation of the structure. The coordinates and work volumes corresponding to each resistivity imaging survey lines are presented in Table 4.1.

Table 4.1 coordinates and work volumes of resistivity imaging survey lines

| No. | Survey line | Coordinates (UTM) | | | | Length of survey line (m) | Depth of investigation (m) |
|-------|-------------|-------------------|----------|---------|----------|---------------------------|----------------------------|
| | | Starting | | Ending | | | |
| | | Easting | Northing | Easting | Northing | | |
| 1 | Line-1 | 368389 | 911141 | 364935 | 910091 | 3611 | 190 |
| 2 | Line-2 | 364773 | 910052 | 361310 | 909014 | 3476 | 190 |
| 3 | Line-3 | 361717 | 909138 | 358218 | 908193 | 3208 | 190 |
| 4 | Line-4 | 358503 | 908170 | 354127 | 909118 | 4199 | 190 |
| 5 | Line-5 | 354555 | 909021 | 351568 | 909698 | 2775 | 190 |
| Total | | | | | | 17,269 | |

Geophysical exploration consists of making indirect measurements from the earth's surface or in boreholes to obtain subsurface information (EM 1110 - 2 - 1804). Accordingly, for the present study geophysical data was utilized by calibrating it from geological features (such as, stratigraphy, lithology, discontinuities and ground water) explored from surface and boreholes data.

4.2.2 Remote Sensing Study

For the present stud remote sensing application was carried out in order to have a general idea of major structural features of rocks, such as faults, shear zone, major joints, fractures and others in the vicinity of the tunnel alignment. To over view the terrain condition of the study area, remote sensing techniques was used. For these purpose DEM with resolution of 20 m (obtained from EMA) was utilized in order to generate ridge lines, drainage map and for identification of geological structures. In addition, Google earth image and geological map with the scale of 1:5000 (obtained from ECDSWC, 2019) were used for terrain view, and geological structure identification.

Software such as Arc GIS 10.3, Surfer 10 and Global mapper 15 were utilized for the present study in order to analyze surface characteristics like topography/morphology, slope, aspect faults and fractures.

According to [Gupta \(2018\)](#) remote sensing application for tunnels need to have subsurface data obtained through drilling, trenching and it is necessary that the geotechnical features or conditions of the rock mass (shear zones, faults, joints, bedding, rock types, groundwater conditions etc.) as observed in the field, interpreted from satellite images and or deduced from drilling, are integrated and projected to tunnel axis for their proper appraisal. So, for the present study, electrical imaging and geological features were later integrated with the remote sensing study.

4.2.3 Permeability Test

In-situ falling head and packer permeability tests were carried out by ECDSWC in soil and rock mass respectively in borehole. The test procedure was undertaken in accordance to the British Code of practice for site investigation ([BS 5930, 1999](#)).

4.2.3.1 Packer Test

Single packer permeability tests were conducted for rock mass sections of the drilled boreholes, where required. For the present study a total of 6 tests from BH-9 and BH-13 were used as secondary data.

The testing method consisted of five consecutive tests or runs, each of ten or five-minute duration, and with a particular corresponding pressure magnitude. The five testing pressures were applied in the order of A-B-C-B-A with increasing and decreasing sequences where, C, stands for the peak applied testing gauge pressure, B, moderate applied testing pressure and equals two-third of the peak applied pressure and A, low applied testing pressure magnitudes and equals one- third of the testing peak gauge pressure. The peak applied testing gauge pressure was obtained after deducting the borehole mid height water column pressure (above groundwater table) from the total testing pressure (0-1 to 0.2bar/m), computed for borehole depth measured to the bottom of test sections.

Table 4.2 Pressure magnitudes typically used for each test stage

| Test Stage | Description | Pressure Step |
|-----------------|-------------|-------------------------|
| 1 st | Low | 0.50 * P _{MAX} |
| 2 nd | Medium | 0.75 * P _{MAX} |
| 3 rd | Peak | P _{MAX} |
| 4 th | Medium | 0.75 * P _{MAX} |
| 5 th | Low | 0.50 * P _{MAX} |

The length of test section was in the range of 3.5 - 5 m. HQ and NQ size pneumatic packers were used in a wire-line drilling system and corresponding borehole diameters.

The resulting Lugeon values of tested sections for each run pressure were computed on the basis of the relation given by [Houlsby \(1976\)](#) (eq. 4.1)

$$(Lu) = (10*Q)/P*L \quad \dots\dots\dots\text{eq. 4.1}$$

Where, ‘Q’ is the average water intake in Lit/minute, ‘P’ is the total testing pressure in bars and ‘L’ is the Length of the tested section in m.

The selection of the representative Lugeon value for the test section was on the basis of plotted flow pattern and guides provided by [Houlsby \(1976\)](#). Accordingly, the reported representative Lugeon value is taken to be the average of the five run values for laminar flow pattern, the average of Lugeon value corresponding to 2nd and 4th testing pressures for Dilation flow pattern, Lugeon value corresponding to peak pressure for Turbulent flow pattern, and Lugeon value corresponding to peak pressure was taken for Turbulent flow pattern, and Lugeon value corresponding to last testing pressure was considered for void filling and washout flow patterns. The corresponding test section permeability (k) value was obtained from the relation that 1Lu units is approximately equals to 1.31×10^{-5} cm/sec.

4.2.4 Groundwater Condition

The groundwater level measurement was taken during the start and completion of daily core drilling activity of a borehole. Ground water table was obtained from three boreholes (BH-9, BH-13 and BH-15) and also from hydrogeological mapping that was made on the Akaki map sheet by [Ephrem Beshawered \(2012\)](#).

4.3 Primary Data Collection/Engineering Geology

The general objective of a site investigation is to assess the suitability of a site for the proposed purpose that involves exploring of surface and sub-surface ground conditions

(Anon, 1999). Hence, it was carried out with strict procedures and integration of results obtained through various methodologies followed in order to obtain the required geological and geotechnical data for planning the development of hydropower headrace tunnel.

Accordingly, for the present study, investigation of the rock mass quality along the headrace tunnel was done based on surface and sub-surface investigations.

Geological mapping of the study area was carried out by reviewing and verifying the previously conducted geological map. This map was done by reviewing and modifying Akaki Beseka sheet that was mapped by GSE (2012) and geological map of Wabe hydropower project that was prepared by ECDSWC (2019).

4.3.1 Geological and Structural Data Collection

4.3.1.1 Geological Mapping

Based on the information gathered from previous works and result of remote sensing evaluation field visit for detailed field geological mapping of the study area was carried out at offset of 500 m from the tunnel alignment at a scale of 1:5,000. Accordingly, different mappable rock units were identified. The geological description (or rock formations) of the rock mass intercepted has provided critical information in the understanding of the characteristics of the rock mass. Besides, it also helped to understand the geological processes. More than 46 rock joint orientations data were collected. Later, structural analysis has been done by using Rock Science software and the results obtained are presented in chapter 5.

4.3.1.2 Discontinuities Survey

Since the physical and mechanical properties of rock masses show substantial changes during the excavation period, parameters which have significant influence on the rock mass properties are determined according to the standard proposed by ISRM (1981) (Table 4.3). The discontinuity data was collected from the field on predesigned recording data sheets. Discontinuity characteristics such as; Orientations, separations, infillings, roughness and many of describing properties of discontinuities are very crucial for description and classification of rock mass (Bieniawski, 1993). Also, they have direct implications on the design stages of the engineering applications (Hoek, 2007 and Syed, 2017). Accordingly, more than 46 discontinuities were recorded and the recorded information was used to assess

the rock mass quality. Later, Rock Mass Rating (RMR) by Bieniawski (1989), Tunneling quality index (Q -system) by Barton et al. (1974), and Geological strength index (GSI) by Hoek et al. (1997-1998) systems were used (Appendix A Fig A-A and A-2).

Table 4.3 Description of degrees of weathering (ISRM, 1981)

| s.n | Term | Description |
|-----|----------------------------|--|
| 1 | Fresh | No visible sign of rock material weathering; perhaps Slight discoloration on major discontinuity surface |
| 2 | Slightly | Weathered Discoloration indicates weathering of rock material and discontinuity surfaces. All the rock material may be discolored by weathering |
| 3 | Moderately weathered | Less than half of the rock material is decomposed or disintegrated to a soil. Fresh or discolored rock is present either as a continuous framework or as core stones |
| 4 | Highly weathered framework | More than half of the rock material is decomposed or disintegrated to a soil. Fresh or discolored rock is present either as a discontinuous or as core stones |
| 5 | Completely weathered | All rock material is decomposed and or disintegrated to soil. The original mass structure is still largely intact |
| 6 | Residual soil | All rock material is converted to soil. The mass structure and material fabric are destroyed. There is a large change in volume, but the soil has not been significantly transported |

Further, in order to estimate the strength of the rock Schmidt hammer rebound hardness tests were undertaken by using N type Proceq H, Silver schmidt hammer on rock outcrop sections (Plate 4.1 (b)). The Silver Schmidt hammer is an integrated electronic device that measures the true rebound coefficient, the so-called “Q”-value (eq.4.2) and it represents the physical rebound coefficient. This value needs no correction for the impact direction which means there is no need to refer to impact direction conversion curves as required with all other test hammers (http://www.proceq.com/proceq_silverschmidt_user_manual_en).

$$Q = 100 * \frac{\text{Energyrestored}}{\text{Energyinput}} \quad \dots\dots\dots\text{eq. 4.2}$$

For the present study 17 stations of rock exposure surface were selected for Schmidt hammer rebound test. To get Schmidt hammer rebound coefficient (Q), initially ten impact readings were undertaken in each case, and the mean value was taken based on ASTM C805 -97 and estimation of the compressive strength is made on the basis of conversion curves as shown in Fig. 4.2.

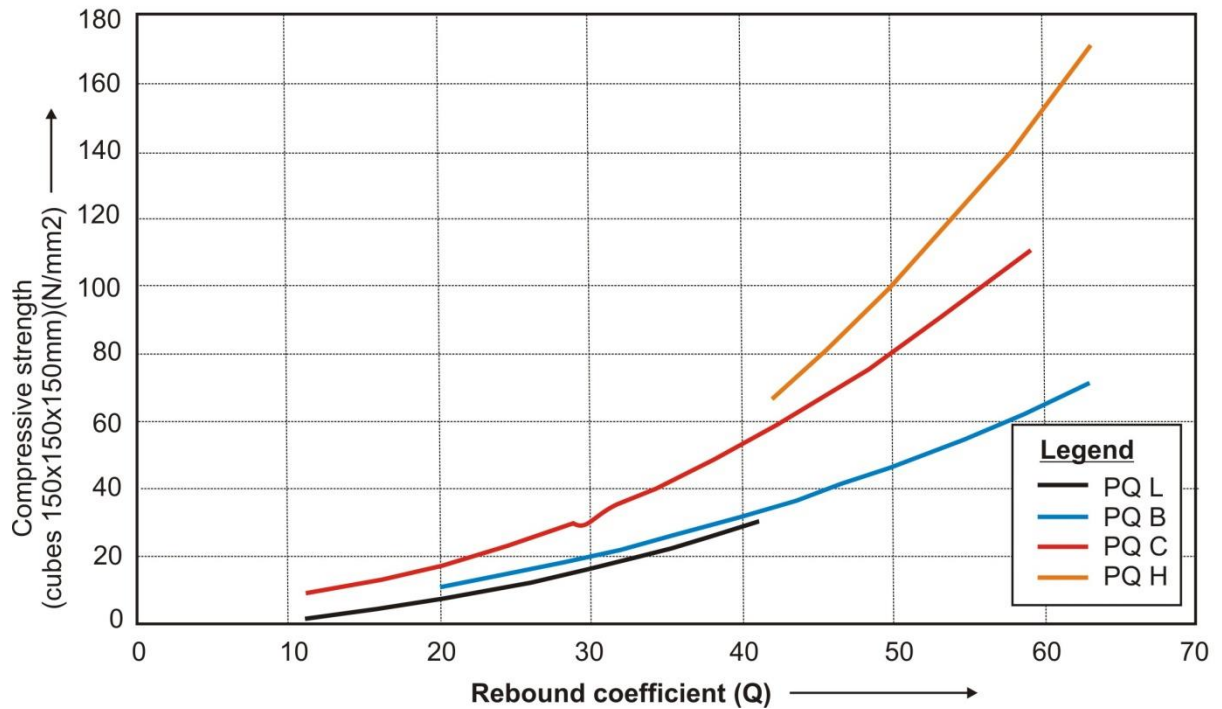


Fig.4.2 BN- Hammer Conversion curve for N type Silver Schmidt hammer (from silver Schmidt operating instructions) (Source: http://www.proceq.com/proceq_silverschmidt_user_manual_en)

Table 4.4 Summary of location for Schmidt hammer data collection.

| S.N | EASTING | NORTHING | ELEVATION | LITHOLOGY | REMARK |
|-----|---------|----------|-----------|-----------|--------|
| 1 | 354276 | 909441 | 1627 | BA_3 | |
| 2 | 355109 | 909197 | 1687 | BA_3 | |
| 3 | 359630 | 907671 | 1766 | BA_3 | * |
| 4 | 355318 | 908981 | 1710 | BA_3 | * |
| 5 | 356504 | 909570 | 1737 | BA_3 | * |
| 6 | 368501 | 911436 | 1719 | BA_3 | * |
| 7 | 359999 | 907987 | 1741 | BA_3 | |
| 8 | 360151 | 907751 | 1759 | BA_3 | |
| 9 | 366864 | 911474 | 1691 | BA_3 | |
| 10 | 363054 | 911184 | 1686 | BA_3 | |
| 11 | 363146 | 910968 | 1695 | BA_3 | |
| 12 | 363328 | 910978 | 1696 | BA_3 | |
| 13 | 357937 | 907648 | 1808 | BA_4 | |
| 14 | 361190 | 907509 | 1828 | BA_4 | * |
| 15 | 362718 | 908151 | 1802 | BA_4 | |
| 16 | 364751 | 909021 | 1823 | BA_4 | |
| 17 | 368175 | 9911436 | 1803 | BA_4 | |

* Location of RQD determination was undertaken

In the present study RQD was determined based on Palmstrom (1982) empirical relation. When no core is available and discontinuity traces are visible in surface exposures or exploratory adits, RQD may be estimated from the number of discontinuities per unit volume.

The suggested RQD relationship for clay-free rock mass is as per eq.4.3:

$$RQD = 115 - 3.3 J_v \quad \dots\dots\dots \text{eq. 4.3}$$

Where, J_v is the discontinuities count, more than 10cm long, in 1mx1m exposed rock surface.

Accordingly, for RQD determination five surface rock exposures were selected and joint volume count was undertaken based on [Palmstorm \(1982\)](#) relation (eq.4.3). The rock exposure for RQD determination was very limited. So, core drilling RQD was integrated with it.

4.3.2 Geotechnical Core Drilling

Geotechnical core logging involves observation, examining and measuring of various aspects of the core to make a quantitative data set that can be used as basic geotechnical information for input into the rock mass classification system ([Bieniawski 1989](#)).

In order to determine the geomechanical parameters such as; identifying and describing foundation materials, collecting soil, and rock samples and conducting both strength and permeability tests of the rock mass exposed along the tunnel alignment, boreholes were drilled by the project authorities. In total, 6 boreholes with a total depth of 606m were drilled along the proposed waterway route. According to [ECDSWC, 2019](#) the selection of borehole locations was mainly made based on surface conditions and geophysical surveying data (Table 4.5).

Table 4.5 Details of boreholes along the proposed waterway (Source: [ECDSWC, 2019](#))

| Bore Hole number | Location | Survey Coordinate(UTM) | | Elevation m.a.s.l. (m) | Termination depth (m) | Termination elevation (m.a.s.l) |
|------------------|------------------------------------|------------------------|----------|------------------------|-----------------------|---------------------------------|
| | | Easting | Northing | | | |
| BH-09 | Intake | 368273.7 | 911105.7 | 1812.0 | 50 | 1762.0 |
| BH-12 | Inlet | 367255.5 | 910799.7 | 1815.0 | - | 1610.0 |
| BH-13 | Alignment | 364371. | 909933.1 | 1765.0 | 156 | 1620.0 |
| BH-14 | Alignment and Middle Shaft | 359987.5 | 908615.4 | 1725.0 | - | 1530.0 |
| BH-15 | Surge Shaft | 354911.6 | 908939.0 | 1695.0 | 117 | 1490.0 |
| BH-16 | Tail Race Tunnel and Outlet portal | 351542.3 | 909698.9 | 1355.0 | 318 | 955.0 |
| Total | | | | | 641 | |

All bore holes have been drilled by ECDSWC by using rotary core drilling method. For the purpose of drilling KMB 1.4, KMB 0.4, and MASENZA wire- line drilling rig machines of

Ethiopian Construction Design and Supervision Works Corporation were used. Further, core drilling and extraction of soil and rock core samples were performed in accordance with Standard Practice for Rock Core Drilling and Sampling of Rock for Site Investigation (ASTM D 2113-99). The drilling operation was made with HQ to NQ borehole size diameter (90mm, and 75.7mm). Later, soil and rock cores were extracted and used for the investigation purpose. In addition, in-situ permeability tests were carried out in the boreholes and, rock core samples were collected for further tests in the laboratory. For the present study borehole logging was done during the field work (Plate 4.1 (a)).



Plate 4.1 (a) Bore hole logging during field work and (b) Field compressive strength estimation using Schmidt hammer

Since the core drilling investigation work has been under progress, all the proposed bore holes were not executed during field data collection stage of this study. Therefore, available length of core drilling for the thesis was 641m. During the present study the required geological and engineering geological information was obtained from the respective drill cores and was recorded. So, for the present study, engineering geological information such as RQD, core drilling samples for laboratory analysis, lithology description, and ground water condition were gathered. This information was used for rock mass characterization.

The geological description on core logging addressed the rock type identification, color and textural description, degree of weathering, mechanical rock strength, intensity of rock fracturing, and the type and extent of secondary infilling minerals. These rock mass properties were determined in accordance to [ISRM \(1981\)](#) strength classification.

According to [Deere et al. \(1967\)](#) RQD is defined as the percentage of intact core pieces longer than 100 mm (4 inches) in the total length of core. So, the RQD data were collected following the eq.4.4.

$$RQD = \sum \frac{\text{Length of pieces cores} > 10 \text{ cm length}}{\text{total length of core run}} * 100 \quad \dots\dots\dots \text{eq. 4.4}$$

4.3.3 Laboratory Testing

The geomechanical parameters of the rock mass along the HRT are fundamental in the designs and support systems of the tunnel ([Irem, 2008](#)). Rock samples were collected during the field geotechnical investigation works from surface and core drilling in order to achieve these geomechanical parameters of rock mechanics. The core samples were collected from boreholes at HRT intake (BH-9) and from HRT alignment (BH-13).

Table 4.6 Summary of laboratory test

| BH or Sample ID | Location | | | UCS (Mpa) | Unit Weight | Specific Gravity(SSD) | Water Absorption | Porosity (%) | Point load(N/mm) | Lithology |
|-----------------|----------|----------|------------------------------------|-----------|-------------|-----------------------|------------------|--------------|------------------|-----------|
| | Easting | Northing | Depth of sampling or Elevation (m) | | | | | | | |
| BH-9 | 368273 | 911105 | 13.56-13.90 | ✓ | ✓ | ✓ | | ✓ | | BA_4 |
| | | | 47.10-47.40 | ✓ | ✓ | ✓ | ✓ | ✓ | | BA_ |
| BH-13 | 364371 | 909933 | 135.65-135-85 | ✓ | | ✓ | ✓ | | | BA_3 |
| | | | 141.15-141.34 | ✓ | | ✓ | ✓ | | | BA_3 |
| SA_1 | 355884 | 908318 | 1766 | | | | | | ✓ | BA_4 |
| SA_2 | 356504 | 909570 | 1737 | | | | | | ✓ | BA_3 |
| SA_3 | 359999 | 907987 | 1741 | | | | | | ✓ | BA_3 |
| SA_4 | 363146 | 910968 | 1698 | | | | | | ✓ | BA_3 |

A total of eight engineering properties and index tests were studied from surface and core samples in order to determine uniaxial compressive strength (UCS), unit weight, specific gravity, water absorption and porosity. These tests were conducted in research, Laboratory

and Training center of the ECDSWC. The details about various laboratory tests conducted including the location and rock unit for present study are presented in Table 4.7.

In addition to the above listed laboratory tests four samples were taken for point load testing during field work.

From eight laboratory test samples, four irregular lump samples were collected for point load test (PLT). These samples were performed in laboratory of ICT Engineering private limited company as per suggested methods by [ASTM D 5731](#). Since point load distance or sample diameter of the lump samples were varied corrections were performed according to [ASTM D 5731](#).

In order to calculate UCS value, eq.4.5 (the relationship between the point load strength (PLS) and UCS and suggested by [Rusnak and Mark, 2000](#)) was used:

$$UCS = 21 * Is(50) \dots\dots\dots eq.4.5$$

Where $Is(50)$ = Point load strength index of a specimen of 50 mm diameter.

4.4 Methodology on data collection and analysis

4.4.1 Preamble

The following sections conclude method of data collection and analysis that have been practiced in this thesis. The input data was collected from field as well laboratory testing and analysis was conducted.

Geology is the most important factor that determines the nature, form and cost of a tunnel ([Bell, 2007](#)) and geology of the rock mass intercepted provided critical information in the understanding of the characteristics of the rock mass, and to understand the geological processes as described in ([Martinsson, 2004](#)). Hence, the route, design and construction of a tunnel are largely dependent on geological considerations.

For the present study, attempts were made on description of relevant factual information, identification of any major features that might influence scheme layout, suitability of the study through remote sensing and engineering geological methods.

4.4.2 Geological and Engineering Geological Investigation

For the present study, systematic geological and the engineering geological investigation was carried out along HRT alignment with offset of 500 m for evaluation of geological and

geotechnical characteristics of the ground along the HRT alignment and slope stability condition of surge shaft and, tunnel entrance was undertaken. Accordingly, the rock mass was divided into a number of rock mass units (BA_3 and BA_4) based on change in lithology and rock mass structural properties and according to the guidelines followed by [Bieniawski, 1989](#) (detail result and discussion was presented in chapter five and six).

According to [Malaya et al.\(2014\)](#) parameters which have significant influence on the rock mass properties encompasses the number of fracture sets and their orientations, persistence, aperture, roughness, filling material, water inflow and weathering. Accordingly, more than 64 discontinuity data were collected along the geological units BA-3 and BA-4 according to the guidelines ([ISRM, 1981](#)). The discontinuities orientation data in the project area were analyzed by stereographic projections in order to get the preferred orientations of different discontinuity sets.

RQD was determined from surface exposure based on [Palmstrom \(1982\)](#) empirical relation and also on core drilling according to the guideline suggested by [Deere et al. \(1967\)](#). Regarding to intact rock strength, it was determined in the field and from the laboratory testing. In the field on 17 selected stations hammer rebound test was determined by using N type Proceq H, Silver Schmidt hammer and four lump samples were collected and analyzed for point load test.

4.4.3 Engineering Geological Assessment

4.4.3.1 Rock Mass Classification

Rock mass classification is an essential element of feasibility studies for any near surface construction project prior to any excavation or disturbances made to earth. In order to perform rock mass classification system, input parameters data were obtained from field and laboratory test results. The rock mass was divided in to segment (rock mass units)by calibrating the geophysical survey results of [ECDSWC ,2019](#) with discontinuity condition such as, fracture density and evenness as displayed by weighted RQD. Those grouped segments are assumed to be more or less uniform in certain geotechnical features.

For the present study three rock mass classification systems, i.e. Rock Mass Rating (RMR) ([Bieniawski, 1989](#)), Q- system ([Barton et al., 1974](#)) and GSI ([Hoek et al., 2002](#)) were used for the characterization and classification of the rock mass. Accordingly, the HRT was divided into three segments and data on all required parameters (orientation, spacing, opening,

roughness, degree of weathering, filling, and groundwater conditions) was collected from each segment to quantify the rock mass by using empirical classification systems.

4.4.3.2 Rock Mass Strength Estimation

In order to estimate the parameters in the Hoek-Brown strength criterion for rock masses, GSI was designed and deformability and strength of rock mass using relationship modified from other classification systems (Hoek et al., 2002). GSI value is related to parameters of Hoek-Brown strength criterion (Hoek, 1994; Hoek and Brown, 1997; Hoek et al., 2002) as discussed in chapter two, section 2.4.2.

For the present study, the generalized Hoek–Brown failure criterion (Hoek et al., 2002) is applied for estimating the strength and deformability of geomechanical rock mass (BA_3 and BA_4). This was performed by employing RockLab 1 was applied based on the data obtained from field measurements and laboratory tests.

4.4.4 Geophysical Characterization of HRT

Bell (2007) presented geophysical investigations can give valuable assistance in determination of subsurface conditions, especially in areas in which the solid geology is poorly exposed. Resistivity techniques have proved useful in locating water tables and buried faults, particularly those that are saturated. As different researchers work (McCann et al., 1997; Smith and Randazzo, 1987), for this thesis, resistivity imaging has been used to locate fault zones, zones of deep weathering and cavities.

4.4.5 Remote Sensing Study

For the present study remote sensing study was carried out to address following relevant aspects (i) Terrain morphology and surface gradients (ii) Geological structure (faults, shear zones etc.); (iii) Slope stability (orientation of structural features vis-à-vis slopes) ;(iv) Surface drainage characters and water channel crossings.

CHAPTER – 5

RESULTS AND DISCUSSION

5.1 General

In this chapter the results of the geological and geotechnical investigation and, remote sensing study of the project are presented. Besides, discussion and interpretation on the results is also made in detail.

5.2 Engineering Geological Assessment

According to [Rahimi et al. \(2014\)](#) the knowledge of the rock mass is fundamental for the tunnel design and it is usually determined in engineering geological study. For the present study, evaluation of geological and geotechnical characteristics of the ground along the HRT alignment was the main objective. Therefore, to describe the ground behavior rock mass composition can be divided into general composition, represented between weakness zones and faults, minerals or rock types which have special properties affecting ground behavior ([Palmström and Stille, 2010](#)).

5.2.1 Geotechnical Units Intercepted Along the Study Area

From the results of the geotechnical site investigation carried out in the present study, geotechnical modeling of the tunnel has been done to understand the engineering properties of the rock mass encountered along the HRT alignment. Accordingly, two major geotechnical units (BA-3 and BA-4) have been identified. These units are basically classified based on their engineering properties directly related to the degree of rock mass weathering, nature of discontinuities and the intact rock strength, through which the most significant parameters influencing the behavior of the rock mass can be defined.

5.2.1.1 Geotechnical Unit One (BA-4)

This geotechnical unit is characterized by slightly weathered and fresh rock mass with closely to widely spaced joints. This unit is encountered along the tunnel alignment from chainage 0+495m to 0+500 m and 0+502m to 1+084 m.

5.2.1.2 Geotechnical Unit Two (BA-3)

This geotechnical unit is characterized by fresh to slightly weathered massive to weakly jointed rock mass. This unit is found along the tunnel alignment from chainage 1+084 m to 14+500 m.

5.2.2 Discontinuity Systems

Geological data is the main framework for all rock mechanics analysis (Anon, 1979). The rock mass has mechanically weak planes and inherent geometrical structural irregularities. Such physical and mechanical properties of rock mass have substantial changes during the excavation phase. The parameters which have significant influence on the rock mass properties encompasses the number of fracture sets and their orientations, persistence, aperture, roughness, filling material, water inflow and weathering (Malaya et al., 2014).

According to Malaya et al. (2014) discontinuities are important input parameters for rock mass strength criteria that have impact on engineering construction designs. Therefore, in the present study the discontinuities in the project area were analyzed by stereographic projections in order to get the preferred orientations of different discontinuity sets.

Based on the field data, joints were plotted on a stereographic projection net with the aid of Dips v.5.1 software (Rocscience, 2002). Accordingly, equal angle lower hemisphere Rose diagram plot of measured joints revealed five major joint sets. Dip/Dip direction of those major joints are; (i) 75°/125° N, (ii) 67°/021° N, (iii) 58°/334° N, (iv) 65°/258° N and (iv) 63°/220°N. Detail of the projection is presented in Table 5.1, Fig. 5.1 and Fig.5.2. The mean attitude of joints (dip/direction) from the stereographic projection is 21.97°/N109.34°.

Table 5.1 Preferred orientations of Major joint sets in the study area

| S.No. | Joint set | Dip amount | Dip direction |
|-------|----------------|------------|---------------|
| 1 | J ₁ | 75° | 125° |
| 2 | J ₂ | 67° | 021° |
| 3 | J ₃ | 58° | 334° |
| 4 | J ₄ | 65° | 258° |
| 5 | J ₅ | 63° | 220° |

5.2.3 Rock Mass Properties

During the present study engineering geological investigations was performed at the site and relevant data pertaining to rock mass properties was collected. This includes data on intact rock strength, RQD, joint number, joint roughness, joint spacing, joint filling, joint alteration number and stress condition. All this data was collected along the geological units BA-3 and BA-4, which was later rated to classify the rock mass. The above mentioned classification parameters are presented and discussed in the following paragraphs.

Intact rock strength - Intact rock strength was obtained both in the field and from the laboratory testing. Accordingly, in the field it was determined by using hammer rebound test and later converted to representative UCS values from the standard conversion graph (http://www.proceq.com/proceq_silverschmidt_user_manual_en). The results shows that UCS value in general ranges from 67 -156 MPa for BA-4 Geotechnical rock unit while, for geotechnical rock unit BA-3 it ranges from 78 -160 MPa.

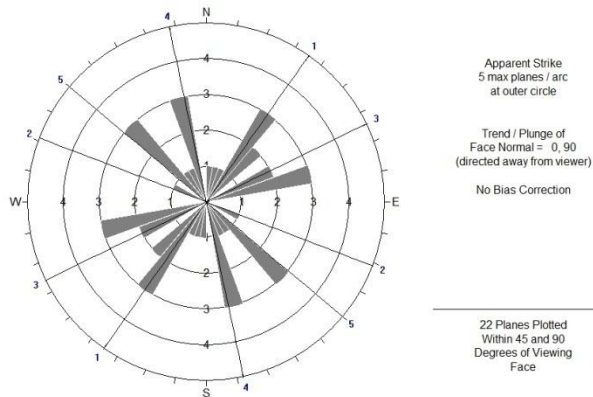


Fig.5.1 Rosette diagram for joints in the study area.

The UCS was also determined from the Core drilling samples through laboratory tests and also from surface rock samples through point load testing. The laboratory test results on UCS are presented in Table 5.2.

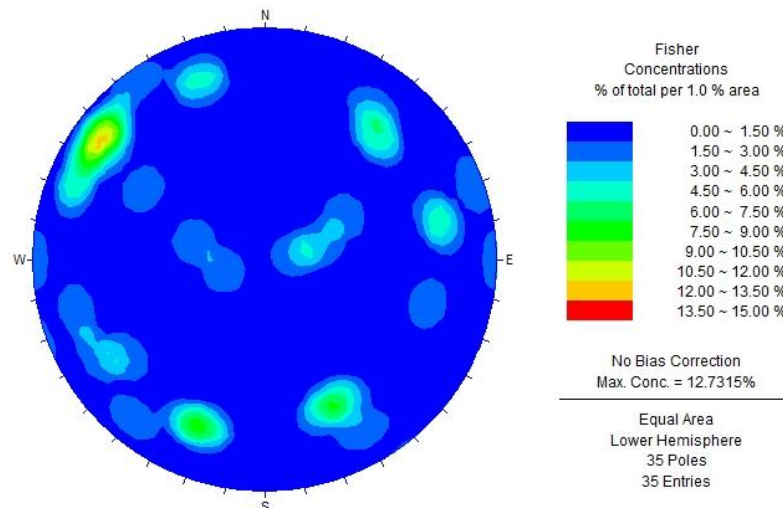


Fig.5.2 Fisher concentrations of joint set in the study area.

The following relationship between the Point Load Strength (PLS) and UCS, suggested by Rusnak and Mark (2000) was used;

$$UCS = 21 * I_s (50) \dots\dots\dots eq. 5.1$$

Where; $I_s (50)$ is the Point load strength index of a specimen of 50 mm diameter and UCS is the uniaxial compressive strength of the intact rock.

Thus, based on the test result (Table 5.2) for rock mass unit BA-3 average UCS value through core testing is 128.05 MPa, whereas through point load testing the average value is 193.2 MPa. Similarly, for rock mass unit BA-4 average UCS value through core testing is 187.8 MPa, whereas through point load testing the value is 194.25 MPa.

Table 5.2 Summary of Laboratory test results on representative rock samples

| Location | | | Lithology | Depth (m) | Laboratory tests | | | |
|----------------------------------|----------|----------|-----------|---------------|--|---------------------------|----------------------|--------------|
| Bore hole | | | | | UCS (MPa) | Unit weight (gm/cc) | Water absorption (%) | Porosity (%) |
| BH_9 | | | BA_4 | 13.56-13.90 | 168.59 | 2.75 | | 3.14 |
| | | | BA_4 | 47.10-47.40 | 207.02 | 2.85 | 0.31 | 3.27 |
| BH_13 | | | BA_3 | 135.65-135.85 | 155.59 | 2.87 | 0.2 | |
| | | | BA_3 | 141.15-141.34 | 100.52 | 2.86 | 0.44 | |
| Test from surface samples | | | | | | | | |
| Sample number | Location | | | | Corrected Point load Index (I_s) in N/mm^2 | Converted UCS value (MPa) | | |
| | Easting | Northing | | | | | | |
| 1 | 355884 | 908318 | BA_4 | | 9.25 | 194.25 | | |
| 2 | 356504 | 909570 | BA_3 | | 9.79 | 205.59 | | |
| 3 | 359999 | 907987 | BA_3 | | 7.64 | 158.34 | | |
| 4 | 363146 | 910968 | BA_3 | | 10.18 | 213.78 | | |

Rock quality Designation (RQD) –RQD for the present study has been obtained in the field as well as from the core drilling. In field study it was estimated by empirical formula ($RQD = 115 - 3.3 \times J_v$) by finding number of joints per cubic meter by using Palmstrom’s Volumetric joint Count (J_v) method (Palmstrom, 1982). Thus, the results obtained from surface exposures shows that RQD value for BA-3 unit ranges from 66 - 85%. Further, for BA- 4 rock unit it was not possible to record the volumetric count due to lack of surface exposure. However, at deeper tunnel level joint number are expected to be decreased. Therefore, it is expected that at tunnel grade in general RQD could be greater than 40% except in shear/weak zones and fractured rock. Moreover, the RQD values obtained from the core drilling for BA-3 unit ranges from 89 to 92% while for BA-4 the value obtained is 91%.

Discontinuity characteristics -The discontinuities observed at the present site are described based on [ISRM \(1981\)](#). The discontinuity parameters that were measured/ observed includes orientation, spacing, persistence, aperture, roughness, number of joints sets, infilling material and hydraulic conditions of the rock mass.

Thus, the discontinuity characterization may be summarized as follows;

- ✚ According to the engineering geological investigation in the study area, the rock mass unit BA-4 showed that spacing of discontinuity ranges from 0.06 to 0.5m and persistence of the joints were measured with the interval between 0.56 to 21m with joint openings from 0.35 to 1cm. Further, the discontinuity surfaces in general were observed as smooth undulating to rough undulating. Regarding filling material, mostly clay infillings was observed within the joints of this rock unit. On surface exposure it was observed that due to erosion, degree of weathering ranges from fresh to highly weathered joint surface.
- ✚ The discontinuity condition surveys on BA-3 outcrops indicate that spacing of discontinuity ranges between 0.06 to 0.75 m and the persistence of the joints have an interval between 1 – 20 m. Besides, joint set of this unit ranges from one joint sets plus random joints to three joint sets. This unit also showed rough undulating to smooth undulating discontinuity surfaces and discontinuity aperture ranges in between 0.2 to 1.5cm. With regards to the filling material, mostly on the surface exposure silty clay infillings was observed within the joints of this rock unit. In addition, quartz vein were also observed as the infillings. In the core samples it was observed that quartz vein is the main joint filling material. Further, it was observed that there are fresh to slightly weathered discontinuity surfaces and dominant portion of the rock exposure shows fresh rock unit. On the surface exposures it was observed that degree of weathering varies from fresh to slightly weathered and dominant portion of the rock exposure shows fresh an altered rock unit.

5.2.4 Ground Water Condition

According to [Zaruba and Mencl \(1976\)](#) inflow of water into the tunnel increases construction costs by about 20 %; as water proofing of the lining and often also drainage behind the lining are necessary. Encountering large quantities of water in weak ground conditions can also lead to rapid formation of cavities around the tunnel excavation. This can produce the potential for significant quantities of wet and loose ground to flow into the tunnel excavation.

For rock mass characterization, condition of ground water is the measure of how much ground water is contained in the rock mass, as observed in the field (Banda, 2013). In the present study area, no surface manifestations of ground water were observed therefore, groundwater conditions were considered dry for surface site condition. However, for rock mass classification ground water rating was considered based on bore hole data. Partly HRT will be passing below the ground water level. Thus, HRT will be passing through completely dry media for Rock unit BA-4 whereas; in BA-3 rock mass unit it will be passing below the ground water level. Information from the drill hole logs revealed that in borehole BH-13 groundwater was recorded at a depth of 70m and in BH-15 it was recorded at a depth of 80m. However, in BH-9, drill hole near to the intake, groundwater was not reported within the full length of the drill hole (50 m).

5.2.5 Permeability Test

According to ECDSWC (2019) in situ falling head and packer permeability tests were carried out in soil and rock mass, respectively in the borehole. The test procedure followed was in accordance to the British Code of practice for site investigation BS5930 (1999) and U.S. Army Corps of Engineers (USACE, 1984).

Single packer permeability tests were conducted for rock mass sections in the drilled boreholes by the project authorities (ECDSWC, 2019). The permeability tests were conducted in accordance to approach proposed by Housby (1976). Thus, the lugeon values of tested sections for each run pressure were analyzed by using following equation (eq. 5.2);

$$Lu = (10*Q)/P*L \quad \dots\dots\dots \text{eq. 5.2}$$

Where; ‘Q’ is average water intake in lit/minute, ‘P’ is total Testing Pressure in bars and ‘L’ is the length of tested section in meters.

The permeability test results, as obtained are presented in Table 5.3. The results presented in Table 5.3 account to permeability tests conducted till the present study however, the tests are ongoing for remaining sections.

5.2.6 Rock Mass Classification in HRT

Rock mass classification is an essential part of engineering projects and it is essential to evaluate the rock mass quantitatively for easy understanding of engineers and support designers (Gupta et al., 2011 and Malaya et al., 2014). The important objectives of the rock mass characterization and classification are; (i) to identify the most significant parameters

influencing the behavior of a rock mass and (ii) to divide a particular rock mass formation into a number of rock mass classes of varying quality (Bieniawski, 1993).

Table 5.3 Summary of permeability test result

| BH-ID. | In-situ permeability test type | | | | In-situ Permeability Condition | |
|--------|--------------------------------|-------------------|-----------------------------|--------------|-------------------------------------|------------------------|
| | Test Section (m) | Lugeon value (Lu) | Permeability Value K (cm/s) | Flow Type | Degree of Permeability (Bell, 2007) | Condition of Rock Mass |
| BH-09 | 5.0-10.0 | Falling Head | 5.65E-03 | | | |
| BH-13 | 10.0-15.1 | Falling Head | 4.18E-03 | | | |
| | 15.0-20.0 | 6 | 7.80E-05 | Laminar | Moderate | Few partly open |
| | 35.0-40.0 | 2 | 2.60E-05 | Dilation | Low | Tight |
| | 42.0-48.0 | 1 | 1.30E-05 | Turbulent | Low | Tight |
| | 60.0-70.0 | 3 | 3.90E-05 | Void filling | Low | Tight |

For the present study three rock mass classification systems, i.e. Rock Mass Rating (RMR) or Bieniawski Geomechanics Classification (Bieniawski, 1989), Q- Index (Barton et al., 1974) and GSI (Hoek et al., 2002) were used for the characterization and classification of the rock mass. For the present study the HRT was divided into three segments and data on all required parameters (orientation, spacing, opening, roughness, the degree of weathering, filling, and groundwater conditions) was collected from each segment to quantify the rock mass by using empirical classification systems. Further, the continuity and uniformity information on rock mass was obtained by calibrating the geophysical survey results (ECDSWC, 2019) with information from logs of drilled boreholes for different depths.

5.2.6.1 Rock Mass Rating (RMR) Classification

The RMR system or the Geomechanics Classification was developed by Bieniawski during 1972-1973 to assess the stability and support requirements of tunnels and has been improved since then. The 1989 version of RMR was used for the rock mass classification in the present study. This engineering classification system, which was modified by Bieniawski in 1989, utilizes the following six rock mass parameters: (i) Uniaxial compressive strength of intact rock material, (ii) Rock quality designation (RQD), (iii) Spacing of discontinuities, (iv) Condition of discontinuities, given as (a) Length, persistence, (b) Separation, (c) Smoothness, (d) Infilling and (e) Alteration / weathering, (v) Groundwater conditions and (vi) Orientation of discontinuities. All parameters are measurable in the field and some of them may also be obtained from borehole data. The rating of each of these parameters is summarized in standard tables, proposed by Bieniawski (1989) to give a RMR value for the rock mass.

In order to apply RMR classification system, the rock mass along the tunnel alignment needs to be divided into number of structural regions, i.e. zones in which certain geological feature

are more or less uniform (Bieniawski, 1989) and each zone is classified and characterized separately (Hoek, 2007).

Table 5.4 RMR values for different geomechanical units along the HRT alignment

| RMR parameters | Geotechnical unit along HRT | | | | | |
|--|-------------------------------------|--------|-------------------------------------|--------|-----------------------------|--------|
| | 0+000 To 1+084 | | 1+084 To 2+675 | | 2+675 To 14+500 | |
| | BA-4 | | BA-3 | | BA-3 | |
| | Value | Rating | Value | Rating | Value | Rating |
| RQD (%) Bore hole | 91 | 20 | 91 | 20 | 89 | 17 |
| Uniaxial compressive Strength (UCS) | 181.21 | 12 | 191.26 | 12 | 191.26 | 12 |
| Spacing (m) | 0.246 | 100. | 0.28 | 10 | 0.21 | 10 |
| Condition of Discontinuities(from surface joint survey) | | | | | | |
| Persistence Mean value (m) | 5.89 | 2 | 5.85 | 2 | 9.7 | 2 |
| Aperture Mean value (cm) | 0.705 | 0 | 0.77 | 0 | 0.81 | 0 |
| Roughness | Smooth –rough | 1-5 | Smooth – rough | 1-5 | Smooth – rough | 1-5 |
| Infilling | Hard filling > 5 mm to none filling | 2-6 | Hard filling > 5 mm to none filling | 2-6 | Free to clayey | 2-6 |
| Weathering | Fresh to slightly weathered | 5-6 | Fresh (generally) | 6 | slightly weathered to fresh | 5-6 |
| Ground water | dry | 15 | dry | 7 | wet | 7 |
| RMR rating | | 69-76 | | 59-68 | | 56-65 |
| Rating Adjustment | fair | -5 | fair | -5 | fair | -5 |
| RMR total | 64-71 | | 54-63 | | 50-60 | |
| Description | Good | | Fair to Good | | Fair to good | |
| Meaning of rock mass classes based on averaged RMR rating | | | | | | |
| RMR mean | 67.5 | | 58.5 | | 55 | |
| Rock mass class | II | | III | | III | |
| Description | Good rock | | Fair rock | | Fair rock | |
| Average stand - up time | 1 year for 10 m span | | 1 week for 5 m span | | 1 week for 5 m span | |
| Cohesion of rock mass (KPa) | 300 - 400 | | 200 - 300 | | 200 - 300 | |
| Friction angle of rock mass(degree) | 35 - 45 | | 25 - 35 | | 25 - 35 | |

For the present study the required data pertaining to RMR was collected for different geotechnical Rock mass units present along the HRT alignment and later it was processed in accordance to RMR classification system (Table A_1 in Appendix A). The resulted RMR values for different geotechnical units along the HRT alignment are presented in Table 5.4. For the present study, the strength values obtained from the Laboratory UCS test, point load test and Schmidt hammer tests were averaged and used as one of the parameters in RMR

classification. However, other required parameters were observed in the field and minimum and maximum range values were used in the rock masses classification.

5.2.6.2 Q - Classification System

In the Q-system the numerical values are defined by six parameters; rock quality designation (RQD), joint roughness (Jr), joint sets (Js), joint alteration (Ja), stress reduction factor (SRF) and joint water reduction (Jw) (Barton et al., 1974). Mathematically tunneling quality index “Q” of the rock mass is calculated by equation no 2.2 which is discussed in Chapter 2.

For the present study the required values for the ‘Q’ parameters were obtained from the surface exposures of the rock mass along the tunnel alignment and for sub- surface through borehole data (for BA-4 overburden stress ranges from 24 to 99 m and for BA-3 it ranges from 63 to 242 m). In general, the major principal stress σ_1 ranges from 0.672 to 8.168 MPa. Since the average uniaxial compressive strength values of the rock from boreholes and point load tests for BA-3 and BA-4 are approximately 166.764 MPa and 189.95 MPa, respectively therefore, the ratio of σ_c / σ_1 varies from 99.45 - 282.66 for rock mass BA-4 and 43.88 -20.416 for BA-3. Further, based on the conditions the standard empirical values were assigned to each of the parameters of the system to calculate the representative Q-index. In general, the numerical values of ‘Q’ system varies from 0.00 (exceptionally poor rock mass) to 1000 (exceptionally good quality rock mass) (Barton et al., 1974). According to Q-system classification, the rock class in the study area varies from ‘poor’ to ‘very good’ rock, as presented in Table 5.5.

5.2.6.3 Geological Strength Index (GSI) System

Geological Strength Index (GSI) provides a measure of the rock mass quality for directly assessing the strength and stiffness of intact and fractured rocks (Hoek et al., 1997). For the present study quick assessment of the GSI has been done on the bases of geological descriptions of the two geomechanical rock units by using modified table for estimating the Geological Strength Index proposed by Hoek et al. (2002), as presented in Fig. 2.1 in Chapter two.

In the present study based on interpolation and calibration of core drilling data and geophysical study results, it has been found that both rock mass units (BA-3 and BA-4) have structural characteristics of well interlocked undisturbed rock mass consisting of cubical

blocks formed by three intersecting discontinuity sets with good to very good surface condition (Fig. 5.3 and Fig.5.4).

5.3 Indirect Estimation of Rock Mass Strength

There have been attempts to assess the strength of the rock mass using a suitable rock mass strength criterion having input derived from the principles outlined in the generalized Hoek-Brown failure criterion with the parameter results from mapping, core logging and laboratory testing (Hoek and Brown 1997). This Failure Criteria was used to estimate the strength and deformation modulus of jointed rock mass using the Geotechnical Strength Index; Hoek and Brown (1997) and Lu (2015) as an input. In the present study, on the bases of Hoek et al. (2002) equations GSI was applied for estimating the strength and deformability characteristics of the rock mass. For this Roc Lab software was utilized.

The required input variables for the computation of various properties through Rock lab and MS computational sheet were obtained for different geotechnical rock unit along the HRT alignment. The mean GSI value as computed for BA-4 and BA-3 geotechnical units was taken as 74 and 79, respectively. The strength parameters as analyzed by using Rock Lab software are presented through Fig.5.5 and Fig.5.6.

Table 5.5 Q values for the different geotechnical rock mass units along the HRT alignment

| Parameters | Geotechnical unit along HRT | | | | | |
|--|--|--------|--|--------|---|--------|
| | 0+000 To 1+084 | | 1+084 To 2+675 | | 2+675 To 14+500 | |
| | BA-4 | | BA-3 | | BA-3 | |
| | Value | Rating | value | Rating | value | Rating |
| RQD(from core drilling) | 91 | | 91 | | 89 | |
| Joint set number (Jn) | One joint sets plus random joints- Two joint sets | 3-4 | One joint sets plus random joints -Three joints | 3-9 | One joint sets plus random joints -Three joints | 3-9 |
| Joint roughness number (Jr) | Smooth undulating -rough undulating | 2-3 | Smooth undulating - rough undulating | 2-3 | Smooth undulating - rough undulating | 2-3 |
| Joint alteration number (Ja) | unaltered joint walls, surface staining only- Silty or sandy clay coatings, small clay fractions (non-softening) | 1-3 | unaltered joint walls, surface staining only- Silty or sandy clay coatings, small clay fractions (non-softening) | 1-3 | Slightly altered joint walls. Non-softening mineral coatings; sandy particles, clay-free disintegrated rock, etc.- Strongly over-consolidated, non-softening, clay mineral fillings (continuous, but <5 mm thickness) | 2-6 |
| Joint water reduction factor (Jw) | Dry excavation or minor inflow | 1 | Dry excavation or minor inflow | 0.66 | Medium inflow or pressure, occasional outwash of joint fillings | 0.66 |
| Stress reduction factor (SRF) | σ_c / σ_1 282.66-99.45 | 1-2.5 | $\sigma_c / \sigma_1 = 43.88-20.416$ | 1 | $\sigma_c / \sigma_1 = 43.88-20.416$ | 1 |
| $Q = \left[\frac{RQD}{J_n} \right] * \left[\frac{J_r}{J_a} \right] * \left[\frac{J_w}{SRF} \right]$ | 9.1-60.66 | | 6.67-40.03 | | 3.26-19.58 | |
| Description | Fair to very good | | Fair to Very good | | Poor to Good | |
| σ_c = unconfined compression strength and σ_1 is major principal stress | | | | | | |



Fig.5.3 GSI for BA-4 geotechnical unit. The drilled Core box shown on left is from BH-9 borehole and GSI value is shown on the right marked over standard chart proposed by Rock Lab Guide by Hoek and Brown, 2002.



Fig. 5.4 GSI for BA-3 geotechnical unit. The drilled Core box shown on left is from BH-13 borehole and GSI value is shown on the right marked over standard chart proposed by Rock Lab Guide by Hoek and Brown, 2002.

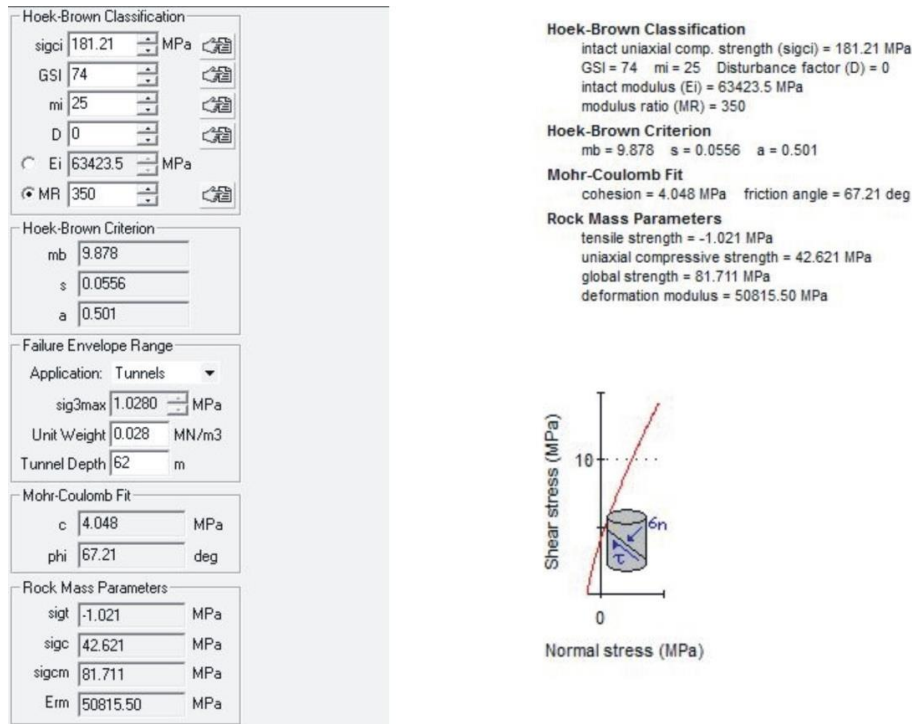


Fig.5.5 Analysis of rock strength using Rock lab for BA-4geotechnical rock unit along HRT alignment

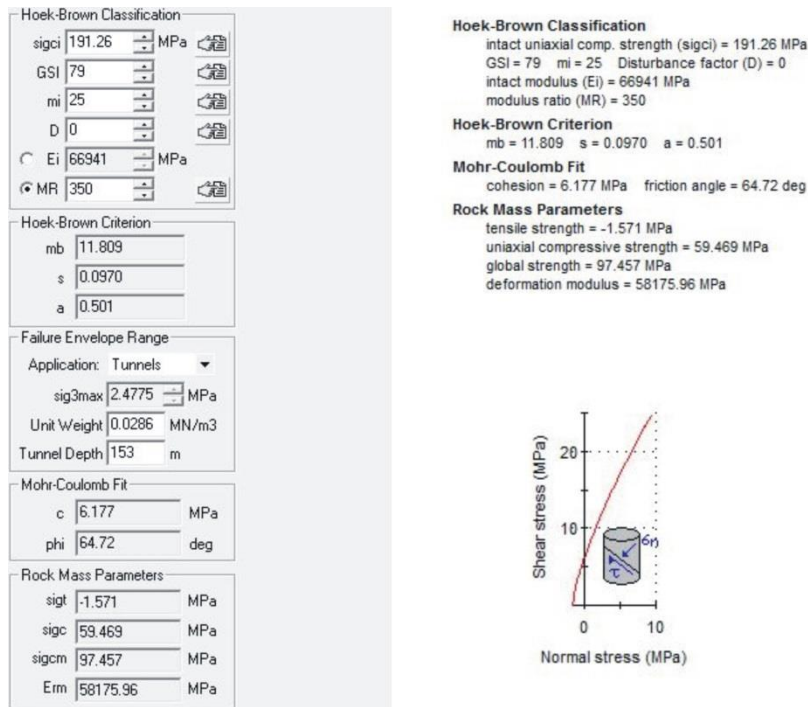


Fig.5.6 Analysis of rock strength using Rock lab for BA-3geotechnical rock unit along HRT alignment

5.4 Geophysical Results and Discussion

As mentioned in Chapter 4, geophysical survey was conducted by ECDSWC in 2019 with the objective to characterize geological features and to assess general ground condition prevailing along the headrace tunnel alignment. For the present study, 2D resistivity imaging

carried out along the HRT alignment was used as a secondary data source. The summarized geophysical report is presented in Appendix B.

5.4.1 2D- Electrical Resistivity Imaging

5.4.1.1 Resistivity Imaging Along Section Line-1

From this section five different anomaly zones can be recognized.

- ✚ The first zone is located on the eastern end of the section line, between electrode numbers 1 to 65. Geological structures as inferred from the high resistivity contrast along section line – 1, seen from the pseudo-section were observed at locations marked by electrode numbers 20, 145 and 165. All these structures dip towards west (Table Fig. B-1, Appendix B). This zone has low resistivity value (7.41-36.65 Ω m) layer of varying thickness with maximum bottom boundary up to 190 meter, and nearly vertical in shape and is open to depth. This might correspond to the weathered part of the basalt.
- ✚ high resistivity zone(65- 80 Ω m) which runs from electrode numbers 65 to 80 and westerly dipping extending to depth below 144m this might be some type of intrusive within the weathered basalt.
- ✚ The third zone is located In the middle of the line (between electrode numbers 80-120) and it is lower resistivity zone(25 -48.62 Ω m) due to a very conductive overburden and the occurrence of shallow groundwater that drains from the eastern to western namely Botu stream.
- ✚ High resistivity (83 Ω m& more) Easterly dipping zone is observed between electrode numbers 130 and 145 and is open to depth. This high resistivity zone may be the response of deep seated dyke.
- ✚ The area observed between electrode numbers 145 and 215 is characterized by resistive values (25- 65.4 Ω m) weathered and fractured ignimbrite zone except high resistivity between electrode numbers 175 and 180 below a depth of 115m.

Generally, on the low resistivity value (see Fig. B-1, Appendix B) between electrode number 47 and 65, 117 and 133, 197 and 213 reflected at the sub sections marked with elliptical outline is considered to be the response of moderately to highly weathered and fractured basalt. Geophysical inferred geological structures as there is high resistivity contrast on the labeled line as seen from the pseudo-section on the electrode numbers 20, 145 and 165 all dips towards western.

5.4.1.2 Resistivity Imaging Along Section Line-2

The pseudo-section of resistivity imaging along section line – 2 demonstrates following;

- ✚ Moderately high resistivity (39- 90 Ω m) layer of varying thickness with maximum bottom boundary was observed between electrodes numbers 1-15. This might be corresponds to the moderately weathered rock.
- ✚ High resistivity zone (39- 73 Ω m) was observed in between location marked by electrode numbers 15 to 55. This might be due to presence of highly to moderately weathered rock.
- ✚ The third zone demonstrated high resistivity (120-140 Ω m), bounded by sharp edged relatively low resistivity zone (120- 140 Ω m) this might be due to highly weathered and fractured rock unit. The alternating resistivity value of high and low zone continue between electrode numbers 130-150 and 150-170 respectively.
- ✚ The fourth zone, lying between electrode numbers 85-140 is characterized by relatively low resistivity (56- 73 Ω m) rock unit. On the top part of the profile, which gets higher to the deep this might be due to different degree of weathering and fracturing.

For the simplicity to all zones sub sections which are marked with elliptical outline around electrode number 25 and 45 as well as around electrical number 105 and 160, are considered to be the response of moderately to highly weathered and fractured basalt. Geological structures as inferred from the high resistivity contrast along section line – 2, seen from the pseudo-section were observed at locations marked by electrode numbers 50, 80 and 115. These structures dip towards east, west and eastern directions, respectively. These structures are generally oriented in different directions (Appendix B, Fig. B-2).

5.3.1.3 Resistivity Imaging Along Section Line-3

In general, geological conditions as inferred from the geophysical survey data along section line-3 may be sub-divided in to five zones of contrasting resistivity distribution;

- ✚ The pseudo section plot along this line has sharp edged low resistivity zone (about 33 Ω m), as observed in between electrode numbers 1 to10, also along shallow depth level and it pinches out under electrode 10. This zone is underlain by moderately high resistivity values (33-83 Ω m) in between electrode numbers 10 to18. This may be because of presence of moderately weathered fractured basalt.
- ✚ The second zone lies in between two anticipated structure (electrode numbers 20 and 30). This zone generally has lower resistivity value at shallow depths. However, low, circular

shaped, high resistivity ($117\Omega\text{m}$) values exist intermittently in this zone. The cause of this high resistivity may be due to presence of fresh basalt like ignimbrite.

- ✚ The vast section of the sub-surface (electrode numbers 30 and 90), mapped as the third layer, is characterized by relatively low to medium resistivity values ($33- 83 \Omega\text{m}$). This zone may be due to the presence of moderate to highly weathered, possibly water saturated, basaltic layer.
- ✚ The fourth layer, which has slightly lower resistivity ($33-83\Omega\text{m}$) on the top than the one above it ($7 - 14 \Omega\text{m}$), is probably due to the presence of weathered basalt rock. This top layer is underlain by a high resistivity ($134 \Omega\text{m}$) layer, dipping due east, might be fresh rock.
- ✚ A higher resistivity layer mapped as the fifth layer is present in between electrode numbers 125 and 135. The resistivity values for this zone were measured in the range of 83 to $100\Omega\text{m}$. These resistivity values are presumed to represent moderately fractured and weathered basaltic formation.

Geological structures as inferred from the high resistivity contrast along section line – 3, as seen from the pseudo-section, were observed at locations marked by electrode numbers 20, 30, 90 and 125. Anticipated structure marked at electrode numbers 20, 30 and 125 generally dips towards west. Structures marked at electrode numbers 20 and 30 are oriented parallel to each other while the structure at electrode numbers 90 dips in the eastern direction (Appendix B, Fig. B-3).

5.4.1.4 Resistivity Imaging Along Section Line-4

From the pseudo-section five different anomaly zones could be noted along section line - 4. These zones can be defined as;

- ✚ The first zone is located on the eastern end of the section line, defined in between electrode numbers 1-26. This zone has low resistivity value ($36\Omega\text{m}$) on top layer and resistivity value increases to $93\Omega\text{m}$ in bottom layer. These resistivity values could possibly be the response of weathered and/or highly fractured formation filled with in the main fracture line.
- ✚ The zone two is marked by high resistivity values ($130- 150\Omega\text{m}$), measured in between electrode numbers 26 to 35. The formation within this zone was observed to be dipping easterly, all along the depth of 190m . This might be due to the presence of intrusive body within the weathered granite.

- ✚ The third zone is marked in between electrode numbers 35 to 50. The lower resistivity zone ($35\Omega\text{m}$) reappear (the extension of zone one or it has similar resistivity observed in between electrode number 1 – 26). This is due to a very conductive overburden and the occurrence of shallow ground water.
- ✚ Further towards west along section line - 4, broader fourth zone was observed. This zone is located in between electrode number 50 and 170. This zone is characterized by wide area of low resistivity ($36- 55\Omega\text{m}$). These resistivity values may be representing weathered and fractured rock unit.
- ✚ Fifth layer was observed to be appearing in pairs as elongated high resistivity value layers ($150\Omega\text{m}$) surrounding the anticipated structure beneath electrode number 195.

Geological structures as inferred from the high resistivity contrast along section line – 4, as seen from the pseudo-section, were observed at locations marked by electrode numbers 34, 50, 159, 170, 195 and 225. Structures at electrode numbers 34 and 50, dips towards east and structures at electrode numbers 159 and 170 are oriented parallel to each other. The structures at electrode numbers 195 and 225 dips in the western direction (Appendix B, Fig. B-4).

5.5 Rock mass study for critical zones

5.5.1 Weak or Critical Zones

For the present study critical zones that have negative influence for HRT design and construction were distinguished. These zones are Geological structures that results into weak rock mass strength. These Geological structures were recognized mainly as faults and lineament. Based on 2D resistivity imaging analysis and remote sensing interpretations seven normal faults and six fracture zones were identified. Accordingly, these faults were observed to be striking northwest and southwest, dipping from 65 to 80° . These faults were characterized to have vertical displacement (throw) ranging from 10 and 20 m. According to [ECDSWC \(2019\)](#) these faults are commonly filled with iron oxides and clays, however at places they are also filled by silica veins.



Plate 5.1 Surface exposures of weak zones or fractured rock along the fault zone in BA_3 rock unit gully exposure

Fractures (linear structures) in the present study area are mainly represented by three dominant systems. These are; (i) NNW to NW (320° - 330°) striking, (ii) WNW (280° - 300°) striking, and (iii) NE (030° - 040°) striking.

The faults in the study area were intercepted at locations; station 0+551 to 0+581, 2+715 to 2+744, 5+265 to 5+290, 12+189 to 12+219 and 13+932 to 13+963. Further, lineaments along HRT were encountered at station 1+739, 2+092, 2+141, 2+984 and 7+294. Similarly, fracture zones were located at station 6+435 to 6+648.

5.6 Remote sensing study Result

The remote sensing study in the present study was mainly employed to supplement the reliable geological information, to overcome the limitation of access to majority of the study area due to extremely mountainous terrain and steep slopes and to execute the present study with short period of time. Moreover, it is well known that application of remote sensing is quite advantageous in terms of time and cost, and it is capable of providing rapid information

on geological characteristics. In this regard, conventional aerial photographs and various types of imagery can be used effectively for large-scale regional interpretation of geologic structure, analyses of regional lineaments, drainage patterns, rock types, soil characteristics, erosion features, and availability of construction materials (Rasher and Weaver, 1990; Gupta, 2003). In general, remote sensing (including aerial photography and satellite imagery) dramatically enhances the geological mapping, processing and visualization procedures and it is used to characterize lithology, structure, and alteration patterns (Soldo et al., 2019).

For the present study remote sensing study was carried out to address following relevant aspects;

- ✚ Terrain morphology and surface gradients
- ✚ Geological structure (faults, shear zones etc.);
- ✚ Slope stability (orientation of structural features);
- ✚ Surface drainage characters and water channel crossings.

Based on Ganas et al. (2005) extraction of topographic feature information from DEMs has become increasingly popular in structural analysis. Digital elevation models (DEMs) data were used to trace tectonic features and mapping geologically and topographically defined structures in many areas (Sarapirome et al., 2002).

During the present study Faults, shear zones and weak zones were identified in the project area based on the field evidences and geomorphologic features as interpreted from the Google Earth image (Fig. 5.7,b) and digital elevation model (DEM) visualization. Thus, the present study area was mapped by using DEM and various features were detected during the interpretation process. All such features were on screen digitized directly from the image and are presented as Fig. 5.9 and 5.10.

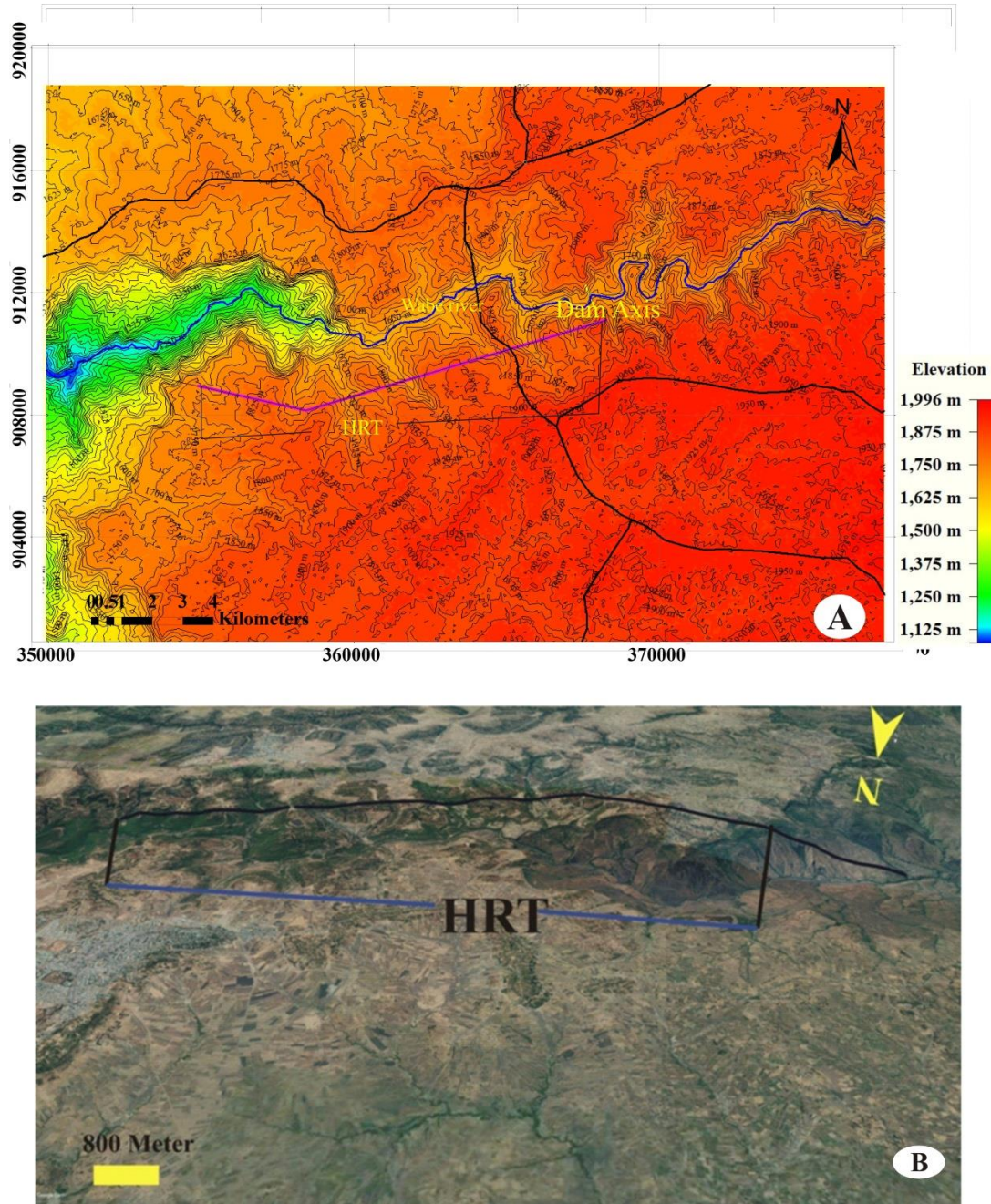


Fig.5.7 (a) Topographic contour map showing morphology of study area and (b) Terrain condition of the study area, as seen through Google Earth image (Source of image b: Google Earth image Landsat/Copernicus; image date 1/24/2019).

5.7 Discussion on results and findings of the study

Wabe hydropower project is proposed to construct across Omo River for the intended use of hydropower production. The project envisages a 4m diameter modified-horse shoe shaped, 15821mlong horizontal head race tunnel (HRT), a pressurized penstock with 3.2m diameter, and 1394long horizontal and 300m vertical shaft tunnel. At downstream end of the

pressurized penstock it trifurcates into three 1.8m diameter steel pipes through a manifold to join the turbine. Each turbine will have an installed capacity of 150MW (ECDSWC, 2019).

The main objective of the present study was to evaluate suitability of HRT through engineering geological and remote sensing method. Thus, the present study mainly encompasses geological mapping at a scale of 1:5000 along HRT alignment, geo-structural surveying, rock mass characterization and classifications, and rock mechanics tests. In the present study the rock mass along HRT has been assessed and classified using three rock mass classification systems i.e., Rock mass rating (RMR) by Biniawski (1989), Tunneling quality index (Q system) by Barton et al. (1974), and Geological strength index (GSI) by Hoek et al. (2002). Thus, based on the result obtained from these classification systems the rock mass was divided into two geotechnical units.

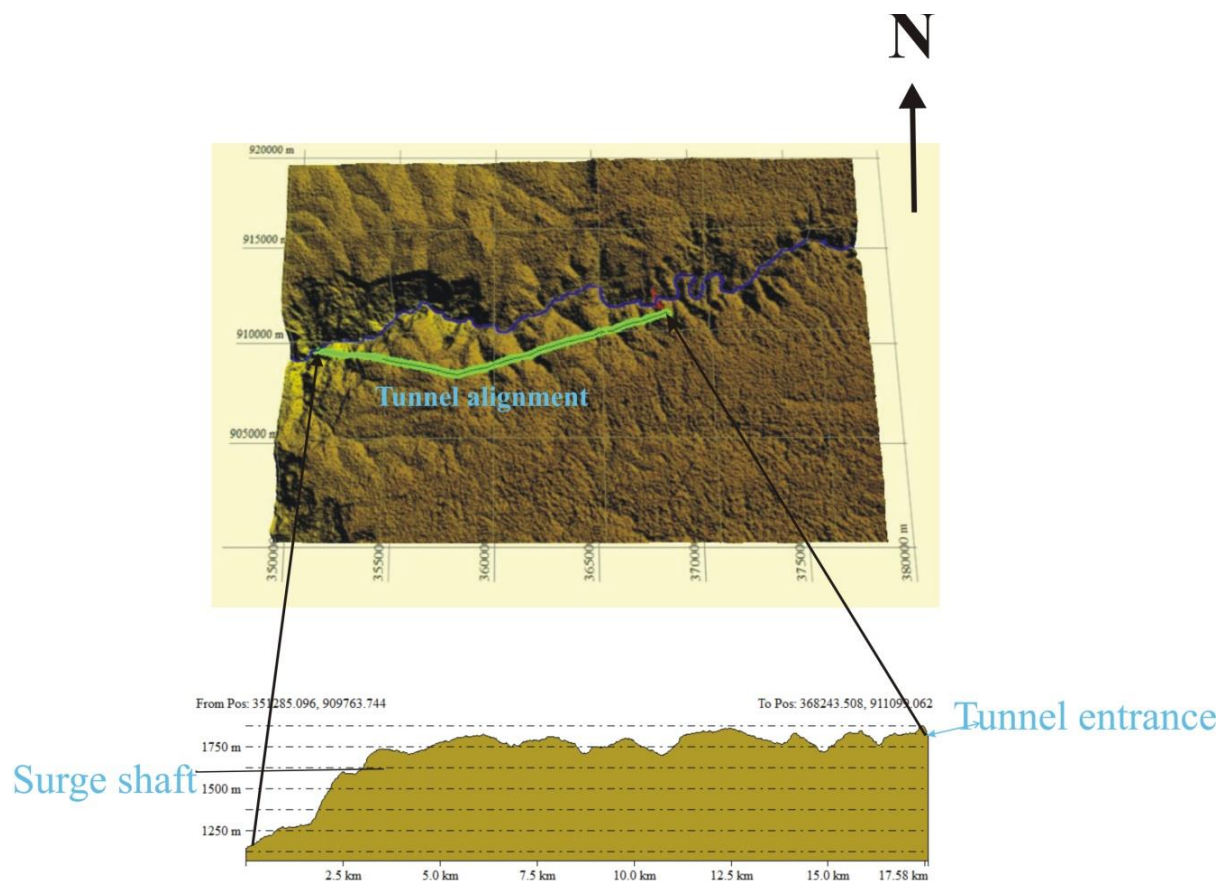


Fig.5.8 Terrain View of the study area (above) with section along the tunnel alignment (bottom)

5.7.1 Geotechnical Conditions along HRT

For the present study, HRT alignment was divided into three segments and generally, HRT will be excavated through Basaltic rock unit. This rock unit was classified in to two geotechnical units (Gtu-1 and Gtu-2 that was described as BA_3 and BA_ respectively, in

section 5.2.1) based on their engineering properties related to the degree of rock mass weathering, nature of discontinuities and intact rock strength. For each unit rock mass classification results are presented in Table 5.7. Further, strength analysis results for rock mass using Rock Lab 1 software are shown in Table 5.8.

In order to classify the rock mass along HRT alignment, all required parameters such as; orientation, spacing, opening, roughness, the degree of weathering, filling, stress reduction factor and groundwater conditions were collected from each segment. The above mentioned classifications parameters of Bieniawski (1989) and Barton et al. (1974) are computed in order to assign empirical value of each geotechnical rock mass unit. The rock mass quality is described based on Table 5.6. Accordingly, RMR computed value of Gtu-1 rock mass unit lies “good” rock (64 – 71) and for rock mass Gtu-2 (0+1084 -13+500) this value describes “fair to good” quality (50-63). According to computed value of Q system, rock mass quality for Gtu-1 lies between “fair” to “very good” (9.1 - 60.66), for Gtu-2 (0+1084 - 2+675) the value lies between “fair” to “very good” (6.67-40.03) and also for Gtu-2 (2+675 – 13+500) the rock mass quality is described from “poor” to “good” (3.26-19.58).

Table 5.6 Classification of rock mass based on RMR and Q-values (Modified after Bieniawski, 1989 and Barton et al 1974).

| Q-system | | RMR | |
|------------|----------------------------|--------|----------------------------|
| Rating | classification/Description | Rating | classification/Description |
| 400-1000 | Exceptionally good | 81-100 | Very Good |
| 100-400 | Extremely good | 61-80 | Good |
| 40-100 | Very good | 41-60 | Fair |
| 10-40 | Good | 21-40 | Poor |
| 4-10 | fair | 0-20 | Very poor |
| 1-4 | poor | | |
| 0.1-1 | Very Poor | | |
| 0.01-0.1 | Extremely poor | | |
| 0.01-0.001 | Exceptionally poor | | |

According to GSI classification, rock mass along HRT alignment is described in the following paragraphs in respect of Hoek et al. (2002). GSI ranges were estimated in Fig.5.3 and Fig.5.4 based on geological description of the two rock unit (BA-3 and BA - 4).Accordingly, averaged GSI value for BA-3 is 74 and this value shows the surface condition of this rock mass is described “good” (rough surface condition and slightly altered). For rock mass (BA-4) mean GSI value is 79 thus, surface very “very good” (very rough un

weathered surface condition).Regarding to the interlocking classification of GSI, both rock mass units are structural characteristics of well interlocked undisturbed rock mass consisting of cubical blocks formed by three intersecting discontinuity sets with “good” to “very good” surface condition (Fig. 5.3 and Fig.5.4).

Hoek and Brown (2002) developed an empirical approach to determine the strength of the jointed rock mass and formulated a failure criterion for jointed rock mass. For the present study Rock mass strengths were calculated using the principles outlined in the generalized Hoek-Brown failure criterion with the required parameter obtained from core logging and laboratory testing results. Hence, based on the value of GSI, evaluation of the rock mass strength has been executed by using Rock Lab software as shown in Fig.5.3 and Fig.5.4. Accordingly, brief information of the rock mass strength parameters is presented in Table 5.8.

Table 5.7 Summary of rock mass classification result for each geotechnical rock mass unit

| Chainage (station) m | Geotechnical unit | Lithology | Rock mass classification | | | | | | | | |
|----------------------|-------------------|-----------|--------------------------|------|------|----------|-------|-------|------|------|------|
| | | | RMR | | | Q system | | | GSI | | |
| | | | Min. | mean | Max. | Min. | mean | Max. | Min. | mean | Max. |
| 0 +000 to 1+084 | Gtu_1 | BA_4 | 64 | 67.5 | 71 | 9.1 | 34.88 | 60.66 | 67 | 74 | 80 |
| 1+084 to 2+675 | Gtu_2 | BA_3 | 54 | 58.5 | 63 | 6.67 | 23.35 | 40.03 | 77 | 79 | 81 |
| 2+675 to 14+500 | Gtu_2 | BA_3 | 50 | 55 | 60 | 3.26 | 11.42 | 19.58 | 77 | 79 | 81 |

Table 5.8 Summary of Rock mass parameters obtained from analyzing geotechnical rock mass along HRT by using Rock Lab 1 software

| Parameters | Geotechnical rock mass along HRT | |
|---|----------------------------------|----------------------------------|
| | BA-4 | BA-3 |
| Input parameters | | |
| Geological strength index(GSI) | 67 – 80 (average value is 74) | 77 – 81 (average value is 79) |
| Intact rock strength (σ_{ci}) Mpa | 181.21 | 191.26 |
| Hoek-Brown constant (mi) | 25 | 25 |
| Intact rock deformation Modulus(E_i)Mpa | 63423.5 | 66941 |
| Tunnel depth(m) | 62 | 153 |
| Disturbance factor | 0 | 0 |
| Rock mass parameters | | |
| Rock mass compressive strength(σ_{cm}) Mpa | 42.62 | 59.469 |
| Rock mass tensile strength (σ_{cm})Mpa | -1.021 | -1.571 |
| Deformation modulus(E_m) Mpa | 50815.5 | 58175.96 |
| Hoek-Brown failure criteria | | |
| Rock mass parameter | | |
| mb | 9.878 | 11.809 |
| S | 0.0556 | 0.0970 |
| A | 0.501 | 0.501 |
| Mohr-Coulomb fit | | |
| Friction angle(ϕ) degree | 67.21 | 64.72 |
| Cohesive strength (c') Mpa | 4.048 | 6.177 |

5.7.2 Discussion on Geophysical Data Results

Based on the result of 2D resistivity imaging survey conducted in the study area, the weathering condition, ground water and anticipated geological structures of HRT is interpreted in detail in 5.4. in this section the interpretation of each surveying line is summarized.

The relatively low resistivity zones, marked with an elliptical outline, on the resistivity imaging section of survey lines are interpreted as the ground may be highly weathered and fractured as compared to the other sub-surface. these zones are intercepted on surveying line-1 (between electrode 47 and 65, 118 and 133, 197 and 214), on survey line-2 (between electrode 19 and 32, 39 and 49, 99 and 114, 153 and 167), survey line-3 (between electrode 45 and 68, 73 and 87, 157 and 182) and survey line-4 (between electrode 58 and 82, 88 and 103, 109 and 132, 197 and 217).

Regarding to ground water condition of HRT, low resistivity value was obtained on survey line-1 at the electrode number 95 and 180, on line-2 at electrode number 25 and 175, on line-3 at electrode number 17 and 115 and 170 and, on line-4 at the electrode number, 25 and 163. This low resistivity values and presence of existing streams shows that on these areas there is high possibility for the occurrence of groundwater.

Furthermore, geophysical inferred geological structure as there is high resistivity contrast on the labeled line as seen from the all pseudo-sections on the electrode numbers specified below the anticipated structures are expected lied. These structures are expected on survey line-1 (at electrode numbers 20, 145 and 165), on line-2 (at electrode numbers 50, 80 and, 115), on line-3 (at electrode numbers 20, 30, 90 and 125) and on line -4 (at the electrode numbers 34, 50, 159, 170, 195 and 225). According to the interpretation result of the 2D resistivity imaging survey HRT, it is considered that the bedrock around Wabe River is composed of moderately weathered basaltic rocks.

5.7.3 Remote Sensing Interpretation

According to Sabins (1996) remote sensing imagery have importance to use for the preparation of maps of terrain classification, interpretation of geological structure, geomorphologic studies, regional engineering soil maps, maps used for route selection, regional inventories of construction materials, groundwater studies, and inventories of drainage networks and catchment areas.

For the present study determination of land forms and reliefs were undertaken. Accordingly, Google Earth image (Fig. 5.7) and digital elevation model (DEM) visualization and interpretation have been used and, faults, shear zones and weak zones were identified in the project area as shown in Fig. 5.9 and Fig. 5.10. Further, an attempt has been made in order to check topographic suitability of HRT using remote sensing with Norwegian rule of thumb rule in tunnel entrance and near to penstock (it is discussed in chapter six).thus, as shown in Fig.5.7, Fig.5.8 and Fig.6.2 the study area is suitable with respect to topographic condition.

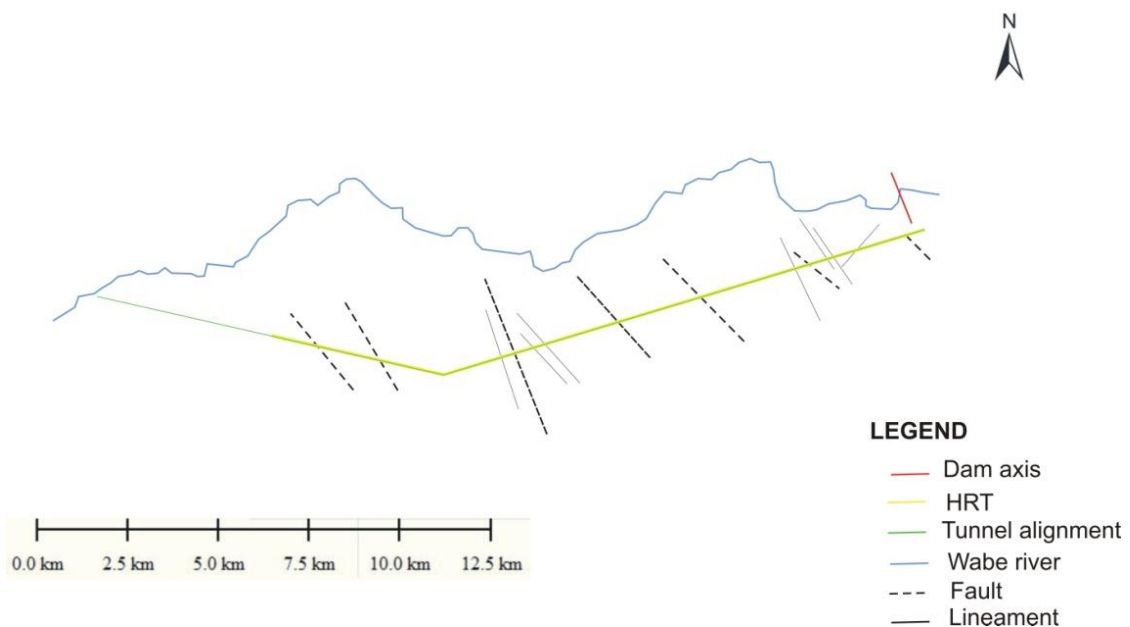


Fig.5.9 Geological structures extracted from DEM (resolution 20m) along HRT tunnel

5.7.4 Overall Assessment of HRT Suitability

For the present study, geological mapping were under taken along the study area and detailed description on each geological unit was presented in previous section (chapter three). Geological and engineering geological study along HRT alignment reveals that HRT drives through two geotechnical units. These rock units are BA-3 (fresh to slightly weathered massive to weakly jointed rock mass) and BA-4 (slightly weathered and fresh rock mass with closely to widely spaced joints). The rock quality expressed in RQD (based on [Deere et al. 1967](#)) which is obtained from the core drilling for BA-3 unit rock quality ranges from “good” to “very good” rock quality (89 to 92%) while BA-4 is “very good” rock quality (91%).

[Bieniawski in 1993](#) states rock mass classification provides a checklist of key parameters for each rock mass type (domain) i.e. it guides the rock mass characterization process.

Classification results in quantitative information for design purposes and enables better engineering judgment and more effective communication on a project. For this thesis, Rock mass classification systems such as, Rock mass rating (RMR) (Bieniawski, 1989), Q – system (Barton et al., 1974), and Geological strength index (GSI) (Hoek et al., 2002) were practiced along HRT alignment, as presented Table 5.7 and 5.8. According to computed averaged RMR value of Gtu-1 and Gtu-2 rock mass unit shows the rock quality lies under “good” and “fair” rock respectively. Similarly, averaged Q-system rating value describes both rock mass unit lies under “Good” rock.

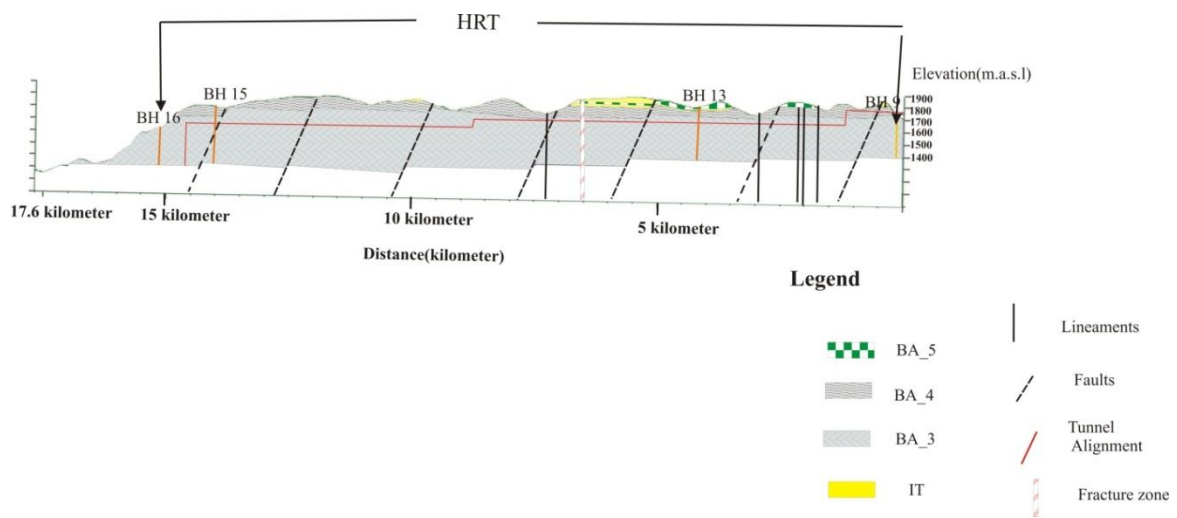


Fig.5.10 Cross section along HRT alignment showing geotechnical rock units and various structures

According to Bell (2007) measurements of the uniaxial compressive strength (UCS) and the vertical stress, showed that overstressing always occurred where the ratio was lower than 2.5. For the present study, remote sensing evaluation of the HRT alignment in respect to topographic shows BA-4 overburden stress ranges from 24 to 99 m and for BA-3 it ranges from 63 to 242 m (as shown in Fig.5.8). So, the major principal stress σ_1 ranges from 0.672 to 8.168 MPa. Since the uniaxial compressive strength values of the rock from boreholes BA-3 and BA-4 are approximately 166.764 MPa and 189.95 Mpa, respectively therefore, the ratio of σ_c / σ_1 varies from 99.45 - 282.66 for rock mass BA-4 and 43.88 - 20.416 for BA-3.

Therefore, along HRT alignment there is no probability of overstressing with respect to topography.

Nilsen and Dahl (1994) states there are possible stability problems associated with weakness zones such as, (i) Cave-in at the working face during tunneling, (ii) Instability at the working face, (iii) Water inflows into the tunnel, (iv) Swelling of smectite, especially when smectite

occurs in combination with other problem- minerals like calcite (solvable) and chlorite (low friction) and(v) Cave-in after completion.

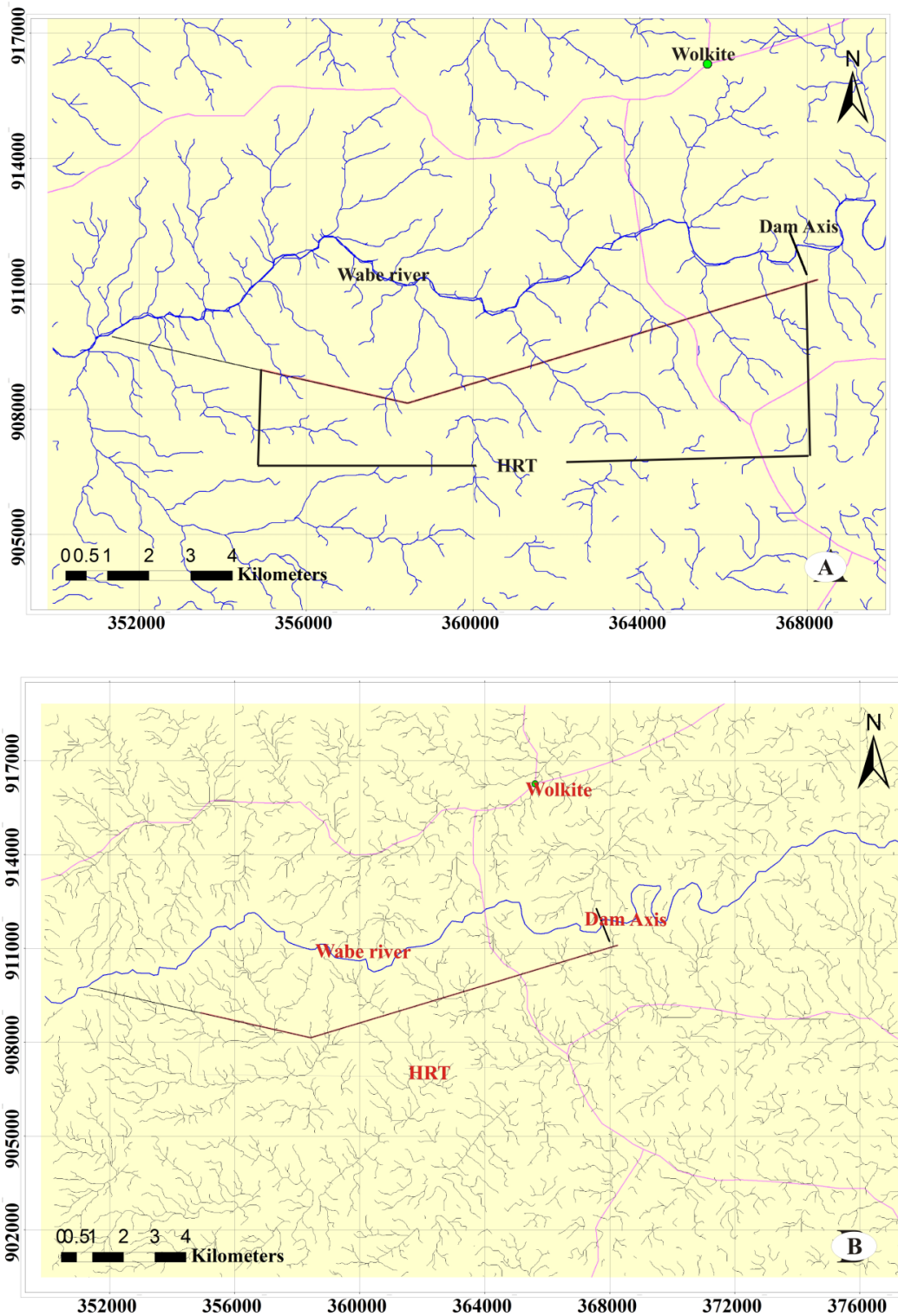


Fig.5.11 (a) drainage patterns map showing drainage systems that cross HRT and (b) ridges along HRT route that indicate geological structures

Geological features are any alignment of features on satellite images such as the various types recognized including topographic, drainage, vegetative, and color alignments. The drainage pattern is apparently being controlled by such structures (Abdullah et al., 2013). Lineaments are linear geological features on the Earth's surface, usually related to the subsurface phenomena or large fractures and faults where their orientation and number give an idea of fracture pattern of rocks (Arlegui, L.E. and Soriano, M.A., 1998). Accordingly, faults were mapped along HRT alignment using drainage patterns and ridgelines (see Fig.5.11 (a) and (b)) as an indicator in addition to geophysical study and field survey.

For the present study, integrated study of remote sensing, field work and geophysical study were undertaken along HRT alignment. Thus, the result reveals the HRT alignment topography is affected by large drainages (see Fig.5.11 (a)) which run across the water way at different locations and seven normal faults and six fractures were identified.

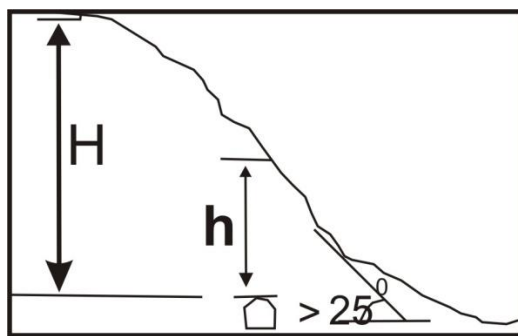
As shown in Fig. 5.9 and 5.10 these geological structures will cross the HRT axis and their orientations are parallel to whole or parts of the tunnel route which trends WNW - ESE. So, engineering geological condition of these structures shows unsafe, highly unfavorable and undesirable where the tunnel is parallel to this orientation.

Moreover, detail analysis of HRT alignment rock support recommendation based on empirical rock mass classification system is presented in chapter six. In this chapter also slope stability condition of Tunnel entrance and surge shaft by kinematics check are evaluated.

CHAPTER – 6 HEADRACE TUNNEL SUITABILITY AND SUPPORT ANALYSIS

6.1 HRT Topographic Condition

According to an Old Norwegian rule of thumb, stress induced problems may arise when the valley side inclination exceeds 25° and the depth of the valley is 500 m or more as shown in Fig. 6.1. When the surface is not horizontal the topography will influence the rock stresses situation. In high valley sides, where hydropower is often located, the stresses situations are totally dominated by topographic effects. In such cases the major principle stress (σ_1) near the surface will be more or less parallel to the valley slope, the minor principle stress (σ_3) will be approximately perpendicular to the slope of the Valley (Nilsen and Thidemann, 1993).



For the present study attempt was made in order to check topographic suitability of HRT using Norwegian rule of thumb rule in tunnel entrance and near to penstock with the aid of remote sensing techniques. Accordingly, as shown in Fig. 6.2 it is suitable.

Fig.6.1 Effect of valley side on stress condition in tunnel

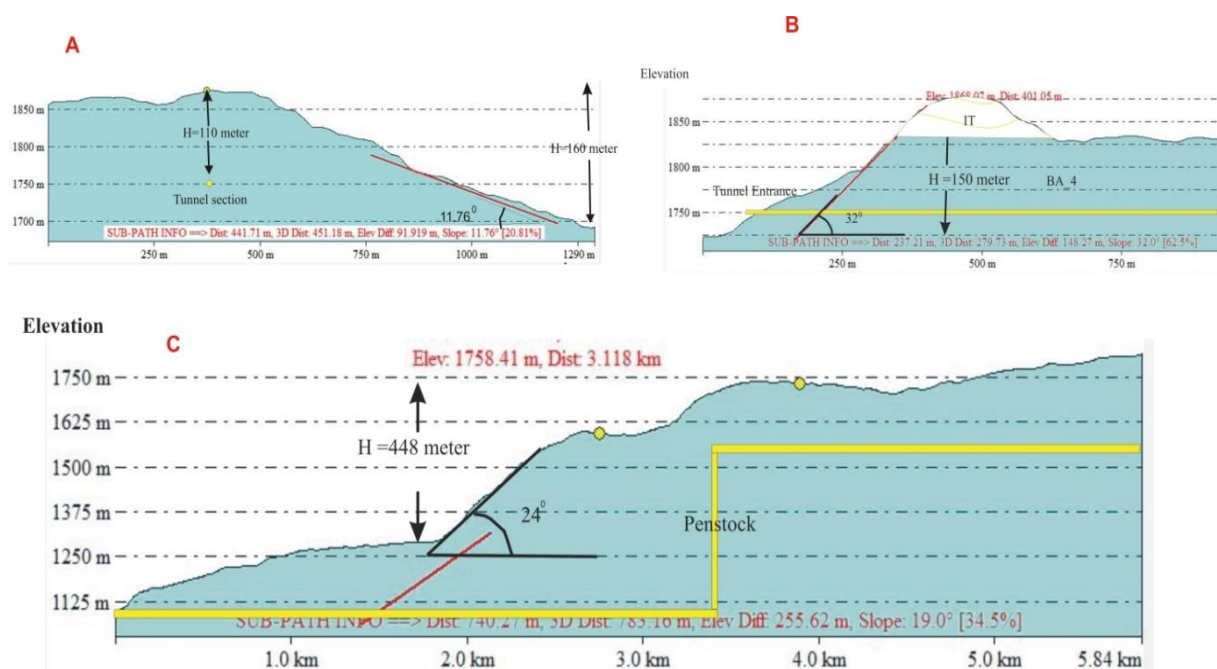


Fig.6.2 Topographic analysis results A) section of near Tunnel entrance. B) HRT entrance profile and C) Tunnel profile near to penstock.

6.2 Kinematic Check

In the present study near to the slope of tunnel entrance and penstock there was lack of joint exposure. However, attempt was made to check the slope stability through kinematic check by using joints exposed along the HRT section. For kinematic analysis structural data, along with slope inclination and a ‘phi circle’ corresponding to angle of friction of the rock mass has been plotted on the equal angle low hemisphere projection. For this purpose, the angle of friction has been estimated from the GSI data. Fig. 6.3 presents the stereo plots to demonstrate Markland test (Markland, 1972) for abutment slope sections. In a rock slope the failure will only occur if the following conditions are satisfied (Markland, 1972; Hoek and Bray, 1981; Sharma et al., 1995; Raghuvanshi, 2019);

$$\text{Plane failure } \alpha f > \alpha p > \phi \quad \dots\dots\dots \text{eq. 6.1}$$

$$\text{Wedge failure } \alpha f > \alpha i > \phi \quad \dots\dots\dots \text{eq. 6.2}$$

Where; αf is the slope angle, αp is the dip of the potential failure plane, αi is plunge of the line of intersection and ϕ is the angle of internal friction of the two wedges forming plane.

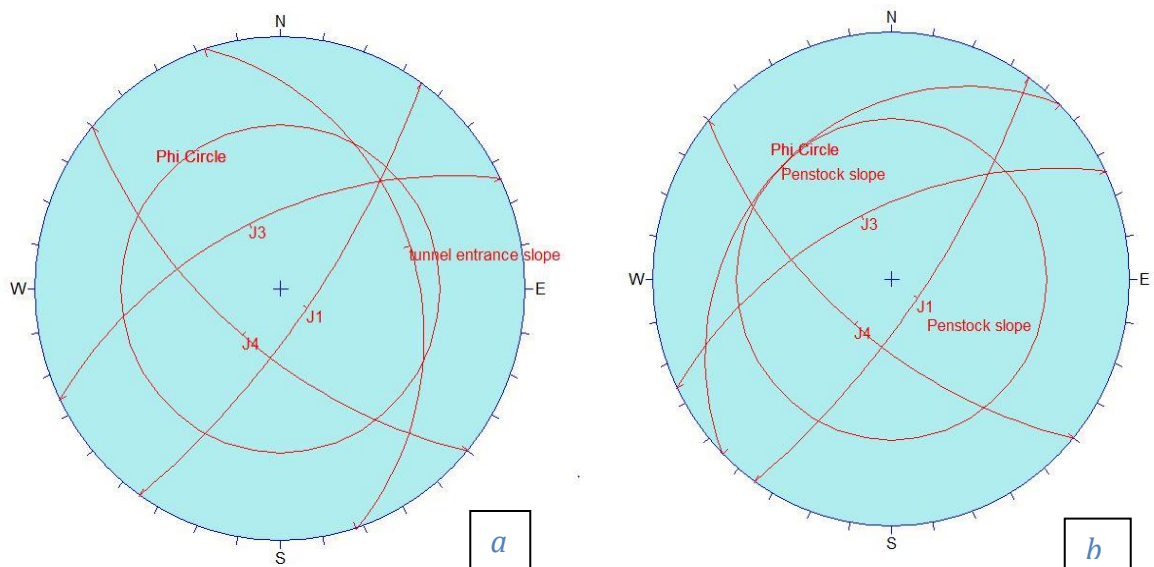


Fig.6.3 Kinematics check for potential mode of failure (a) for tunnel entrance slope. (b) for slope near to penstock

In order to perform kinematic check, three major joints were considered ($75^{\circ}/125^{\circ}$, $58^{\circ}/334^{\circ}$ and $63^{\circ}/220^{\circ}$). Tunnel entrance slope angle and dip of the potential slope angle is 32° and 72° whereas for penstock slope angle and dip of potential slope angles are 315° and 24° . According to kinematics check analysis, both slope sections do not satisfy condition for plane mode of failure. However, there is a possibility for wedge mode of failure in the tunnel entrance slope whereas; there is no potential for wedge failure near to the penstock slope. It has been found that the road slope cut at the left side slope sections satisfy the kinematics condition for wedge mode of failure defined by joints J2 and J3. In the present study this analysis was made with limited point structural data and along HRT alignment. Therefore, it is recommended to make a detailed slope stability analysis during excavation and construction period, where there will be rock exposure and detailed structural data on both of the abutments will be available.

6.3 Engineering Geological Evaluation and HRT Support Analysis

Different rock mass classification systems provide significant input to design rock engineering parameters for tunnel support analysis (Panda et al., 2014). In the present study, tunnel supports are recommended based on values as obtained from RMR (Bieniawski, 1989) and Q (Barton et al., 1974) classification systems. Table 6.1 shows summary of Rock mass classification values that were used for HRT support recommendation.

Table 6.1 Summary of Rock mass classification results

| Rock mass class classification | Geotechnical rock unit | |
|--------------------------------|------------------------|--------------|
| | BA-4 | BA-3 |
| GSI value range | 67 – 80 | 77 – 81 |
| RMR ₈₉ value range | 64 – 71 | 50 – 63 |
| Q system value range | 9.1 – 60.6 | 3.26 – 40.03 |

6.3.1 Recommended HRT Support Based on RMR

For the present study, the excavation and support systems were worked out using guidelines in accordance with RMR classification system. In-situ stress, shape of the tunnel and excavation methods is the main factors affecting the guidelines of rock reinforcement (Bieniawski, 1989). As shown in Table 6.2 (marked as blue color box) permanent supports were recommended based on support guidelines (Table 2.3, Chapter 2) after computing RMR values for geomechanical rock mass units.

For BA-4, RMR value ranges from 64 to 71 which indicate good rock mass class. Thus, Table 6.2 suggests that HRT could be excavated by Full face, 1–1.5 m advance and to complete support 20 m from the face. Locally, bolts in crown 3m long, spaced 2.5 m with

occasional wire mesh is recommended. Similarly, For BA-3, RMR value ranges from 50 to 63 which indicate fair to good rock mass. Therefore, for fair rock mass class Table 6.2 suggests that HRT could be excavated by top heading and bench, with a 1.5 to 3 m advance in the top heading. Support should be installed after each blast and the support should be placed at a maximum distance of 10 m from the face. Systematic rock bolting, using 4 m long 20 mm diameter fully grouted bolts spaced at 1.5 to 2 m in the crown and walls, is recommended. Wire mesh, with 50 to 100 mm of shotcrete for the crown and 30 mm of shotcrete for the walls, is recommended.

Table 6.2 Estimated support and excavation based on Guidelines for excavation and support of 10 m span horseshoe shaped rock tunnels constructed using drill and blast method at a depth of < 900 m, in accordance with the RMR system (after Bieniawski, 1989) *

| Rock mass class | Excavation | Rock bolts (20 mm diameter, fully grouted) | Shotcrete | Steel sets |
|----------------------------------|--|--|--|---|
| I- Very good rock RMR: 81–100 | Full face, 3 m advance | Generally, no support required except spot bolting | | |
| II- Good rock RMR: 61–80 | Full face, 1–1.5 m advance complete support 20 m from the face. | Locally, bolts in crown 3m long, spaced 2.5 m with occasional wire mesh | 50 mm in crown where required | None |
| III- fair rock RMR: 41–60 | Top heading and bench 1.5–3 m advance in top heading. Commence support after each blast. Complete support 10m from the face. | Systematic bolts 4 m long, spaced 1.52 m in crown and walls with wire mesh in the crown. | 50–100 mm in crown and 30 mm insides | None |
| IV- Poor rock RMR: 21–40 | Top heading and bench 1.0–1.5 m advance in top heading Install support currently with excavation, 10 m from the face. | Systematic bolts 4–5 m long, spaced 1–1.5 m in crown and wall with wire mesh | 100–150 mm in crown and 100 mm insides | Light to medium ribs spaced 1.5m where required |
| V- Very poor rock RMR: <20 | Multiple drifts 0.5–1.5 m advance in top heading. Install support currently with excavation. Shotcrete as soon as possible after blasting. | Systematic bolts 5–6 m long, spaced 1–1.5 m in crown and walls with wire mesh, Bolt invert | 150–200 m in the crown, 150 mm in sides, and 50 mm on the face | Medium to heavy ribs spaced 0.75 m with steel lagging and forepoling if required. Close invert. |

* Shape: horseshoe. Width: 10 m. Vertical stress: 25 MPa. Construction method: drilling and blasting.

6.3.2 Recommendation for HRT Support Based on Q System

For the present study Q value is also applied in addition to RMR value to estimate the support measure for a tunnel of a given dimension, and the usage of excavation by defining the Equivalent Dimension (De) of the excavation (Barton et al., 1974). This was computed by using equation 2.21. For the HRT alignment, ESR was determined from Table 2.5, Chapter 2 and the value of ESR was taken as 1.6. Therefore, for an excavation span of 5 m, the equivalent dimension, $De = 5/1.6 = 3.12$.

Therefore, using the computed value of De and by plotted it against Q value support categories were determined from chart (Fig. 6.3 updated by Grimstad and Barton, 1993).

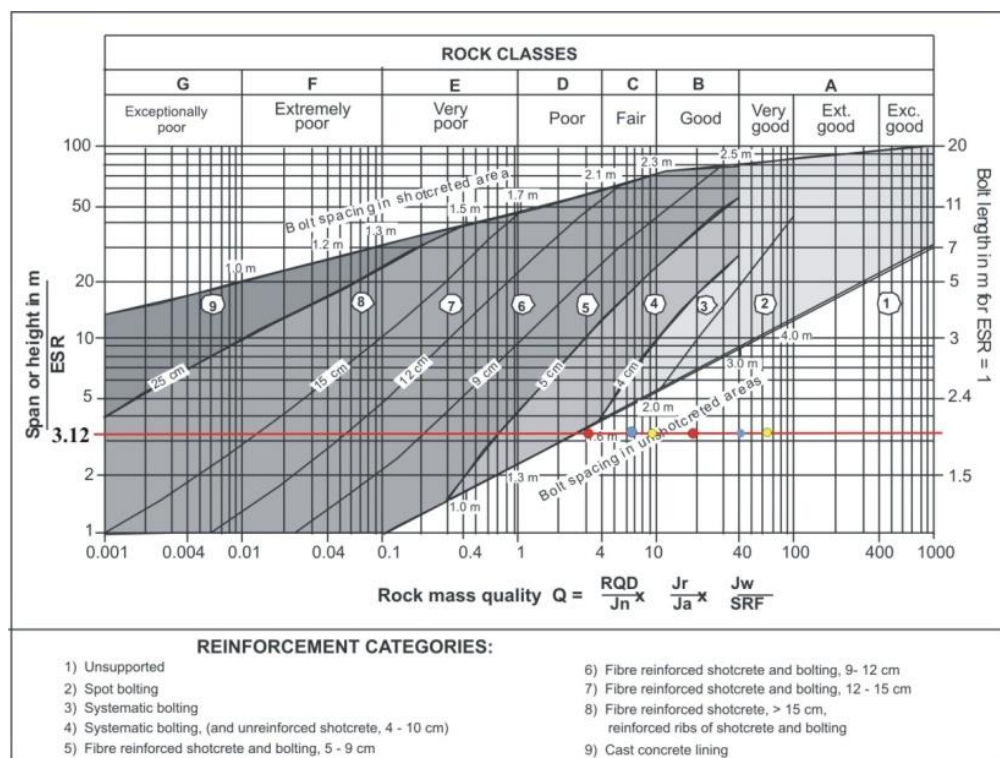


Fig.6.4 Estimated support categories on the bases of the tunneling quality index Q (After Grimstad and Barton, 1993, reproduced from Palmstrom and Broch, 2006).

Table 6.3 Maximum unsupported span and reinforcement categories for geotechnical rock mass unit (according to Q system)

| Geomechanica rock unit | Q value | Excavation support ratio (ESR) | Equivalent dimension (De) in m for 5m excavation span | Length of rock bolt (L) in m | Maximum unsupported span (Smax) in m | Reinforcement category |
|------------------------|--------------|--------------------------------|---|------------------------------|--------------------------------------|------------------------|
| BA_4 | 9.1 - 60.6 | 1.6 | 3.12 | 1.72 | 7.74 – 16.52 | 1 (unsupported) |
| BA_3 | 6.67 - 40.03 | 1.6 | 3.12 | 1.72 | 6.83 - 14 | 1 (unsupported) |
| | 3.26 - 19.58 | 1.6 | 3.12 | 1.72 | 5.13 – 10.51 | 1 (unsupported) |

Barton et al (1980) also proposed empirical relationships to determine rock bolt length (L) and maximum unsupported spans (Smax). L and Smax were determined based on equation 2.22 and 2.23, respectively in order to supplement the support recommendations. Therefore, the computed values of L and Smax are listed in Table 6.3.

According to support guidelines of Q system presented by Grimstad and Barton, 1993, both rock units falls in unsupported reinforcement category for excavation span of 5 m.

6.4 Summery on General Suitability of HRT

The topography head difference between the intake and the power house is about 650m. The tunnel axis orientation varies S 730° W and N 78° W direction (see Fig.6.4) with bed slope 0.1 % (5.7°).The proposed HRT will be excavated through Basaltic rock with rock mass classification and characterization of” Fair” to “Good”. According to the results of the rock mass classifications, the possible underground excavation rock supports for the proposed tunnel suggested and the details are presented in the above sections (Table 6.2 and Table 6.3).

From integrated study of remote sensing and engineering geological study, detailed geological features were identified and mapped along natural rock exposures at the surface (see Fig.5.9).In the study area, faults were observed to be striking northwest and south west, dipping from 65 to 80°. These faults were characterized to have vertical displacement (throw) ranging from 10 and 20 m. Fractures (linear structures) in the present study area are mainly represented by three dominant systems. These are; (i) NNW to NW (320°-330°) striking, (ii) WNW (280°-300°) striking, and (iii) NE (030°-040°) striking.

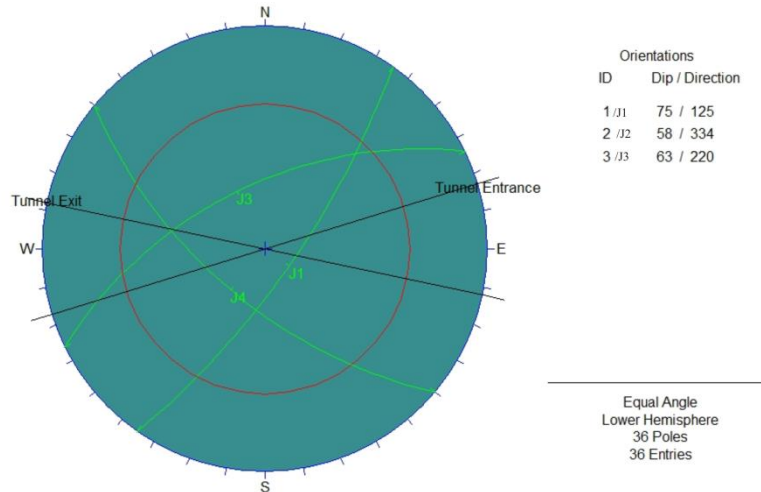


Fig.6.5 stereographic plot of major joint set and tunnel axis orientation

According to Bell (2007) faults generally mean non-uniform rock pressures on a tunnel and generally problems increase as the strike of a fault becomes more parallel to the tunnel opening. So, the intercepted faults along HRT alignment were within unsafe condition with respect to tunnel axis orientation. Thus, based on the recommendation of Bell (2007) necessitate special treatment at times is recommended such as the construction of box sections with invert arches.

Furthermore, the stereographic projection of joints measured along the HRT alignment and the rock mass consists of five sets joints with dip amount/dip direction; J1:75°/125°, J2: 67°/021°, J3: 58°/334°, J4: 65°/258° and J5:63°/220°. As discussed in chapter five (Fig.5.1 and Fig.5.2) the mean joint orientation lies under favorable with respect to tunnel axis.

Remote sensing data products (aerial photographs and satellite images) give direct information on the landscape - the surface features of the Earth, and therefore geomorphological investigations are most easy to carry out based on such data (Gupta,2018). Besides, terrain condition of HRT was carried out using Norwegian rule of thumb rule in tunnel entrance and near to penstock. Accordingly, as shown in Fig. 6.2 it is suitable terrain condition on selected slope.

CHAPTER – 7

CONCLUSION AND RECOMMENDATIONS

7.1 Conclusion

Wabe hydropower project is proposed to be constructed across Omo River for the intended use of hydropower production. The project envisages a 4m diameter modified-horse shoe shaped, 15,821m long horizontal head race tunnel (HRT), a pressurized penstock with 3.2m diameter, and 1394 m long horizontal and 300m vertical shaft tunnel. At downstream end of the pressurized penstock it trifurcates into three 1.8m diameter steel pipes through a manifold to join the turbine. Each turbine will have an installed capacity of 150 MW (ECDSWC, 2019).

For the present study, remote sensing application and mainly engineering geological methods were integrated for evaluation of HRT. Generally, this work encompasses geological mapping at a scale of 1:5000, geostructural surveying, geophysical data analysis, rock mass Classifications, and rock mechanics tests. Besides, topographic condition of tunnel entrance and slope near to penstock was evaluated and according to Old Norwegian thumb rule these slopes were topographically evaluated for its suitability for HRT alignment.

Remote sensing, geophysical investigations and engineering geological integration study shows that there are seven normal faults and six fractures that will cross the HRT axis and the intercepted structures were within unsafe condition with respect to tunnel axis orientation.

According to the information obtained from the field and rock material properties determined in the laboratory, rock mass along HRT has been assessed. Further, the rock mass was classified through three rock mass classification systems i.e., Rock mass rating (RMR) (Biniawski, 1989), Tunneling quality index (Q system) (Barton et al., 1974), and Geological strength index (GSI) (Hoek et al., 2002). Based on the result, two major geotechnical units (BA-3 and BA-4) have been identified. These units are basically classified based on their engineering properties directly related to the degree of rock mass weathering, nature of discontinuities and the intact rock strength, through which the most significant parameters influencing the behavior of the rock mass can be defined. The results of rock mass classification through Q system indicates that the rock mass quality in general varies from poor to very good whereas classification through RMR system indicates that the rock mass quality in general varies in the range of Fair to good. The GSI value for rock mass ranges from 67 to 81 which suggest rock mass to be good blocky undisturbed to very good massive rock.

Further, BA-4 geotechnical rock unit was classified as good rock by RMR. Thus, the HRT within BA-4 rock unit could be excavated by Full face, 1–1.5 m advance complete support 20 m from the face. Also, locally, bolts in crown 3m long, spaced 2.5 m with occasional wire mesh is recommended. Similarly, BA-3 was classified as fair to good rock mass by RMR classification. Therefore, the HRT within BA-4 rock unit could be excavated by top heading and bench, with a 1.5 to 3 m advance in the top heading. Support should be installed after each blast and the support should be placed at a maximum distance of 10 m from the face. Systematic rock bolting, using 4 m long 20 mm diameter fully grouted bolts spaced at 1.5 to 2 m in the crown and walls, is recommended. Also, wire mesh, with 50 to 100 mm of shotcrete for the crown and 30 mm of shotcrete for the walls, is recommended.

The result obtained from Q system indicates that Q value for BA-4 in general varies from 9.1 to 60.6 and for rock mass unit BA-3 it ranges from 3.26 to 19.58. Thus, on the basis of above rating values for 5 m excavation span, the support assessment shows that the HRT lies in unsupported category. Further, GSI rock mass classification was undertaken using RockLab software and the result indicates GSI values to range from 67 to 81. Further, these values were utilized for strength and deformation modulus estimation based on [Hoek and Brown \(2002\)](#).

From the result of 2D resistivity imaging survey conducted along HRT alignment, the geological material is classified according to resistivity value and it is considered that the bedrock of study area is composed of moderately weathered basaltic rocks. In addition, terrain condition of HRT was carried out using Norwegian rule of thumb rule in tunnel entrance and near to penstock. Accordingly, it is suitable terrain condition on selected slope.

Based on the outcome from the present study, the site is found reasonably feasible for the proposed HRT alignment except the intercepted geological structures and from the findings recommendations are forwarded.

7.2 Recommendations

This study was undertaken as a study for academic purpose under various limitations within it. The main technical limitation encountered was limited rock exposures to obtain sufficient joint exposures, especially around tunnel entrance and on penstock slope. Besides, during the field work (January, 2019) for the present study proposed geotechnical core drilling investigation work by ECDSWC has not accomplished.

Based on the present study following recommendations are forwarded;

- ✚ The present study documents systematic study on geological and geotechnical conditions evaluation for the design of the tunnel project. Additional research or study is recommended for a better understanding of the engineering geology of HRT, surge shaft and tunnel entrance for reliability of geotechnical design parameters and tunnel excavation and support of the project.

- ✚ In accordance to Traditional Norwegian tunneling philosophy, it is allowed a relative large extent of the investigations to be undertaken during construction. Investigations made during construction like tunnel face mapping which provides detailed information as a basis for particular decisions to be taken. Therefore, this study recommends construction stage investigation should be carried out for more detailed information on geological and geotechnical conditions.

REFERENCE

- Abbate, E. and Sagri, M. (1980). Volcanites of Ethiopian and Somali plateaus and major tectonic lines, *Atti-convegni Lincei*.**47**: 219-227.
- Abbate, E., Bruni, P. and Sagri, M.(2015). Geology of Ethiopia: a review and geomorphological perspective. *World geomorphological landscapes*. **8**:33-64.
- Abebe Tsegaye, Mazzarini, F., Innocenti, F. and Manetti, P. (1998). The Yerer-Tullu Wollel Volcano-tectonic Lineament: a trans tensional structure in central Ethiopia and the associated magmatic activity. *Journal of African Earth Sciences*.**26**: 135-150.
- Abdullah, A., Nassr, S. and Ghaleeb, A. (2013). Remote Sensing and Geographic Information System for Fault Segments Mapping a Study from Taiz Area , Yemen. *Journal of Geological Research*.1 – 16.
- Anon. (1999). *Code of Practice on Site Investigations, BS 5930*. British Standards Institution, London, 206 pp.
- Anon. (1979). Classification of rocks and soils for engineering geological mapping. *Bulletin of the International Association of Engineering Geology*.**19**: 364–371.
- Arlegui, L.E. and Soriano, M. A. (1998). Characterizing lineaments from satellite images and field studies in the central Ebro basin (NE Spain). *International Journal of Remote Sensing*. **19** (16): 3169–3185.
- American Standard for Testing Material (ASTM) (1993). *Annual book of ASTM standards*. American Society of Testing and Materials. West Conshohocken, PA.
- Barton, N., Løset, F., Lien, R., and Lunde, J. (1980). Application of the Q-system in design decisions. **In: Bergman, M., ed., Subsurface space, 2**: New York Pergamon. 553-561.
- Bell, F. G. (2007). *Engineering geology*. Amsterdam, Elsevier, 581 pp.
- Barton, N.R., Lien, R., and Lunde, J. (1974). Engineering classification of rock masses for the design of tunnel support. *Rock Mechanics journal*. **6**:189-239.

- Bieniawski, Z.T. (1993) Classification of rock masses for engineering: The RMR system and future trends. **In:** *Hudson, J.A., ed.*, pp.553-573. *Comprehensive Rock Engineering, Volume 3: Oxford, Pergamon Press, New York.*
- Bieniawski, Z.T. (1989). *Engineering Rock Mass Classifications*. Wiley, New York, 251 pp.
- Bieniawski, Z.T. (1976). The Geomechanics Classification in Rock Engineering Applications. *proc. 4th Inter. Cong. Rock., Montreux., 2:36-48.*
- Bieniawski, Z.T. (1973). Engineering classification of jointed rock masses. *Transaction of the South African Institution of Civil Engineers, 15:* pp. 335-344.
- Billi, P. (2015). Geomorphological Landscapes of Ethiopia. *World Geomorphological Landscapes*. 3-32 pp.
- Blanford, W.T. (1870). *Observations on the geology and zoology of Abyssinia, made during the progress of the British expedition to that country in 1867–68*. Macmillan, London, 487 pp.
- Bommer, J.J. and Pinho, R. (2006). Adapting earthquake actions in Eurocode-8 for performance-based seismic design. *Earthquake Eng. Structural Dynamics, 35:* pp.29-55.
- Cosar, S. (2004). Application of rock mass classification systems for future support design of the Dim Tunnel near Alanya. Published Ph.D. thesis, Middle East Technical University.
- Davidson, A. and Rex, D.C. (1980). Age of volcanism and rifting in southwestern Ethiopia. *Nature, 283:* 657-658.
- Deere, D.U. (1964). Technical description of rock cores for engineering purposes. *Rock Mechanics Engineering Geology journal. 1:* 17-22.
- ECDSWC (Ethiopian Construction Design and Supervision works Corporation) (2019). Pre-feasibility and feasibility studies of Wabe hydropower project, pre-feasibility main report (final). Unpublished Technical report, ECDSWC, Addis Ababa, Ethiopia, 112 pp.

- ENEL and ELC (Enel Power & Electro Consult) (2004). Gilgel Gibe Hydropower Project Final Report on Project Implementation. Unpublished Technical Report, Addis Ababa, Ethiopia.
- Ephrem Beshawered (2012). Geology of the Akaki area. Geological Survey of Ethiopia Memoir 26, 93 pp.
- FAO (1997). Soil Map of Ethiopia.
- Ganas , A., Pavlides, S. and Karastathis, V. (2005). DEM-based morphometry of range-front escarpments in Attica, central Greece, and its relation to fault slip rates. *Geomorphology*. **65**: (3-4). pp. 301–319.
- Geological survey of Czech (GSC).(2018).Remote sensing data and analysis for geological mapping - quick guide. Unpublished technical report, GSC, Czech. 10 pp.
- Geremew Lamessa, Tilahun Mammo and Raghuvanshi, T. K. (2019). Homogenized earthquake catalog and b- value mapping for Ethiopia and its adjoining regions. *Geoenvironmental Disasters*. 24 pp.
- Giday Wolde Gabriel, Aronson J.L. and Walter, R.C. (1990). Geology, geochronology, and rift basin development in the central sector of the Main Ethiopia Rift. *Geol Soc Am Bull*. **102**:439–458.
- Gregnanin, A. and Piccirillo, A.M. (1974). Considerazioni sulle serie vulcaniche e sulla struttura dell'Altopiano Etiopico centrale. *Mem MusTridentino Sci Nat*. **20**:79–100.
- Grimstad, E., and Barton, N.(1993). Updating the Q-system for NMT. **In: Kompen, Opsahll, and Berg, eds.**, International Symposium on Sprayed Concrete-Modern use of wet mix sprayed concrete for underground support, Norwegian Concrete Association, Oslo.
- Gupta, R.P.(2018). Remote Sensing Geology - Geological applications. *Springer, Verlag Gmbh,Germany*. 291- 415.
- Gupta, R.P. (2003). *Remote sensing geology*, 2nd ed., Springer, Berlin, 655 pp.

- Hoek, E., Carranza-Torres C. and Corkum, B. (2002). Hoek–Brown failure criterion – 2002 Edition. **In:** *Proceedings of the north American Rock Mechanics Society*, pp.267-273, Toronto, Canada.
- Hoek, E. and Brown, E.T. (1997). Practical estimates of rock mass strength. *Int. J. Rock Mech. Min Sci.***34**:1165-1186.
- Hoek, E. and Bray, J.W. (1989). *Rock Slope Engineering*, 3rd ed., Institute of Mining and Metallurgy, London, 358 pp.
- Hoek, E. and Brown, E.T. (1980). *Underground Excavations in Rock*, Inst. of Mining and Metallurgy, Stephen Austin and Sons Ltd., London, 106 pp.
- [https://www.academia.edu/6546821/managing](https://www.academia.edu/6546821/managing_power_house-back-slope-) power house-back-slope- A case study &sa=u&ved.pdf accessed on 20.03.2019.
- <https://www.google.nl/earth/> Accessed on: 1.24.2019.
- <http://www.proceq.com> proceq_silverschmidt_user_manual_en .pdf accessed on 20.02.2019.
- Institute of Geophysics Space Science and Astronomy Addis Ababa University (IGSSA) (2018). Site Specific Seismic Hazard Assessment Draft Report for Wabe Hydropower Project Site. Unpublished technical report, IGSSA, Addis Ababa, Ethiopia, 21 pp.
- Irem, A. (2008). Determination of the rock mass characteristics and support systems of the new Ulus tunnel, Aknkara. Unpublished Msc Thesis, middle east technical university, Ankara. 168 pp.
- Irwin, W. H., Logan, M. H. and Klein, I. R. A. E., 1970 .Tunnel Site Investigations and Geologic Factors Affecting Mechanical Excavation Methods .Retrieved from <http://www.onlinepubs.trb.org/onlinepubs/hrr/1970/339/339-004.pdf> on 10.02.2019.
- International Society for Rock Mechanics (ISRM) (1981). *Rock Characterization Testing and Monitoring* (Brown, E.T, ed.) Pergamon Press Ltd, Great Britain, 211 pp.
- Jeganathan I , C., Pramod, K., Kshama, G., Rahul, D. G., Anand, K. S., Kirti, A. and Ramesh, H. (2017). Remote sensing and GIS for civil engineering applications and remote sensing and GIS for civil engineering applications and human. *International Journal of Advancement in Remote Sensing, GIS and Geography* .**5** (1): 1-18.

- Lu, Y. (2015). Deformation and failure mechanism of slope in three dimensions. *J. Rock Mech. Geot. Eng.* **7**:109–119.
- Marie, J. ,1998. Tunneling: Mechanics and Hazards. Retrieved on 2016 September 9 from <http://www.umich.edu/~gs265/tunnel.html> on 11.04.2019.
- McCann, D.M., Culshaw, M.G. and Fenning, P.J. (1997). Setting the standard for geophysical surveys insite investigation. **In:** *Modern Geophysics in Engineering Geology*, Engineering Geology Special Publication No. 12, McCann,D.M., Eddleston, M., Fenning, P.J. and Reeves, G.M. (Eds.), Geological Society, London, pp. 3–34.
- Mohammad , R. H., Sofyan, R. and Harry, P.(2017). Geotechnical investigation on headrace tunnel construction at hydropower field of papua province. **In:** *The 2nd Join Conference of Utsunomiya University and Universitas Padjadjaran*, pp.66-70.The second Geological Engineering Study Program, Faculty of Earth Technology and Energy, Trisakti University, Jakarta, Indonesia.
- Nilsen, B. and Thidemann, A. (1993). *Hydropower Development - Rock Engineering*, Tapir Press, Trondheim.**9**:156 pp.
- Ocepec, D. (2006). New Trends in Rock Mass Characterization for Designing Geotechnical Structures published Ph.D. thesis Geoinženiringd.o.o.Ljubljana, Slovenia.
- Palmstrom, A. and Einar Broch, E. (2006). Use and misuse of rock mass classification systems with particular reference to the Q-system. *Tunn Undergr Space Technol.* **21(6)**:575–593.
- Panda, M.K., Mohanty, S., Pingua, B M. P. and Mishra, A. K. (2014). Engineering geological and geotechnical investigations along the head race tunnel in Teesta Stage- III hydroelectric project , India. *Eng. Geol.* **181**: 297–308.
- Rahimi , B.,Shahriar, K. and Sharifzadeh, M.(2014).Evaluation of rock mass engineering geological properties using statistical analysis and selecting proper tunnel design approach in Qazvin–Rasht railway tunnel. *Tunnelling and Underground Space Technology.***41**:pp.206–222.
- Ritter, W., 1879, Die Statik der Tunnelgewölbe: Berlin, Springer.

- Rusnak, J. and Mark, C.(2000). Using the point load test to determine the uniaxial compressive strength of coal measure rock. 19th Int. Conf. on ground control in mining, Morgantown, WV, pp.362-371.
- Samuel Kinde & Samson Engeda (2010). Tunnel Collapse of Gilgel Gibe2 Project Engineer's Perspective. Unpublished Report, Addis Ababa, Ethiopia.
- Sarapirome, S., Surinkum, A. and Saksutthipong, P. (2002). Application of DEM data to geological interpretation: Thong Pha Phumarea, Thailand. **In: Proceedings of the 23rd Asian Conference on Remote Sensing.** ACRS 02, Kathmandu, Nepal.
- Serafim, J.L., Pereira, J.P. (1983).Considerations of the geomechanics classification of Bieniawski. **In: Proceedings of the international symposium on engineering geology and underground construction,** 1:33–44. LNEC, Lisbon, Portugal.
- Sharma, V.M. and Saxena, K.R. (2001). *In-Situ Characterization of rocks - measurement and characterization of rock mass jointing.* A. A. Balkema publishers, Tokio, Japan, 40 pp.
- Singh, M., Rao, K S. and Ramamurthy, T. (2002). Strength and Deformational Behavior of a Jointed Rock Mass.*Rock Mechanics and Rock Engineering Journal.*3: 35-39.
- Soldo, L.,Vendramini, M. and Eusebio ,A.(2019).Tunnels design and geological studies. *Tunnelling and Underground Space Technology.* 82–98.
- Strauss A, Bien J, Neuner H, et al.(2020). Sensing and monitoring in tunnels testing and monitoring methods for the assessment of tunnels. *Structural Concrete.* pp.1– 21.
- Syed, A. (2015). *Rock Mass Classification Systems.* Geotechnical Institute and National Centre of Excellence in Geology publishers, University of Peshawar, Freiberg Germany, pp.286.
- Vinassa de Regny, P. (1931). La geologiadelle AlpiDancale. *Boll Soc Geol It.* **50**:1–24.
- Wickham, G.E., Tiedemann, H R. and Skinner, E.H. (1972).Support determination based on geologic predictions, **In: North American Rapid Excavation and Tunneling Conference** (Lane, K.S.A.G., L. A., ed.), pp. 43-64. Society of Mining Engineers of the American Institute of Mining, Metallurgical and Petroleum Engineers, Chicago, New York.

Willow Run Laboratories of the Institute of Science and Technology (WRLIST)
(1972).*Tunnel-Site Selection by Remote Sensing Techniques* (Wagner et al.,ed.) The
University of Michigan,101 pp.

APPENDIX

APPENDIX: A Rock mass classification systems

Table A-1. Rock Mass Classification RMR system ratings (Bieniawski, 1989)

| A. CLASSIFICATION PARAMETERS AND THEIR RATINGS | | | | | | | |
|---|--------------------------------------|--|---|--|--|--|--|
| Parameter | | Range of values | | | | | |
| 1 | Strength of intact rock material | Point-load strength index | >10 MPa | 4 - 10 MPa | 2 - 4 MPa | 1 - 2 MPa | For this low range - uniaxial compressive test is preferred |
| | | Uniaxial comp. strength | >250 MPa | 100 - 250 MPa | 50 - 100 MPa | 25 - 50 MPa | |
| | Rating | 15 | 12 | 7 | 4 | 2 1 0 | |
| 2 | Drill core Quality RQD | | 90% - 100% | 75% - 90% | 50% - 75% | 25% - 50% | < 25% |
| | Rating | | 20 | 17 | 13 | 8 | 3 |
| 3 | Spacing of discontinuities | | > 2 m | 0.6 - 2 . m | 200 - 600 mm | 60 - 200 mm | < 60 mm |
| | Rating | | 20 | 15 | 10 | 8 | 5 |
| 4 | Condition of discontinuities (See E) | | Very rough surfaces Not continuous No separation Unweathered wall rock | Slightly rough surfaces Separation < 1 mm Slightly weathered walls | Slightly rough surfaces Separation < 1 mm Highly weathered walls | Slickensided surfaces or Gouge < 5 mm thick or Separation 1-5 mm Continuous | Soft gouge >5 mm thick or Separation > 5 mm Continuous |
| | Rating | | 30 | 25 | 20 | 10 | 0 |
| 5 | Groundwater | Inflow per 10 m tunnel length (l/m) | None | < 10 | 10 - 25 | 25 - 125 | > 125 |
| | | (Joint water press)/ (Major principal σ) | 0 | < 0.1 | 0.1, - 0.2 | 0.2 - 0.5 | > 0.5 |
| | General conditions | | Completely dry | Damp | Wet | Dripping | Flowing |
| | Rating | | 15 | 10 | 7 | 4 | 0 |
| B. RATING ADJUSTMENT FOR DISCONTINUITY ORIENTATIONS (See F) | | | | | | | |
| Strike and dip orientations | | Very favourable | Favourable | Fair | Unfavourable | Very Unfavourable | |
| Ratings | Tunnels & mines | 0 | -2 | -5 | -10 | -12 | |
| | Foundations | 0 | -2 | -7 | -15 | -25 | |
| | Slopes | 0 | -5 | -25 | -50 | | |
| C. ROCK MASS CLASSES DETERMINED FROM TOTAL RATINGS | | | | | | | |
| Rating | 100 ← 81 | | 80 ← 61 | 60 ← 41 | 40 ← 21 | < 21 | |
| Class number | I | | II | III | IV | V | |
| Description | Very good rock | | Good rock | Fair rock | Poor rock | Very poor rock | |
| D. MEANING OF ROCK CLASSES | | | | | | | |
| Class number | I | | II | III | IV | V | |
| Average stand-up time | 20 yrs for 15 m span | | 1 year for 10 m span | 1 week for 5 m span | 10 hrs for 2.5 m span | 30 min for 1 m span | |
| Cohesion of rock mass (kPa) | > 400 | | 300 - 400 | 200 - 300 | 100 - 200 | < 100 | |
| Friction angle of rock mass (deg) | > 45 | | 35 - 45 | 25 - 35 | 15 - 25 | < 15 | |
| E. GUIDELINES FOR CLASSIFICATION OF DISCONTINUITY conditions | | | | | | | |
| Discontinuity length (persistence) | < 1 m | | 1 - 3 m | 3 - 10 m | 10 - 20 m | > 20 m | |
| Rating | 6 | | 4 | 2 | 1 | 0 | |
| Separation (aperture) | None | | < 0.1 mm | 0.1 - 1.0 mm | 1 - 5 mm | > 5 mm | |
| Rating | 6 | | 5 | 4 | 1 | 0 | |
| Roughness | Very rough | | Rough | Slightly rough | Smooth | Slickensided | |
| Rating | 6 | | 5 | 3 | 1 | 0 | |
| Infilling (gouge) | None | | Hard filling < 5 mm | Hard filling > 5 mm | Soft filling < 5 mm | Soft filling > 5 mm | |
| Rating | 6 | | 4 | 2 | 2 | 0 | |
| Weathering | Unweathered | | Slightly weathered | Moderately weathered | Highly weathered | Decomposed | |
| Rating | 6 | | 5 | 3 | 1 | 0 | |
| F. EFFECT OF DISCONTINUITY STRIKE AND DIP ORIENTATION IN TUNNELLING** | | | | | | | |
| Strike perpendicular to tunnel axis | | | Strike parallel to tunnel axis | | | | |
| Drive with dip - Dip 45 - 90° | | Drive with dip - Dip 20 - 45° | | Dip 45 - 90° | | Dip 20 - 45° | |
| Very favourable | | Favourable | | Very unfavourable | | Fair | |
| Drive against dip - Dip 45-90° | | | Drive against dip - Dip 20-45° | | Dip 0-20 - Irrespective of strike° | | |
| Fair | | | Unfavourable | | Fair | | |

* Some conditions are mutually exclusive . For example, if infilling is present, the roughness of the surface will be overshadowed by the influence of the gouge. In such cases use A.4 directly.

** Modified after Wickham et al (1972).

Table A-2. Description of ratings for input parameters of Q-system (After Barton et al 1974).

| DESCRIPTION | VALUE | NOTES |
|---|-------------------------|---|
| 1. ROCK QUALITY DESIGNATION | RQD | |
| A. Very poor | 0 - 25 | 1. Where RQD is reported or measured as ≤ 10 (including 0), a nominal value of 10 is used to evaluate Q. |
| B. Poor | 25 - 50 | |
| C. Fair | 50 - 75 | |
| D. Good | 75 - 90 | 2. RQD intervals of 5, i.e. 100, 95, 90 etc. are sufficiently accurate. |
| E. Excellent | 90 - 100 | |
| 2. JOINT SET NUMBER | J_n | |
| A. Massive, no or few joints | 0.5 - 1.0 | |
| B. One joint set | 2 | |
| C. One joint set plus random | 3 | |
| D. Two joint sets | 4 | |
| E. Two joint sets plus random | 6 | |
| F. Three joint sets | 9 | 1. For intersections use $(3.0 \times J_n)$ |
| G. Three joint sets plus random | 12 | |
| H. Four or more joint sets, random, heavily jointed, 'sugar cube', etc. | 15 | 2. For portals use $(2.0 \times J_n)$ |
| J. Crushed rock, earthlike | 20 | |
| 3. JOINT ROUGHNESS NUMBER | J_r | |
| a. Rock wall contact | | |
| b. Rock wall contact before 10 cm shear | | |
| A. Discontinuous joints | 4 | |
| B. Rough and irregular, undulating | 3 | |
| C. Smooth undulating | 2 | |
| D. Slickensided undulating | 1.5 | 1. Add 1.0 if the mean spacing of the relevant joint set is greater than 3 m. |
| E. Rough or irregular, planar | 1.5 | |
| F. Smooth, planar | 1.0 | |
| G. Slickensided, planar | 0.5 | 2. $J_r = 0.5$ can be used for planar, slickensided joints having lineations, provided that the lineations are oriented for minimum strength. |
| c. No rock wall contact when sheared | | |
| H. Zones containing clay minerals thick enough to prevent rock wall contact | 1.0 (nominal) | |
| J. Sandy, gravely or crushed zone thick enough to prevent rock wall contact | 1.0 (nominal) | |
| 4. JOINT ALTERATION NUMBER | J_a | ϕ_r degrees (approx.) |
| a. Rock wall contact | | |
| A. Tightly healed, hard, non-softening, impermeable filling | 0.75 | 1. Values of ϕ_r , the residual friction angle, are intended as an approximate guide to the mineralogical properties of the alteration products, if present. |
| B. Unaltered joint walls, surface staining only | 1.0 | 25 - 35 |
| C. Slightly altered joint walls, non-softening mineral coatings, sandy particles, clay-free disintegrated rock, etc. | 2.0 | 25 - 30 |
| D. Silty-, or sandy-clay coatings, small clay-fraction (non-softening) | 3.0 | 20 - 25 |
| E. Softening or low-friction clay mineral coatings, i.e. kaolinite, mica. Also chlorite, talc, gypsum and graphite etc., and small quantities of swelling clays. (Discontinuous coatings, 1 - 2 mm or less) | 4.0 | 8 - 16 |

Conti'd

| 4, JOINT ALTERATION NUMBER | J_a | ϕ/r degrees (approx.) | |
|---|-------------|---|---|
| b. Rock wall contact before 10 cm shear | | | |
| F. Sandy particles, clay-free, disintegrating rock etc. | 4.0 | 25 - 30 | |
| G. Strongly over-consolidated, non-softening clay mineral fillings (continuous < 5 mm thick) | 6.0 | 16 - 24 | |
| H. Medium or low over-consolidation, softening clay mineral fillings (continuous < 5 mm thick) | 8.0 | 12 - 16 | |
| J. Swelling clay fillings, i.e. montmorillonite, (continuous < 5 mm thick). Values of J_a depend on percent of swelling clay-size particles, and access to water. | 8.0 - 12.0 | 6 - 12 | |
| c. No rock wall contact when sheared | | | |
| K. Zones or bands of disintegrated or crushed | 6.0 | | |
| L. rock and clay (see G, H and J for clay | 8.0 | | |
| M. conditions) | 8.0 - 12.0 | 6 - 24 | |
| N. Zones or bands of silty- or sandy-clay, small clay fraction, non-softening | 5.0 | | |
| O. Thick continuous zones or bands of clay | 10.0 - 13.0 | | |
| P. & R. (see G.H and J for clay conditions) | 6.0 - 24.0 | | |
| 5. JOINT WATER REDUCTION | | | |
| | J_w | approx. water pressure (kgf/cm ²) | |
| A. Dry excavation or minor inflow i.e. < 5 l/m locally | 1.0 | < 1.0 | |
| B. Medium inflow or pressure, occasional outwash of joint fillings | 0.66 | 1.0 - 2.5 | |
| C. Large inflow or high pressure in competent rock with unfilled joints | 0.5 | 2.5 - 10.0 | 1. Factors C to F are crude estimates; increase J_w if drainage installed. |
| D. Large inflow or high pressure | 0.33 | 2.5 - 10.0 | |
| E. Exceptionally high inflow or pressure at blasting, decaying with time | 0.2 - 0.1 | > 10 | 2. Special problems caused by ice formation are not considered. |
| F. Exceptionally high inflow or pressure | 0.1 - 0.05 | > 10 | |
| 6. STRESS REDUCTION FACTOR | | | |
| | | SRF | |
| a. Weakness zones intersecting excavation, which may cause loosening of rock mass when tunnel is excavated | | | |
| A. Multiple occurrences of weakness zones containing clay or chemically disintegrated rock, very loose surrounding rock any depth) | | 10.0 | 1. Reduce these values of <i>SRF</i> by 25 - 50% but only if the relevant shear zones influence do not intersect the excavation |
| B. Single weakness zones containing clay, or chemically disintegrated rock (excavation depth < 50 m) | | 5.0 | |
| C. Single weakness zones containing clay, or chemically disintegrated rock (excavation depth > 50 m) | | 2.5 | |
| D. Multiple shear zones in competent rock (clay free), loose surrounding rock (any depth) | | 7.5 | |
| E. Single shear zone in competent rock (clay free). (depth of excavation < 50 m) | | 5.0 | |
| F. Single shear zone in competent rock (clay free). (depth of excavation > 50 m) | | 2.5 | |
| G. Loose open joints, heavily jointed or 'sugar cube', (any depth) | | 5.0 | |

Conti'd

| DESCRIPTION | VALUE | | | NOTES |
|--|---------------------|---------------------|---------|---|
| 6. STRESS REDUCTION FACTOR | | | | SRF |
| b. Competent rock, rock stress problems | | | | |
| | σ_c/σ_1 | σ_t/σ_1 | | 2. For strongly anisotropic virgin stress field |
| H. Low stress, near surface | > 200 | > 13 | 2.5 | (if measured): when $5 \leq \sigma_1/\sigma_3 \leq 10$, reduce σ_c |
| J. Medium stress | 200 - 10 | 13 - 0.66 | 1.0 | to $0.8\sigma_c$ and σ_t to $0.8\sigma_t$. When $\sigma_1/\sigma_3 > 10$, |
| K. High stress, very tight structure (usually favourable to stability, may be unfavourable to wall stability) | 10 - 5 | 0.66 - 0.33 | 0.5 - 2 | reduce σ_c and σ_t to $0.6\sigma_c$ and $0.6\sigma_t$, where |
| L. Mild rockburst (massive rock) | 5 - 2.5 | 0.33 - 0.16 | 5 - 10 | σ_c = unconfined compressive strength, and |
| M. Heavy rockburst (massive rock) | < 2.5 | < 0.16 | 10 - 20 | σ_t = tensile strength (point load) and σ_1 and |
| c. Squeezing rock, plastic flow of incompetent rock under influence of high rock pressure | | | | |
| N. Mild squeezing rock pressure | | | 5 - 10 | σ_3 are the major and minor principal stresses. |
| O. Heavy squeezing rock pressure | | | 10 - 20 | 3. Few case records available where depth of crown below surface is less than span width. Suggest SRF increase from 2.5 to 5 for such cases (see H). |
| d. Swelling rock, chemical swelling activity depending on presence of water | | | | |
| P. Mild swelling rock pressure | | | 5 - 10 | |
| R. Heavy swelling rock pressure | | | 10 - 15 | |
| ADDITIONAL NOTES ON THE USE OF THESE TABLES | | | | |
| When making estimates of the rock mass Quality (Q), the following guidelines should be followed in addition to the notes listed in the tables: | | | | |
| 1. When borehole core is unavailable, RQD can be estimated from the number of joints per unit volume, in which the number of joints per metre for each joint set are added. A simple relationship can be used to convert this number to RQD for the case of clay free rock masses: $RQD = 115 - 3.3 J_v$ (approx.), where J_v = total number of joints per m^3 ($0 < RQD < 100$ for $35 > J_v > 4.5$). | | | | |
| 2. The parameter J_n representing the number of joint sets will often be affected by foliation, schistosity, slaty cleavage or bedding etc. If strongly developed, these parallel 'joints' should obviously be counted as a complete joint set. However, if there are few 'joints' visible, or if only occasional breaks in the core are due to these features, then it will be more appropriate to count them as 'random' joints when evaluating J_n . | | | | |
| 3. The parameters J_r and J_a (representing shear strength) should be relevant to the weakest significant joint set or clay filled discontinuity in the given zone. However, if the joint set or discontinuity with the minimum value of J_r/J_a is favourably oriented for stability, then a second, less favourably oriented joint set or discontinuity may sometimes be more significant, and its higher value of J_r/J_a should be used when evaluating Q. The value of J_r/J_a should in fact relate to the surface most likely to allow failure to initiate. | | | | |
| 4. When a rock mass contains clay, the factor SRF appropriate to loosening loads should be evaluated. In such cases the strength of the intact rock is of little interest. However, when jointing is minimal and clay is completely absent, the strength of the intact rock may become the weakest link, and the stability will then depend on the ratio rock-stress/rock-strength. A strongly anisotropic stress field is unfavourable for stability and is roughly accounted for as in note 2 in the table for stress reduction factor evaluation. | | | | |
| 5. The compressive and tensile strengths (σ_c and σ_t) of the intact rock should be evaluated in the saturated condition if this is appropriate to the present and future in situ conditions. A very conservative estimate of the strength should be made for those rocks that deteriorate when exposed to moist or saturated conditions. | | | | |


APPENDIX: B

Resistivity Images along the Tunnel Route

APPENDIX: C.

Table of Site Discontinuity Survey Data

APPENDIX: D Point load Laboratory test result



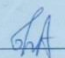
ICT ENGINEERING PRIVATE LIMITED COMPANY

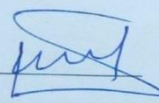
POINT LOAD STRENGTH (ASTM D 5731)


LAB NUMBER : KT MSC 167/20
 CLIENT : Kibrewosen Jira
 PROJECT : For Thesis MSc
 TYPE OF TESTS : Point Load
 TEST SPECIFIED BY : Kibrewosen Jira
 SAMPLED BY : Kibrewosen Jira
 SUBMITTED BY : Kibrewosen Jira On: 07.05.2020
 REPORTED TO : Kibrewosen Jira On: 14.05.2020

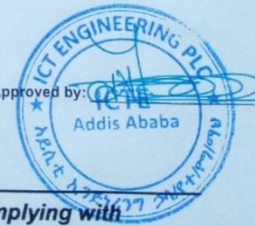
| Sl. No. | Sample No. | Sample Depth (m) | Sample type | Point Load Distance or sample Diameter (mm) | Load | Area | Stress | Correction Factor $F=(d/50)^{0.45}$ | Corrected Pint Load I_s (N/mm) ² | Water Absorption % |
|---------|------------|------------------|-------------|---|--------|---------------------|---------------|--|--|--------------------|
| | | | | | P (KN) | d ² (mm) | $I_s / P/d^2$ | | | |
| 1 | SA 1 | — | Quarry Rock | 41 | 17 | 1681 | 10.11 | 0.91 | 9.25 | Nil |
| 2 | SA 2 | — | Quarry Rock | 38 | 16 | 1444 | 11.08 | 0.88 | 9.79 | Nil |
| 3 | SA 3 | — | Quarry Rock | 39 | 13 | 1521 | 8.55 | 0.89 | 7.64 | Nil |
| 4 | SA 4 | — | Quarry Rock | 40 | 18 | 1600 | 11.25 | 0.90 | 10.18 | Nil |

REMARK : Samples description are not given by the Client.

Tested by: 

Checked by: 

Approved by: 
 Addis Ababa



We stand Committed to the highest performance standards, fully complying with requirements of the Quality Management System (QMS) and our esteemed Clients.

BUSINESS OFFICE:
 Sub City : Kirkos, Woreda: 03
 House # 524 near Senay Higher Clinic
 P.O Box: 120563- Gotera Post Office, Addis Ababa, ETHIOPIA
 Tel.: +251 11 470 2517, Fax: +251 11 470 2399
 E-mail: icteplc@ethionet.et

CENTRAL LABORATORY:
 Sub City : Kirkos, Woreda: 03
 House # 524 near Senay Higher Clinic
 P.O Box: 120563- Gotera Post Office, Addis Ababa, ETHIOPIA
 Tel.: +251 911 68 0487, Fax: +251 11 470 2399
 E-mail: n.akhtar1974@yahoo.com